12-2013

Repair of the airway epithelium after chlorine-induced injury.

Sadiatu Musah
University of Louisville

REPAIR OF THE AIRWAY EPITHELIUM AFTER CHLORINE-INDUCED INJURY

By

Sadiatu Musah

B.S., University of Ghana, 2004

M.S., University of Northern Iowa, 2008

A Dissertation

Submitted to the Faculty of the

School of Public Health and Information Sciences of the University of Louisville

in Partial Fulfillment of the Requirements

Doctor of Philosophy

Department of Environmental and Occupational Sciences

University of Louisville

December 2013

REPAIR OF THE AIRWAY EPITHELIUM AFTER CHLORINE-INDUCED INJURY

By

Sadiatu Musah

B.S., University of Ghana, 2004

M.S., University of Northern Iowa, 2008

A Dissertation Approved on

November 22, 2013

by the following Dissertation Committee:

_____

Gary W. Hoyle, Ph.D., Dissertation Director

_____

David Tollerud, M.D., M.P.H.

_____

Qunwei Zhang, M.D., M.P.H., Ph.D.

_____

Daniel Conklin, Ph.D.

DEDICATION

This dissertation is dedicated to my sister Naa Amponsah Dodoo whose selfless dedication and tremendous help has contributed to my success.

ACKNOWLEDGEMENTS

I am very grateful to my mentor, Dr. Gary Hoyle, for his patience and guidance. I would also like to appreciate the other members of my committee, Dr. David Tollerud, Dr. Qunwei Zhang, and Dr. Daniel Conklin. A big thank you also goes to the entire staff and faculty in the department of Environmental and Occupational Health Sciences. My appreciation also goes to my father Sura, and my sister Zubaida, for their encouragement and support. I would also like to thank the members of my church family in Louisville, Kentucky. Last but in no way the least, I would like to thank the members of the Hoyle Lab, Jing Chen, Connie Schlueter, David Humphrey, and Yiqun Mo for all their help.

ABSTRACT

REPAIR OF THE AIRWAY EPITHELIUM AFTER CHLORINE-INDUCED INJURY

Sadiatu Musah

November 22, 2013

Chlorine is a widely used toxic chemical that is considered a chemical threat agent. Chlorine inhalation injures airway epithelium, and efficient epithelial repair is necessary to restore normal lung structure and function. Regeneration of injured tissues typically proceeds through the proliferation and differentiation of stem or progenitor cells. Knowledge of underlying mechanisms that regulate these processes during airway epithelial repair is lacking. This dissertation characterizes respiratory epithelial repair after chlorine injury to investigate potential signaling pathways that could be manipulated to regulate stem/progenitor cells in airway repair.

Repair of the pseudostratified tracheal epithelium after chlorine-induced injury was characterized in C57BL/6 mice by morphometric analysis of tracheal sections following standard histological staining and specific staining for proliferating cells and epithelial cell types. Surviving basal epithelial cells served as progenitor cells for tracheal epithelial regeneration after chlorine injury. In areas where repair was inefficient owing to few remaining basal cells, airway fibrosis was observed. To investigate potential signaling pathways that could be manipulated to facilitate epithelial repair after chlorine-induced injury, the low-

affinity nerve growth factor receptor (NGFR) and the Wnt/β-catenin pathway were examined. Pharmacological treatment of isolated tracheal epithelial cells with NGFR ligands did not influence the growth of tracheal basal cells in vitro. Overexpression of nerve growth factor (NGF) in airway epithelium or mutation of NGFR increased the pool of stem cells that formed a differentiated pseudostratified epithelium in vitro. Treatment of chlorine-exposed mice with NGF did not impact epithelial repair in vivo. Minimal effect of NGF overexpression on epithelial repair in transgenic mice was observed. NGFR mutation resulted in increased sensitivity of mice to chlorine-induced airway injury, but unexpectedly protected mice from the development of fibrosis. Stimulation of Wnt/β-catenin signaling with lithium chloride prevented the formation of pseudostratified epithelium in vitro. Chlorine inhalation in mice activated β-catenin signaling in the tracheal epithelium. Treatment of mice with lithium chloride or the Wnt/β-catenin signaling modulator ICG-001 reduced collagen content in the lung after chlorine exposure. This work highlights the potential contribution of NGFR and Wnt/β-catenin signaling to airway epithelial repair and identifies potential therapeutic targets for inhibiting chlorine-induced airway fibrosis.

TABLE OF CONTENTS

LIST OF FIGURES

CHAPTER I: INTRODUCTION

Chlorine Health Effects

Chlorine is a gaseous chemical agent with multiple industrial uses, including the production of polyvinyl chloride, paper, pharmaceuticals, chlorinated solvents, and for the purification of water [1, 2]. About 15 million tons of chlorine are produced in the United States annually and transported predominantly by rail across states [2]. The potential sources of chlorine gas exposure to humans include accidental train derailment during transportation [3], occupational exposures, and also through accidental mixtures of chlorine bleach with household cleaners that contain acid [1, 2]. Chlorine is also considered a chemical threat agent that could be deliberately released in an attack on the U.S. populace [4].

Inhalation of chlorine results in acute health effects such as chest tightness, shortness of breath, obstruction of the small airways, and pulmonary edema [1]. Long-term effects of chlorine exposure include chronic bronchitis and decrements in lung function [5-7].

Human Exposures and Effects

A myriad of adverse respiratory effects have been reported with acute, high level accidental chlorine exposures. In a train derailment accident that led to the release of high levels of chlorine, exposed individuals exhibited respiratory

abnormalities such as expiratory obstruction and pulmonary edema within 48 hours of chlorine inhalation [8]. In an assessment of individuals who were also accidentally exposed to chlorine in a train derailment, victims developed severe airway inflammation and exhibited acute respiratory distress syndrome [3]. A study of healthy individuals accidentally exposed to high chlorine concentrations in a pulpmill revealed airflow obstruction and air trapping in pulmonary function tests performed a day after the exposure [6]. Individuals accidentally exposed to high chlorine levels during a leak in a chlorination system exhibited symptoms such as dyspnea, tachycardia, and tachypnea [9]. In a population of healthy workers who accidentally inhaled high concentrations of chlorine gas in an industrial accident, airway obstruction was observed in 10 out of the 19 exposed individuals [10].

Alterations in pulmonary function measurements have been associated with long-term effects of acute, high level chlorine exposures. In a study of pulmonary function in a 12-year follow-up of individuals accidentally exposed to high chlorine concentration in a train derailment, persistence in airflow obstruction and increased airway reactivity were observed [6]. In a 4-year prospective cohort study among workers in a metal production plant who accidentally inhaled high concentrations of chlorine, a transient decrease in airway function and an increase in airway hyperreactivity were reported [11]. Exposure to high levels of chlorine gas has been associated with an asthma-like condition described as reactive airway dysfunction syndrome (RADS) or irritant-induced asthma, a condition characterized by airway obstruction and bronchial

hyperresponsiveness [12-15]. In a case study involving an individual accidentally exposed to chlorine in an industrial accident, RADS was observed 6 years after the exposure incident [13]. During an assessment of the respiratory health among construction workers exposed to chlorine gas 18 to 24 months after exposure incidents, 41% of these workers exhibited bronchial hyperresponsiveness due to RADS [16]. In individuals accidentally exposed to sub-lethal doses of chlorine gas in a paper factory, symptoms of RADS were reported 30 months post-exposure [15]. In a study to reassess the long-term outcome of individuals diagnosed with acute irritant-induced asthma due to irritant gas exposure, results revealed persistence of respiratory symptoms with no improvement in bronchial hyper-responsiveness in 27% of subjects examined 9 years following exposure [14]. In a prospective observational study after an acute accidental exposure to high levels of chlorine gas, RADS was reported in 3 out of 12 affected individuals several months after chlorine inhalation [9]. During an evaluation of the long-term respiratory health effects of workers accidentally exposed to high chlorine gas concentrations in an industrial factory, RADS was observed in 2 out of 5 participants in a follow-up 8 months after the incident [12].

Pathological changes in the airways have been linked to reports of irritant-induced asthma or RADS due to chlorine exposure. Biopsy specimens from individuals diagnosed with RADS revealed increased thickness in basement membrane without reversibility of obstruction after inhalation of albuterol [17]. In a study of patients diagnosed with RADS as a result of chlorine exposure, biopsy specimens showed increased airway subepithelial fibrosis which was positively

correlated with response to methacholine challenge [18]. In the case study of an individual diagnosed with RADS, it was observed from bronchial biopsies that histological changes were partially reversible while bronchial responsiveness to methacholine was completely reversible upon treatment with inhaled steroids after 5 months [19]. In a 10-year follow-up of individuals with a history of irritant induced-asthma, results from bronchial biopsies revealed thickness in basement membrane which was associated with bronchial responsiveness to methacholine [20]. Taken together, the results of these studies indicate that acute, high level exposures to chlorine can produce chronic airway disease in some individuals.

Chronic effects of low levels chlorine exposure have been associated with diverse respiratory symptoms and alterations in lung function. In a cross-sectional survey to investigate lung health among pulpmill workers, it was reported that chlorine or chlorine dioxide exposure incidents were associated with elevated respiratory symptoms and increased airflow obstruction [21]. In this same population of workers, analysis of first-aid reports related to chlorine exposure incidents among workers was used as a predictor of lung health over a 7-year period of observation. Results revealed a significant decline in lung function among workers who had been accidentally exposed to chlorine compared with non-exposed workers [22]. In a survey of the respiratory and irritative symptoms among construction workers in a bleaching plant over a 3 to 6 month period, cough-like and flu-like symptoms were reported as recurrent incidents after repeated low level accidental exposures to chlorine [23]. In a follow-up study to determine the prevalence of persistent respiratory symptoms in

these workers 18 to 24 months after occupational exposure to chlorine had ended, 82% of the workers still exhibited respiratory symptoms, 23% reported bronchial obstruction, and 29% exhibited airway hyperreactivity [16].

Animal Models of Chlorine-Induced Lung Injury

Lung injury caused by inhalation of chlorine has been demonstrated in various animal models. In one study, A/J mice exposed to 800 ppm chlorine for 5 minutes (min) exhibited airway epithelial loss, inflammation, oxidative stress, and increased airway reactivity to methacholine [24]. Acute chlorine exposure in C57BL/6 and FVB/N mice resulted in epithelial cell death, pulmonary edema, and neutrophil inflammation [25]. Exposure of mice to 800 ppm chlorine for 5 min resulted in death of epithelial cells by apoptosis, elevated protein in bronchoalveolar lavage fluid, airway smooth muscle hyperplasia, and airway hyperreactivity [26]. Song and colleagues exposed C57BL/6 mice to 400 ppm chlorine for 30 min and reported increased airway reactivity and decreased alveolar fluid clearance [27]. BALB/C mice exposed to a chlorine concentration of 400 ppm for 30 min exhibited increased unfolded protein response signaling in the lungs [28]. Exposure of male Sprague Dawley rats to up to 400 ppm chlorine for 30 mins resulted in decreased ascorbate and glutathione levels, as well as extensive airway epithelial loss and hypoxemia [29]. Similar exposure of rats also resulted in endothelial dysfunction characterized by the loss of endothelial nitric oxide synthase [30].

Other studies have investigated subacute and longer term effects of chlorine exposure. Fanucchi and colleagues exposed rats to 400 ppm chlorine

for 30 min and observed decreased levels of ascorbate and reduced glutathione concentrations, epithelial hyperplasia, increased mucus production, and airway hyperreactivity 7 days after exposure [31]. Yildirim and colleagues exposed rats to chlorine and observed a thickening of the airway septa and interstitial fibrosis after 45 days [32]. Demnati and colleagues exposed rats to 1,500 ppm chlorine for 5 min and assessed animals after 3 months. Their results revealed histological abnormalities in the airway epithelium and smooth muscle as well as physiological abnormalities including increased lung resistance and airway hyperreactivity [33].

Aside from rodent models of chlorine exposure, other studies have investigated the effect of chlorine in large animals. Female sheep exposed to up to 350 ppm chlorine for 30 min exhibited a rapid and dose-dependent development of acute respiratory distress syndrome (ARDS) characterized by decreased PaO_2-to-FiO_2 ratio, transient hypotension and decreased cardiac output [34]. Gunnarsson and colleagues exposed pigs to 140 ppm chlorine for 10 min through mechanical ventilation and observed sloughing of bronchial epithelium, infiltration of inflammatory cells, hypoxemia, pulmonary hypertension, and pulmonary edema [35]. It is apparent from the various studies of chlorine exposure in these different animal models that chlorine injury does produce diverse structural and functional changes in the airways.

Mechanisms of Chlorine Toxicity

The biological effect of chlorine inhalation has been observed to be dependent on the concentration and duration of chlorine exposure with injury

extending to distal parts of the respiratory system as the concentration of chlorine increases [36]. Chlorine exhibits a high reactivity towards water to form hydrochloric acid (HCl) and hypochlorous acid (HOCl) [1, 2, 36]. Damage to the respiratory tract resulting from chlorine inhalation is thought to be caused by the oxidative nature of chlorine and HOCl rather than by the acidic nature of HCl because of the neutralizing effect of the significant concentration of bicarbonate in lung epithelial lining fluid (ELF) [37]. When inhaled, elemental chlorine can also react directly with biological molecules in ELF, which include low molecular weight antioxidants, amino acid functional groups of proteins, and amino-phospholipids [36]. HOCl and other reactive byproducts of chlorine can directly injure and kill cells of the respiratory tract through oxidative damage. It has been hypothesized that with chlorine inhalation, the predominant site of adsorption and reaction is the upper airways with progressive loss in concentration as chlorine travels into the lower airways [2]. The high concentrations of low molecular weight antioxidants such as ascorbic acid, uric acid, and glutathione in ELF have been reported to influence the uptake of chlorine in the proximal airways by acting as scavengers for chlorine and HOCl [36].

The exact mechanism by which chlorine kills cells is not understood. One potential mechanism of chlorine toxicity is through induction of mitochondrial dysfunction. Studies have shown that HOCl interferes with the mitochondrial membrane potential by inducing the mitochondrial permeability transition of cells and ultimately leading to cell death [38-40]. Chlorine and HOCl can also react with amino acid functional groups of proteins leading to the formation of

chloramines which have longer half-lives and can also injure biological tissues. Additionally, HOCl has been associated with DNA damage and the DNA repair enzyme ADP-ribose polymerase [41]. Chloramines and HOCl have also been suggested to be involved with the activation of inflammatory pathways [37]. The recruitment of inflammatory cells such as neutrophils leads to the production of reactive oxygen species such as superoxide, hydrogen peroxide, and hydroxyl radicals as well as the production of additional HOCl. Recruitment of inflammatory cells leads to the generation of nitric oxide synthase which in turn leads to the formation of additional free radicals such as nitric oxide and peroxynitrite which further contribute to airway injury [42]. Thus, although multiple types of potential mechanisms for chlorine-induced cytotoxicity have been identified, the relative importance of each and how they may interact to produce cell death are not known.

Airway Epithelial Repair

In animal studies, chlorine inhalation has been observed to produce injury to the pseudostratified respiratory epithelium with extensive loss of airway epithelial cells [25, 29, 43]. In mice, the pseudostratified epithelium of the respiratory tract has been reported to be composed of about 55% ciliated cells and 30% basal cells, with the remainder being secretory cells (most of which are Clara cells) and neuroendocrine cells. However there are significant regional variations in the distribution of cell types within the proximal airways, as well as differences among inbred mouse strains [44]. The pseudostratified epithelium in mice is restricted to the trachea and bronchi, and it transitions to a simple

epithelium devoid of basal cells in the mainstem or lobar bronchi. In larger species including humans, the pseudostratified epithelium is lined by about 30% ciliated cells, 30% basal cells, and 30% secretory cells, and extends further into the respiratory tract to the level of the terminal bronchioles [45].

Unlike epithelial cells in tissues such as the gut and skin that turn over rapidly, epithelial cells of lung are slow-renewing but can be stimulated for increased self-renewal after injury [46]. Regeneration of the airway epithelium is needed to restore normal barrier and host defense function after injury [47]. Repair of epithelial tissues is thought to be carried out by the coordinated action of resident stem cells (rare cells with an extensive capacity for self-renewal and differentiation) and progenitor cells (more abundant cells with a finite capacity for self-renewal and differentiation) [48]. The normal repair response of the airway after injury usually involves the migration of remaining progenitor cells to cover denuded airways, proliferation, and differentiation of progenitor cells or local populations of stem cells to restore the integrity of the epithelium [46, 47]. Basal cells are an example of a type of progenitor or stem cell involved in epithelial repair.

Basal cells have been implicated as progenitor cells responsible for repair of the tracheal and bronchial epithelium in mice after injury [49, 50]. In addition, a subset of airway basal cells has been implicated as a multipotent stem cell population in the regeneration of pseudostratified epithelium after injury [51]. Evidence from lineage-tracing studies shows that basal cells are capable of extensive self-renewal and are able to differentiate into ciliated and Clara cells

[50, 52]. Basal cells have been identified by markers including the transcription factor transforming related protein 63 (TRP63; p63) [50], cell surface markers such as integrin alpha-6 (ITGA6) [50], the cytoskeletal proteins keratin 5 and keratin 14 (K5 and K14) [50, 53, 54], and the low-affinity nerve growth factor receptor (NGFR) [50].

Although repair of the airway has been characterized in specific injury models such as naphthalene [55] and sulfur dioxide [50, 56], information about repair of the tracheal epithelium after acute exposure to chlorine is lacking. Since naphthalene-induced injury is specific to only Clara cells [55], and the dose of sulfur dioxide used in previous studies resulted in a different extent of epithelial damage [50, 56] compared to chlorine injury [25], repair mechanisms may differ. Since efficient repair of injured epithelium after chlorine exposure is necessary for the restoration of normal lung structure and function, our objective was to evaluate potential signaling mechanisms that could mediate repair of the tracheal epithelium after chlorine injury. Among the signaling pathways investigated in this study are NGFR signaling and the Wnt/β-catenin pathway.

Nerve Growth Factor (NGF) and Receptor Signaling

Nerve growth factor (NGF) is a member of the neurotrophin family, which binds to NGFR to induce signaling associated with this receptor. The neurotrophin family also includes brain-derived neurotrophin factor (BDNF) and neurotrophin-3 (NT-3) [57]. These growth factors bind to the trk family of receptors, as well as to NGFR. NGF was initially identified from its effect on

nerve cells to promote differentiation and survival. It is now established however, that NGF affects non-neuronal cells as well [57].

NGFR, also known as the low-affinity p75 neurotrophin receptor, is a member of the death receptor family. In addition to being a marker for basal cells in the lung, NGFR is also expressed in basal stem cells in other organs such as the esophagus and oral mucosa [58, 59]. Embryonic stem cells have been shown to express NGFR which stimulates proliferation in these cells [60]. Treatment of NGFR-expressing mouse embryonic stem cells with NGF enhanced proliferation but not differentiation in these cells [60]. These results provided evidence for NGFR being involved in a potential stem/progenitor cell signaling pathway. NGF has also been shown to contribute to repair of the lung epithelium by promoting the proliferation and self-renewal of Clara cells after naphthalene injury [55]. To date however, no study has investigated the significance of NGF in repair of the respiratory epithelium after chlorine injury, which would be more typical of that caused by toxic industrial chemicals. The contribution of signaling pathways implicated in stem cell function to the regulation of basal cell proliferation and differentiation is of particular interest because of the potential to stimulate repair of the respiratory epithelium after chemical lung injury.

Wnt/β-Catenin Signaling

Another signaling pathway implicated in stem cell modulation is Wnt/β-catenin signaling [61]. Wnt proteins are a family of cysteine-rich glycoproteins involved in embryonic development, homeostasis, and stem cell renewal [62]. Wnt ligands bind to Frizzled receptors, a family of seven trans-membrane

proteins and G-protein coupled receptors [63, 64]. Frizzled receptors are differentially expressed in the developing and adult lungs [62, 63]. The canonical pathway of Wnt signaling involves activation of the nuclear transcription factor β-catenin by increasing its stability [62, 64].

It has been reported that inactivation of Wnt/β-catenin signaling in mouse embryonic airway epithelial cells results in abnormal lung development [62]. Additionally, continued activation of β-catenin signaling in vivo also results in abnormal differentiation of epithelial cells [62, 65]. Activation of Wnt/β-catenin signaling has been implicated in the regulation of stem cells in various tissues including the lung [61, 64-67]. It has been observed that activation of Wnt/β-catenin signaling regulates airway stem cell numbers and contributes to the regeneration and repair of lung epithelium after injury [65, 67]. Conditional stabilization of β-catenin in the embryonic lung resulted in increased stem cells numbers due to the inhibition of differentiation rather than increased proliferation [65]. Additionally, sustained activation of β-catenin signaling in tracheal epithelial cells cultured from adult mice promoted differentiation of basal cells towards ciliated cell lineage but inhibited Clara cell differentiation [68]. Manipulation of Wnt/β-catenin signaling would serve as a potential pathway to stimulate epithelial repair after injury.

Study Objectives

Since repair of the airway epithelium after injury is necessary in order to restore the integrity of the respiratory system, the objectives of this study were to characterize respiratory epithelial repair after chlorine injury and to investigate

potential signaling pathways that may regulate stem/progenitor cells in the repair the airway after injury. The ultimate goal of this line of investigation is to develop strategies for stimulating basal cells to facilitate repair of the respiratory epithelium in ways that could be therapeutically beneficial.

The hypotheses to be tested are that repair of chlorine injury to the respiratory tract is carried out by airway basal cells and that NGFR signaling and the Wnt/β-catenin pathways are associated with basal cell repair of the respiratory epithelium following chlorine-induced injury. To test these hypotheses, the following objectives were investigated:

1. To characterize epithelial repair in mouse trachea after chlorine injury.

2. To determine the role of NGFR signaling in the repair of the tracheal epithelium following chlorine-induced injury.

3. To determine the contribution of Wnt/β-catenin signaling in the repair of the respiratory epithelium after chlorine injury.

CHAPTER II: CHARACTERIZATION OF EPITHELIAL REPAIR IN MOUSE TRACHEA AFTER CHLORINE INJURY

Introduction

Chlorine is a widely used industrial compound and is considered a chemical threat agent that could be intentionally released in an attack on the U.S. populace [4]. Chlorine inhalation injures epithelial cells of both the upper and lower airways leading to acute effects of pulmonary edema, pneumonitis, and pulmonary function abnormalities [2, 42]. High-level chlorine exposure results in sloughing of the pseudostratified airway epithelium of the proximal airways composed primarily of secretory, ciliated, and basal cells [25, 26, 29]. Repair of the airways after injury involves the coordinated action of local progenitor cells and stem cells to restore the integrity of the epithelium [46, 47, 69]. Understanding these processes following chlorine lung injury may suggest strategies for treating injury or accelerating epithelial repair. In mice, basal cells function as progenitor cells to repair tracheal and bronchial epithelium, whereas Clara cells are progenitor cells in bronchiolar epithelium [48-50]. Although the identity of tissue-specific stem cells in the airways is not completely established, current evidence suggests that subsets of basal cells and Clara cells function as stem cells for repair and long-term maintenance of the tracheobronchial and bronchiolar epithelium, respectively [49, 51, 53, 70, 71]. In the mouse tracheobronchial epithelium, most basal cells express the cytoskeletal protein keratin 5 (K5) whereas only a subset of these cells express keratin 14 (K14)

during steady state [45, 49, 69]. Lineage-tracing studies show that both K5- and K14-expressing basal cells are capable of extensive self-renewal and differentiation into ciliated and Clara cells [50, 52]. Because efficient repair of injured epithelial cells is necessary for restoration of normal lung structure and function, we sought to characterize repair of the tracheal epithelium in mice after acute chlorine injury. This study reports that after chlorine-related tracheal injury, epithelial repair occurs faster in the proximal trachea than in distal trachea/mainstem bronchus with basal cells initiating repair and serving as progenitor cells for the restoration of the tracheal epithelium.

Materials and Methods

Animals

All experiments involving animals were approved by the University of Louisville Institutional Animal Care and Use Committee and were conducted in accordance with the Institute of Laboratory Animal Resources Guide for the Care and Use of Laboratory Animals [72]. Male C57BL/6 mice (6 to 8 week old) were purchased from the Jackson Laboratory. Mice were randomly assigned to chlorine exposed or unexposed groups and exposed to a target dose of 240 ppm-hr chlorine in a whole body exposure chamber [25]; deviation between target and actual doses averaged 1.25%.

For time-course experiments, mice were injected intraperitoneally with 10 mg/kg of 5-ethynyl-2'-deoxyuridine (EdU) [73] from Life Technologies (Grand Island, NY) 17 hrs prior to euthanasia at different times after exposure (days 2, 4, 7, or 10) to label proliferating cells. Mice were euthanized for collection of tracheal tissue by injection with tribromoethanol (375 mg/kg intraperitoneally) followed by exsanguination. Tracheal tissues were collected, fixed in 10% neutral buffered formalin overnight and divided into 3 equal pieces along the proximal-distal axis (designated proximal, middle, and distal) before embedding in paraffin.

Histology, EdU Detection, and Immunofluorescence

For histological evaluation of tracheal structure, hematoxylin and eosin staining was performed on paraffin-embedded tracheas. To label proliferating cells in tracheal sections, EdU was detected using the Click-It EdU kit (Life Technologies, Grand Island, NY) according to the manufacturer's protocol. For dual EdU and immunofluorescence staining, EdU staining was performed first, followed by immunostaining. Briefly, sections were deparaffinized and rehydrated, and antigen retrieval was performed with 10 mM sodium citrate, pH 6.0, containing 0.05% Tween-20 at 95 ^{o}C for 30 min where necessary (for K5 and K14). This was followed by EdU detection and incubation in blocking solution (1% bovine serum albumin, 5% normal goat or donkey serum, and 0.3% Triton X-100) for 30 min at room temperature. After washing, slides were incubated with primary antibodies for 1 hr at room temperature. The following primary antibodies and dilutions were used: rabbit anti-K5 from Covance (Princeton, NJ) (1: 1,000; catalog # PRB-160P); mouse anti-K14 from Thermo Scientific (Fremont, CA) (1: 1,000; catalog # MS-115-P1); mouse anti-acetylated tubulin (AcTub) from Sigma-Aldrich (St Louis, MO) (1: 20,000; catalog # T7451); and goat anti-Clara cell secretory protein (CCSP), kindly provided by Dr. Gurmukh Singh (VA Medical Center, Pittsburgh, PA) (1: 1,000). After washing, slides were incubated with secondary antibodies for 1 hr at room temperature. The following antibodies (Life Technologies, Grand Island, NY) were used at a dilution of 1:500: Alexa Fluor 594 donkey anti-rabbit IgG for K5 immunofluorescence, Alexa Fluor 594 goat anti-mouse IgG for K14, Alexa Fluor

594 donkey anti-mouse IgG for AcTub, and Alexa Fluor 594 donkey anti-goat IgG for CCSP immunofluorescence. Sections were washed, coverslipped with Prolong Gold antifade reagent with DAPI (Life Sciences), and viewed by epifluorescence.

Immunohistochemistry

To detect alpha-smooth muscle actin in fibrotic tracheal sections, immunohistochemical staining was performed. Briefly, sections were deparaffinized and rehydrated, and endogenous peroxidases were inactivated with methanol containing 0.3% hydrogen peroxide for 30 min. This was followed by incubation in blocking solution (3% bovine serum albumin, 5% normal goat serum, and 0.3% Triton X-100) for 30 min at room temperature. Slides were washed thereafter and incubated with alpha-smooth muscle actin antibody (Sigma Aldrich, St Louis, MO) (1: 5,000; catalog # A5228) for 1 hr at room temperature. After washing, slides were incubated with biotinylated goat anti-mouse antibody (Jackson ImmunoResearch) (1: 3,500) at room temperature for 1 hr. Sections were washed and incubated with streptavidin-conjugated horseradish peroxidase (Jackson ImmunoResearch) (1: 2,000) for I hr at room temperature. After washing, slides were developed by incubation in 50 mM Tris-HCl, pH 7.6, containing 0.006% hydrogen peroxide and 200 µg/ml diaminobenzidine (DAB) for 15 min in the dark. Sections were washed, counterstained with Gill's hematoxylin (Sigma Aldrich), dehydrated, and coverslipped with Permount. Trichrome staining to detect collagen in fibrotic

sections was performed according to the manufacture's protocol (Sigma Aldrich, St Louis, MO).

Morphometry

Cross sections were cut at random depths of proximal, middle, and distal trachea for sampling of the entire trachea. Digital images encompassing the full circular profile of tracheal cross sections were captured and analyzed. Morphometric analysis [74, 75] was performed using point/intercept counting methods and Image J software (ImageJ: Image processing and analysis in java [76]. Re-epithelialization of the trachea was assessed by scoring the epithelium overlying intercepts of the basement membrane as normal, reparative, squamous, or none. This information was used to derive the percentage of basement membrane surface area covered by the different epithelial structures. A flow chart of the process used to perform morphometric analysis is shown in Fig 1. A representative image demonstrating scoring of re-epithelialization using intercept counting is shown in Fig 2A. For evaluation of epithelial immunostaining, the volume of structures of interest (EdU, K5, K14, CCSP, or AcTub labeling of airway epithelial cells) was measured by point counting and normalized to basement membrane surface area measured by intercept counting. The volume of structure of interest (i) relative to basement membrane surface area was expressed as VS (i,bm) and calculated using the equation VS (i,bm) = 2(Pi)(k)/π(Ibm), where Pi is the number of points overlying the structure of interest, k is the line length per test point, and Ibm is the number of intersections of lines with the basement membrane [74, 75]. For K5 and K14, the

volume of K5- or K14-expressing cells was measured by counting points that fell anywhere within a labeled cell, including unlabeled nuclei surrounded by cytoplasmic staining. For CCSP and AcTub, the volume of stained material was measured by counting only points that fell on CCSP or AcTub staining. The volume fraction of EdU-stained nuclei was calculated as points that fell on EdU-labeled nuclei within the epithelium divided by total points that fell on nuclei within the epithelium. A representative image demonstrating scoring of nuclear staining using point counting is shown in Fig 2B.

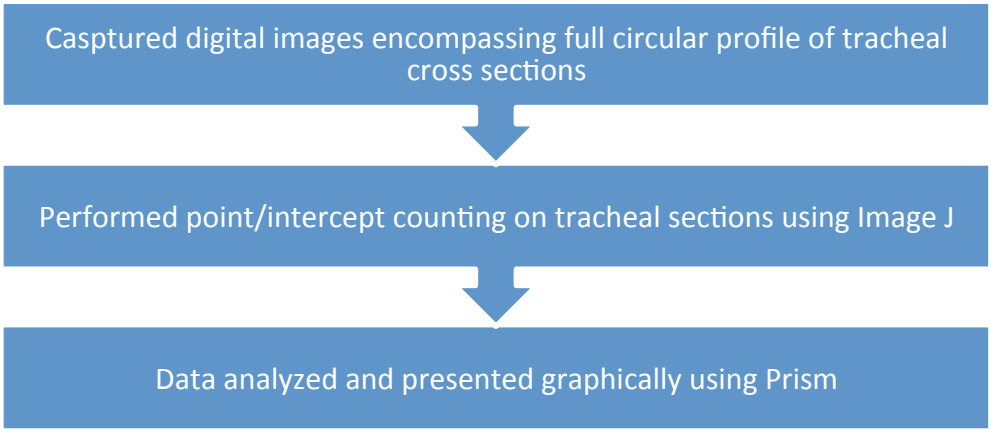

Figure 1. Flow chart of morphometric analysis of trachea sections.

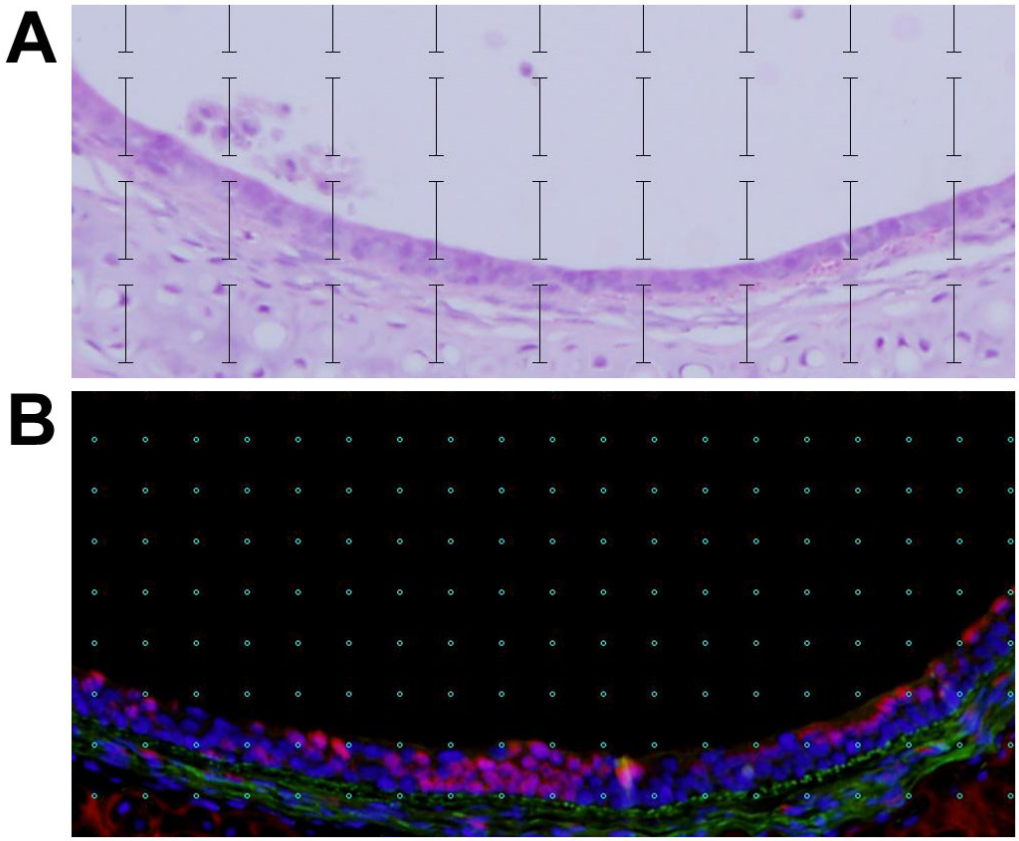

Figure 2. Representative images of morphometric analysis using ImageJ.

A. Representative portion of image showing vertical grid used for intercept counting. B. Representative portion of image showing grid used for point counting.

Statistical Analysis

Data are presented as group means ± standard error of the mean (SEM). Statistical analysis was performed using Prism 4.0a (GraphPad; La Jolla, CA). Group means were compared between chlorine-exposed and unexposed animals using one-way analysis of variance (ANOVA) with Dunnett's multiple comparison test. Effects of chlorine exposure among groups (e.g. proximal, middle, and distal trachea) were analyzed by one-way ANOVA with Bonferroni's multiple comparison test. Differences were considered statistically significant at $p < 0.05$.

Results

Histology of Tracheal Epithelium in Chlorine-Exposed Mice

Adult male mice were exposed to a target chlorine dose of 240 ppm-hr (1 hr exposure). The effects of chlorine exposure in the trachea were initially analyzed by hematoxylin and eosin staining (Fig 3) and quantitated by morphometric analysis (Fig 4). Preliminary studies indicated differential effects of chlorine along the proximal-distal axis of the trachea, so proximal, middle, and distal portions of the trachea were analyzed separately. In unexposed mice, examination of tracheal sections revealed a pseudostratified epithelium in proximal, middle, and distal trachea (Fig 3A-C and 4). Chlorine exposure resulted in sloughing of most if not all of the tracheal epithelium as observed at day 2 (Fig 3D-F and 4). At this time a thin layer of squamous epithelium could be observed lining portions of the tracheal lumen (Fig 3D), whereas other areas appeared to be entirely denuded of epithelium (Fig 3E and F). Denuded areas contained eosinophilic material (possibly fibrin), inflammatory cells, and dead epithelial cells. Epithelial repair proceeded faster in the proximal trachea than in the middle or distal portions. On day 4 after exposure, many areas of proximal trachea had regenerated a normal pseudostratified epithelium (Fig. 4A). Other areas contained undifferentiated, generally cuboidal cells that tended to form multiple layers producing a pluristratified, reparative epithelium (Fig 3G and 4C). Middle and distal trachea appeared to be in earlier stages of repair, including squamous and simple cuboidal epithelia, and often still had areas devoid of epithelial cells, particularly in the distal trachea (Fig 3H and I, Fig 4). On day 7,

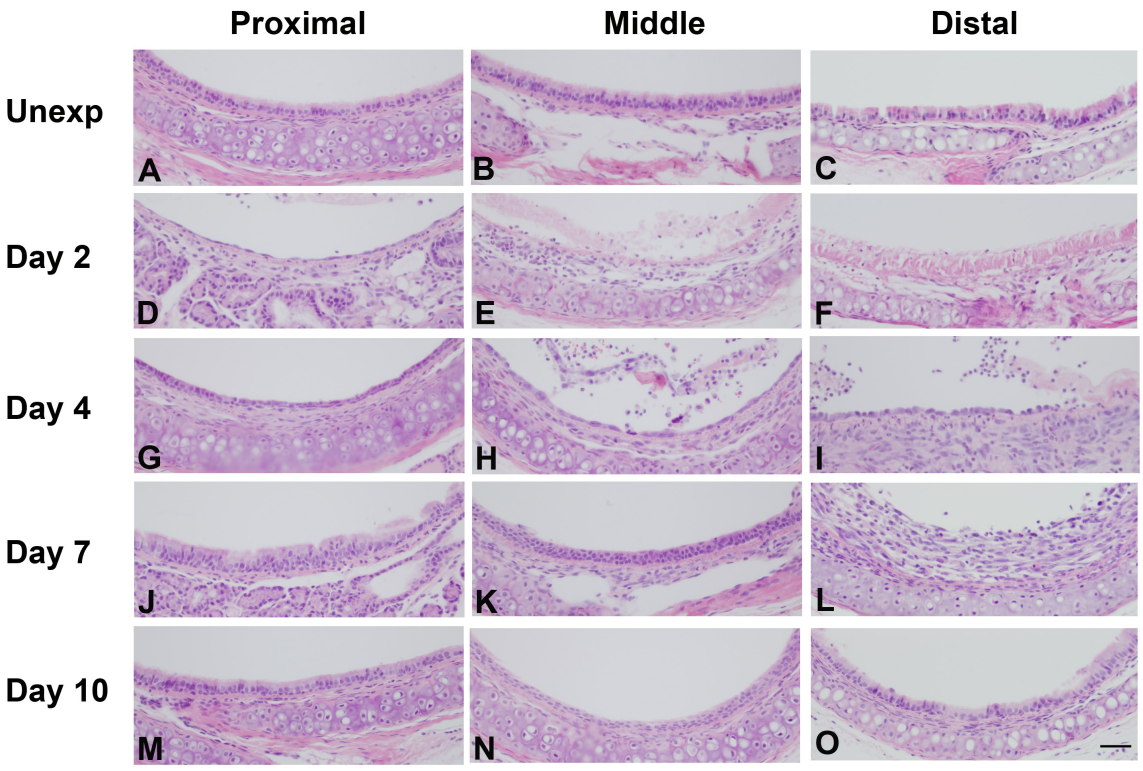

Figure 3. Histology of tracheal epithelium in chlorine-exposed mice.

Tracheas were collected for histological analysis from chlorine-exposed mice 2, 4, 7, and 10 days after exposure or from unexposed mice (Unexp). Scale bar in Panel O represents 40 μm for all panels.

the proximal trachea showed primarily a pseudostratified epithelium (Fig 1J), whereas and middle and distal trachea showed a mixture of pseudostratified, reparative (Fig 1K), and unrepaired (Fig 1L) epithelium (Fig 2). Areas of inefficient repair were observed mostly in distal trachea and were characterized by fibrotic lesions (Fig 1L). On day 10, distal sections showed a mixture of areas with well repaired pseudostratified epithelium (Fig. 1O) along with poorly repaired areas with fibrotic lesions. Fibrotic lesions grew from the tracheal wall and protruded into the lumen to partially obstruct the airway (Fig 3). Similar but more pronounced occlusive fibrotic lesions were also observed in mainstem and lobar bronchi (not shown).

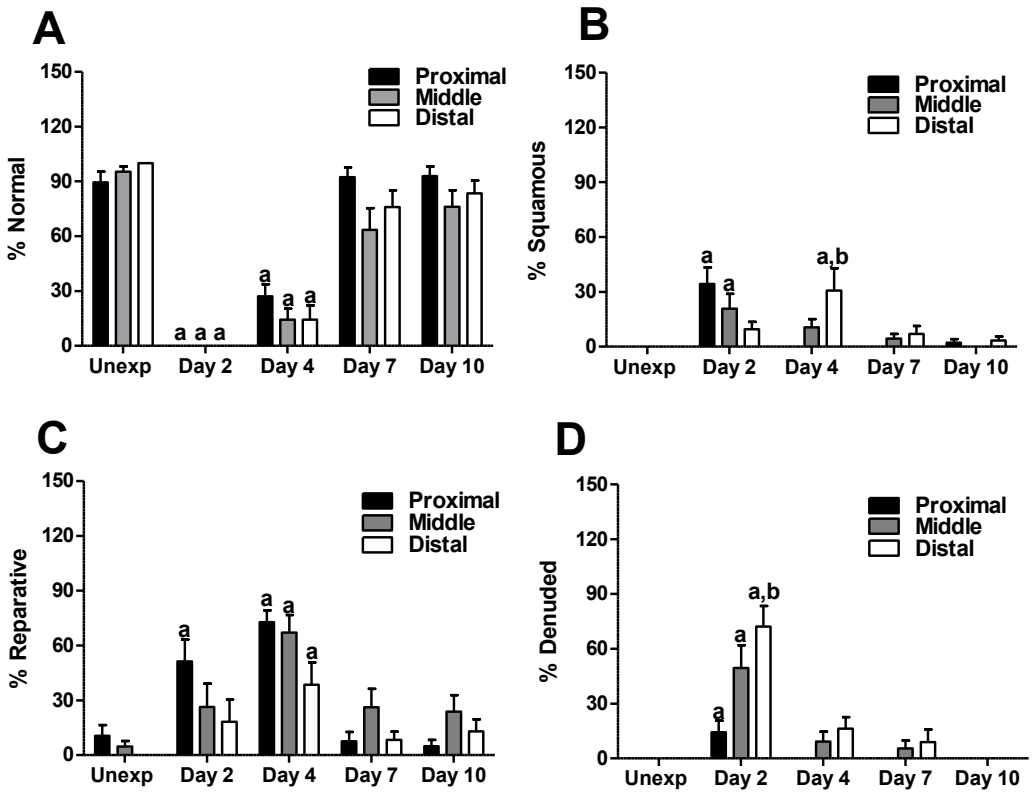

Figure 4. Morphometric analysis of tracheal epithelium in chlorine-exposed mice. Tracheal epithelium was evaluated in H&E-stained sections as described in Materials and Methods. The graphs depict the percentage of basement membrane surface area covered by normal (A), squamous (B), reparative (C), or no (D) epithelium in proximal, middle, and distal trachea. a, $p < 0.05$ vs. unexposed; b, $p < 0.05$ vs. proximal.

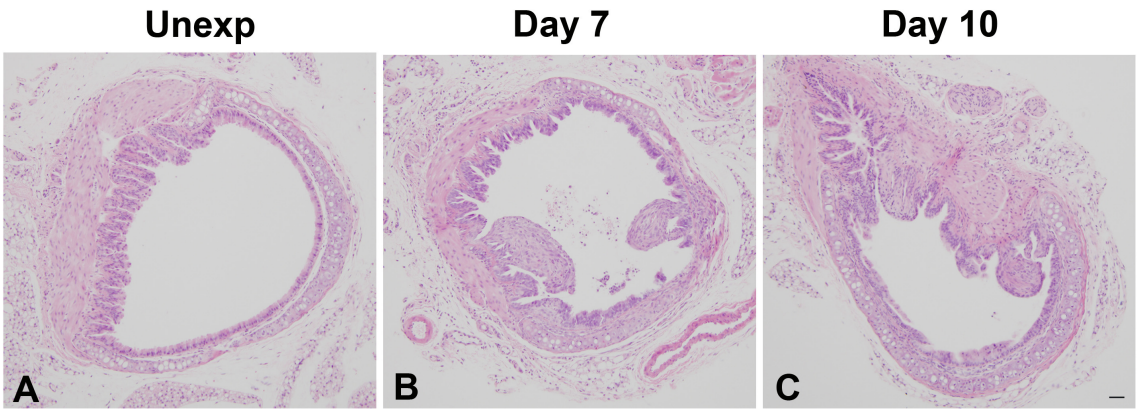

Figure 5. Airway fibrosis in chlorine-exposed mice. Tracheas were collected for histological analysis from chlorine-exposed mice 7 and 10 days after exposure or from unexposed mice. Note fibroproliferative lesions on days 7 and 10. Scale bar in Panel C represents 50 μm for all panels.

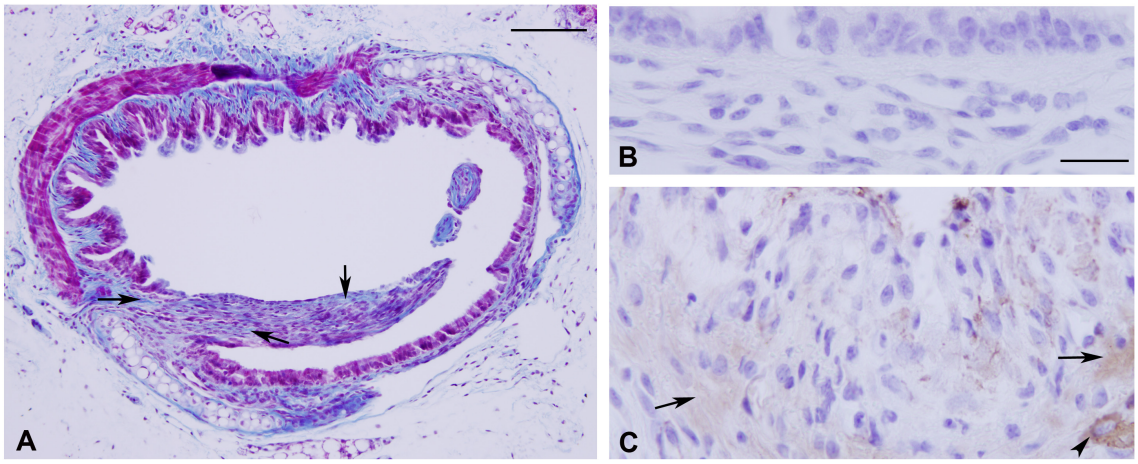

Figure 6. Markers of airway fibrosis after chlorine exposure in mice.

Tracheas from mice exposed to chlorine were collected after 7 days and stained for trichrome (A), or alpha-smooth muscle actin (B) and (C). A. Trichrome staining of distal trachea showing collagen fibers in fibrotic section. Arrows indicate blue staining of collagen fibers in fibrotic area after trichrome staining. Scale bar represents 100 μm. B. Immunohistochemical staining for alpha-smooth muscle actin in distal trachea showing efficient repair. C. Staining for alpha-smooth muscle actin in fibrotic region of distal trachea showing inefficient repair. Arrows indicate brown staining of smooth muscle actin. Arrowhead represents smooth muscle actin staining in muscle. Scale bars in panels B and C represent 20 μm.

Cell Proliferation and Differentiation after Chlorine Injury in Mice

Cellular proliferation during tracheal repair after chorine exposure was detected by EdU labeling (Fig 7) and quantitated by morphometry (Fig. 8). Minimal proliferation was observed in unexposed mice (Fig 7A-C and Fig 8), but proliferation increased after chlorine exposure (Fig 7D-L). A peak in EdU staining was observed in the proximal trachea on day 2 (Fig 7D and Fig 8) whereas peak proliferation in the middle and distal trachea was observed on day 4 (Fig 7H and I and Fig 8). Proliferation returned to nearly normal levels by day 7 in proximal trachea and day 10 in middle and distal trachea (Fig 8).

To determine the contribution of basal cells to proliferation and repair of the tracheal epithelium, we performed EdU detection in conjunction with immunofluorescence for the basal cell markers K5 (Fig 9) or K14 (Fig 10) and quantitated the results by morphometry (Fig 11). Images of tissue staining in middle trachea are shown; similar processes occurred in proximal and distal trachea although with somewhat different kinetics. Even within the same section, it was also apparent that areas in close proximity could be at different stages of the repair process. Expression of K5 was observed in almost all basal cells in unexposed mice (Fig 9A). In contrast, there were minimal or no K14-expressing cells in unexposed mice (Fig 10A and 11B). Following chlorine exposure, both K5 and K14 staining could be seen in squamous epithelium during the early stage of repair (Fig 9B and 10B). Abundant K5- and K14-expressing cells were observed in pluristratified reparative epithelium on day 4 in both basal and luminal locations; EdU staining was common in cells expressing these markers at

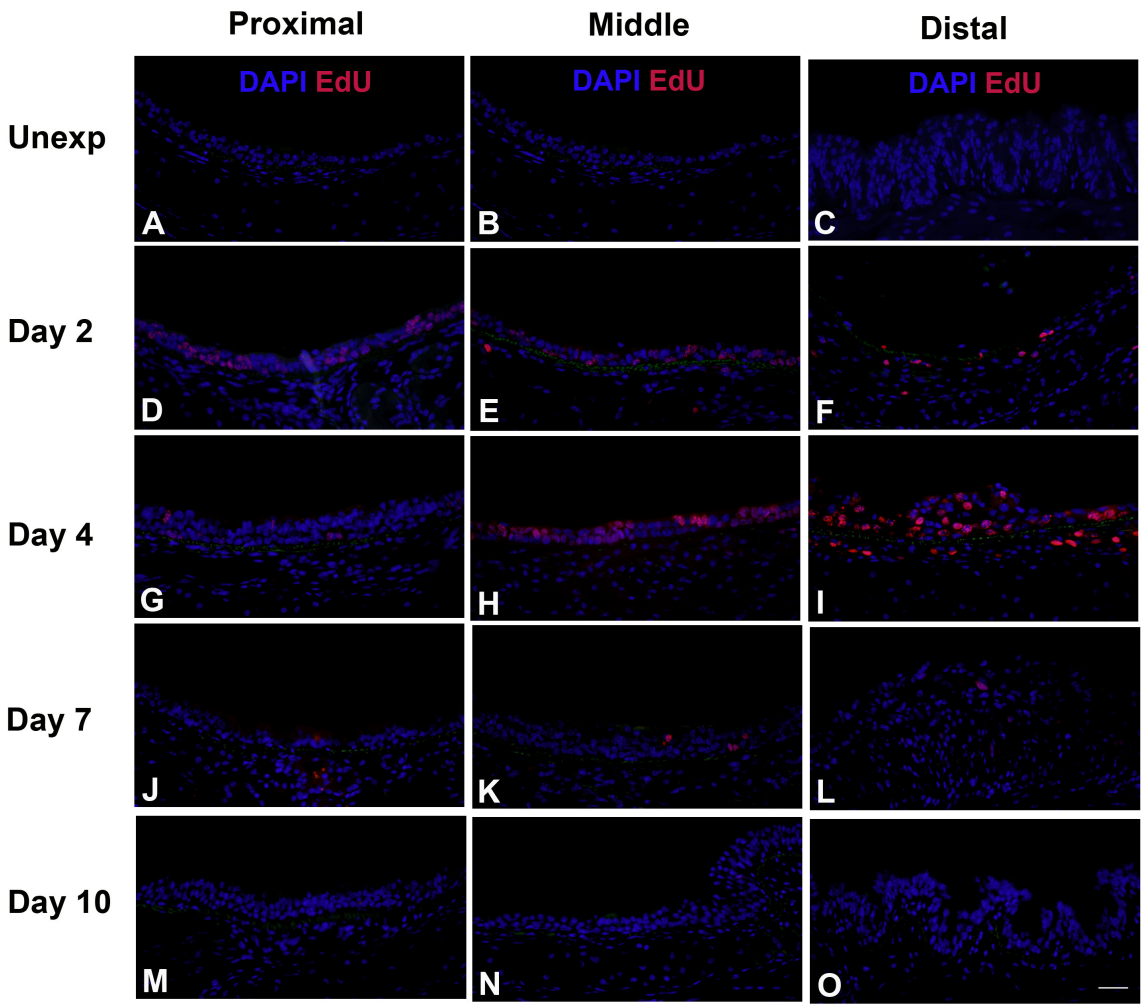

Figure 7. Cell proliferation in tracheal epithelium after chlorine-induced injury. Mice were exposed to chlorine and injected with EdU 17 hr prior to euthanasia and collection of tracheas 2, 4, 7, or 10 days after exposure. Tracheal sections were stained for EdU (red), and DAPI was used to visualize nuclei (blue). Green is tissue autofluorescence to aid in the visualization of airway structure. Scale bar in Panel O represents 40 μm for all panels.

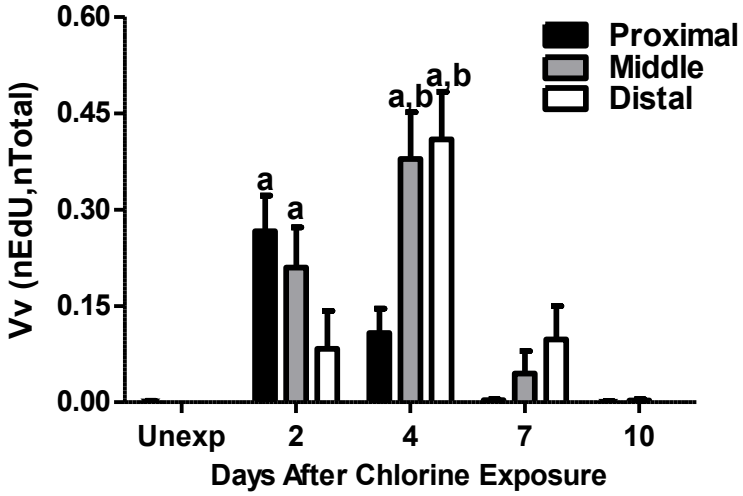

Figure 8. Morphometric analysis of cell proliferation in tracheal epithelium after chlorine injury. Cell proliferation was assessed in EdU-stained tracheal sections as described in Materials and Methods. The graphs depict the volume density (Vv) of EdU-labeled nuclei (nEdU) relative to total nuclei in tracheal epithelium (nTotal). a, $p < 0.05$ vs. unexposed; b, $p < 0.05$ vs. proximal.

this stage (Fig 9C and 10C). K5 and K14 continued to be expressed at day 7, but proliferating cells were significantly reduced (Fig 9D and 10D). At this stage K5 and K14 staining was becoming more restricted to a basal location, although many of the stained cells continued to exhibit increased cellular and nuclear size compared with basal cells in unexposed mice. On day 10, K5 staining was observed predominantly in a basal location in mostly smaller cells similar to normal basal cells, although some larger cells, both in basal and luminal locations continued to be observed (Fig 9E). K14 expression was reduced compared with earlier times, but was still observed in excess of that in unexposed mice (Fig 10E). Essentially no cellular proliferation was detected at this time. Morphometric analysis revealed a nonsignificant trend toward decreased volume of K5-expressing cells at day 2 followed by recovery to normal levels by day 4 (Fig 11A, although the distribution of the staining was altered, as shown in Fig 9). The volume of K14-expressing cells increased dramatically in chlorine-exposed mice, peaking on days 2-4 and becoming lower, but still readily detectable, on day 10 (Fig 11B). An assessment of K5- and K14-expressing cells that were proliferating revealed similar kinetics with a peak in these populations at day 2 in proximal trachea and day 4 in middle and distal trachea, with proliferation returning to near zero by day 10 (Fig 11C and D).

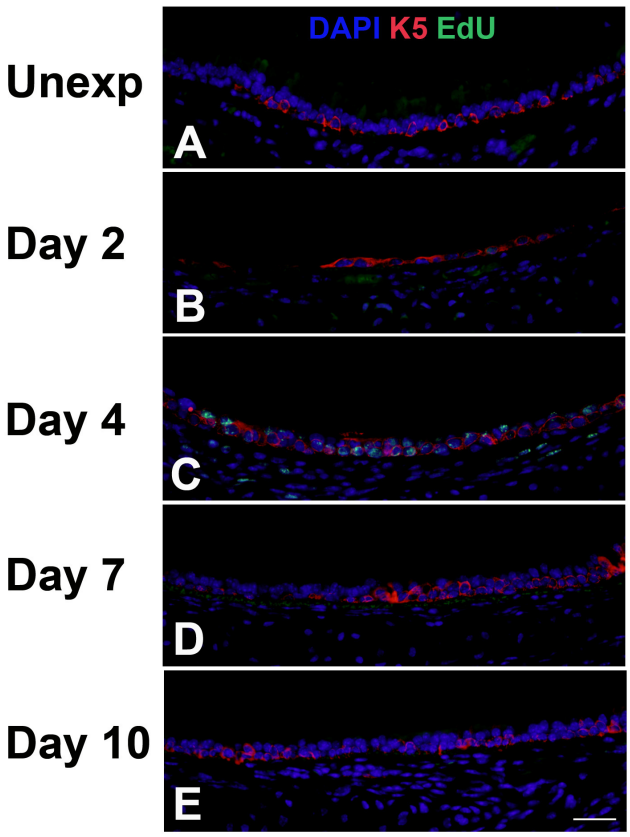

Figure 9. Cell proliferation and K5 expression in middle trachea after chlorine injury. Mice were exposed to chlorine and injected with EdU 17 hr prior to euthanasia and collection of tracheas. Tracheal sections were stained for EdU (green) and K5 (red), and nuclei were labeled with DAPI (blue). Scale bar in Panel E represents 40 μm for all panels.

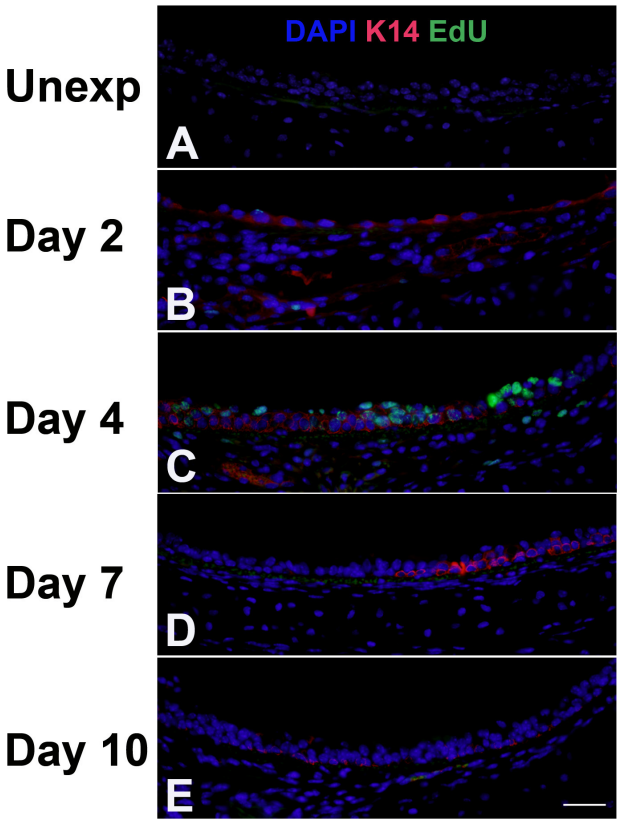

Figure 10. Cell proliferation and K14 expression in middle trachea after chlorine injury. Mice were exposed to chlorine and injected with EdU 17 hr prior to euthanasia and collection of tracheas. Tracheal sections were stained for EdU (green) and K14 (red), and nuclei were labeled with DAPI (blue). Scale bar in Panel E represents 40 μm for all panels.

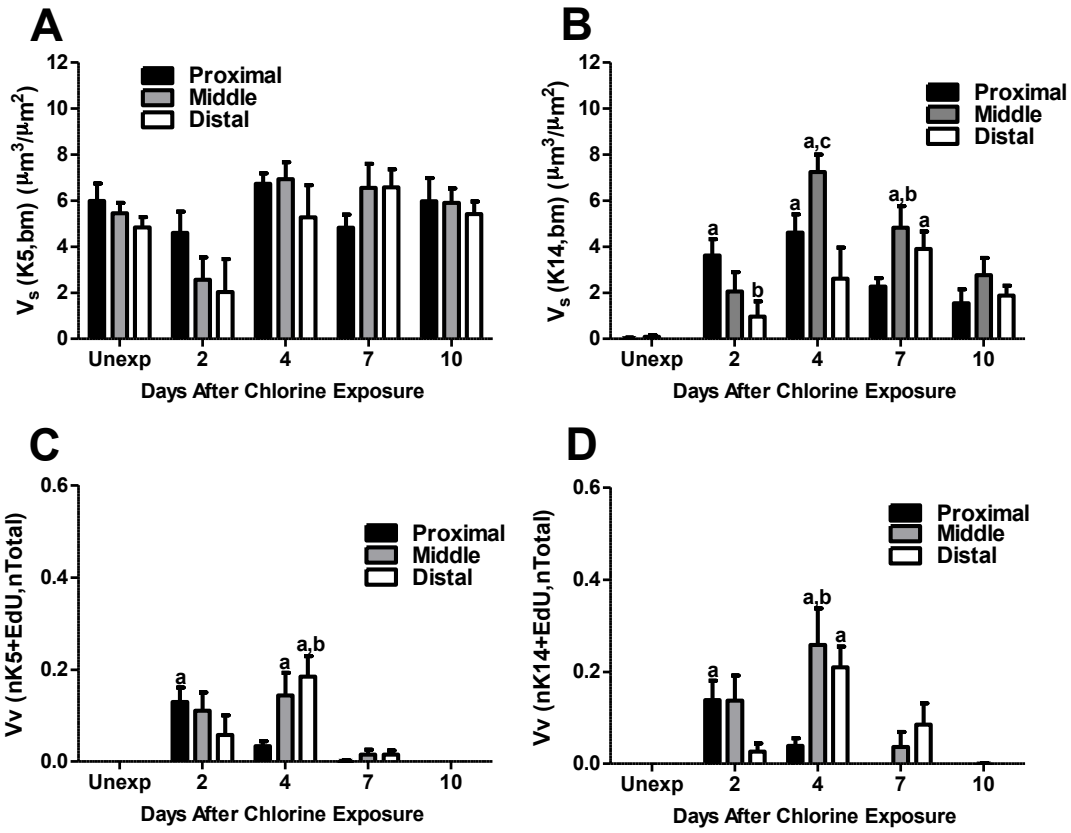

Figure 11. Morphometric analysis of basal cell markers K5 and K14 in tracheal epithelium after chlorine injury. Tracheal sections stained for EdU in conjunction with either K5 or K14 were evaluated as described in Materials and Methods. (A) Volume of K5-expressing cells relative to basement membrane surface area. (B) Volume of K14-expressing cells relative to basement membrane surface area. a, $p < 0.05$ vs. unexposed; b, $p < 0.05$ vs. proximal; c, $p < 0.05$ vs. distal. (C) Proliferation in K5 cells measured as volume density of EdU-labeled nuclei in K5-expressing cells relative to the total epithelial nuclear volume. a, $p < 0.05$ vs. unexposed; b, $p < 0.05$ vs. proximal. (D) Proliferation in K14 cells measured as volume density of EdU-labeled nuclei in K14-expressing

cells to the total epithelial nuclear volume. a, $p < 0.05$ vs. unexposed; b, $p < 0.05$ vs. proximal.

EdU detection in conjunction with immunofluorescence for either Clara cell (CCSP, Fig 12) or ciliated cell (AcTub, Fig 13) markers was performed and quantitated by morphometric analysis (Fig 14). CCSP expression was detected in unexposed mice (Fig 12A), and was more abundant in the distal trachea compared with the proximal and middle trachea (Fig 14A). Chlorine exposure led to the loss of virtually all CCSP-expressing cells from the trachea (Fig 12B and 14A). During stages when proliferation was high (days 2-4), minimal if any CCSP-expressing cells were detected (Fig 12C and 14A). Expression of CCSP was observed at later times during repair at days 7 and 10 (Fig 12D, 12E, and 14A), but CCSP expression was not observed in any areas of the epithelium where there were proliferating cells. Expression of the ciliated cell marker AcTub appeared to be evenly distributed throughout the trachea in unexposed mice (Fig 13A and 14B). Chlorine exposure resulted in the loss of ciliated cells from the tracheal epithelium, and virtually no ciliated cells were observed on days 2 and 4 after chlorine exposure (Fig 13B, 13C, and 14B). Ciliated cells were observed at later times during repair (days 7 and 10) but no proliferating cells were seen in areas of the trachea where ciliated cells had differentiated (Fig 13D and 13E). On day 10, the volume of AcTub staining was increased in the proximal and distal trachea of chlorine-exposed mice compared with unexposed (Fig 14B).

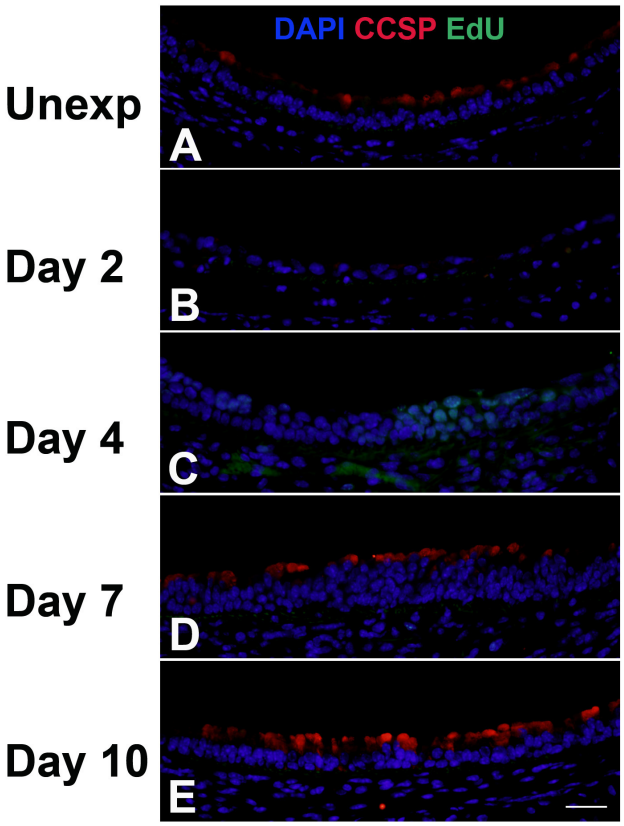

Figure 12. Cell proliferation and expression of Clara cell marker CCSP in middle trachea after chlorine injury. Mice were exposed to chlorine and injected with EdU 17 hr prior to euthanasia and collection of tracheas 2, 4, 7, and 10 days after exposure. Tracheal sections were stained for EdU (green) and CCSP (red), and nuclei were labeled with DAPI (blue). Scale bar in Panel E represents 40 μm for all panels.

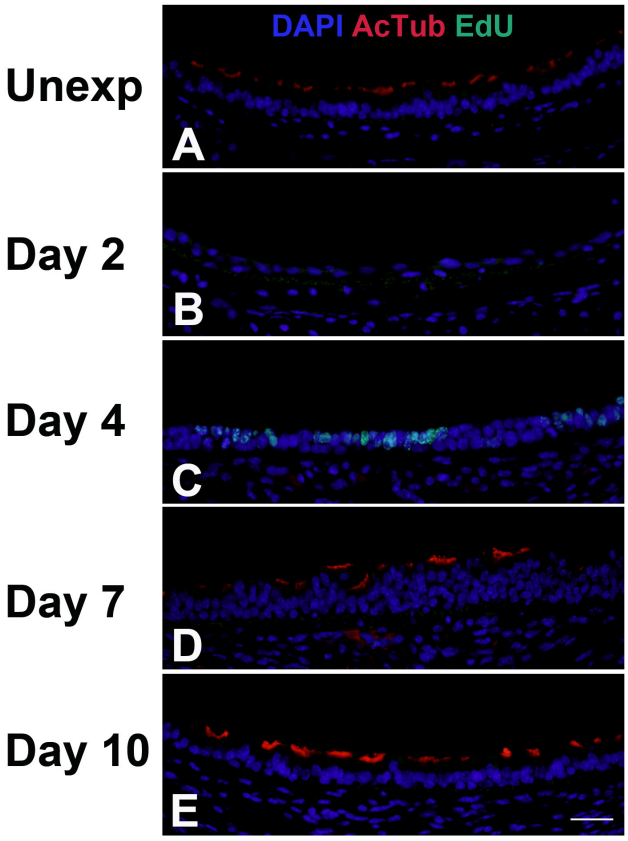

Figure 13. Cell proliferation and expression of ciliated cell marker AcTub in middle trachea after chlorine injury. Mice were exposed to chlorine and injected with EdU 17 hr prior to euthanasia and collection of tracheas 2, 4, 7, and 10 days after exposure. Tracheal sections were stained for EdU (green) and AcTub (red), and nuclei were labeled with DAPI (blue). Scale bar in Panel E represents 40 μm for all panels.

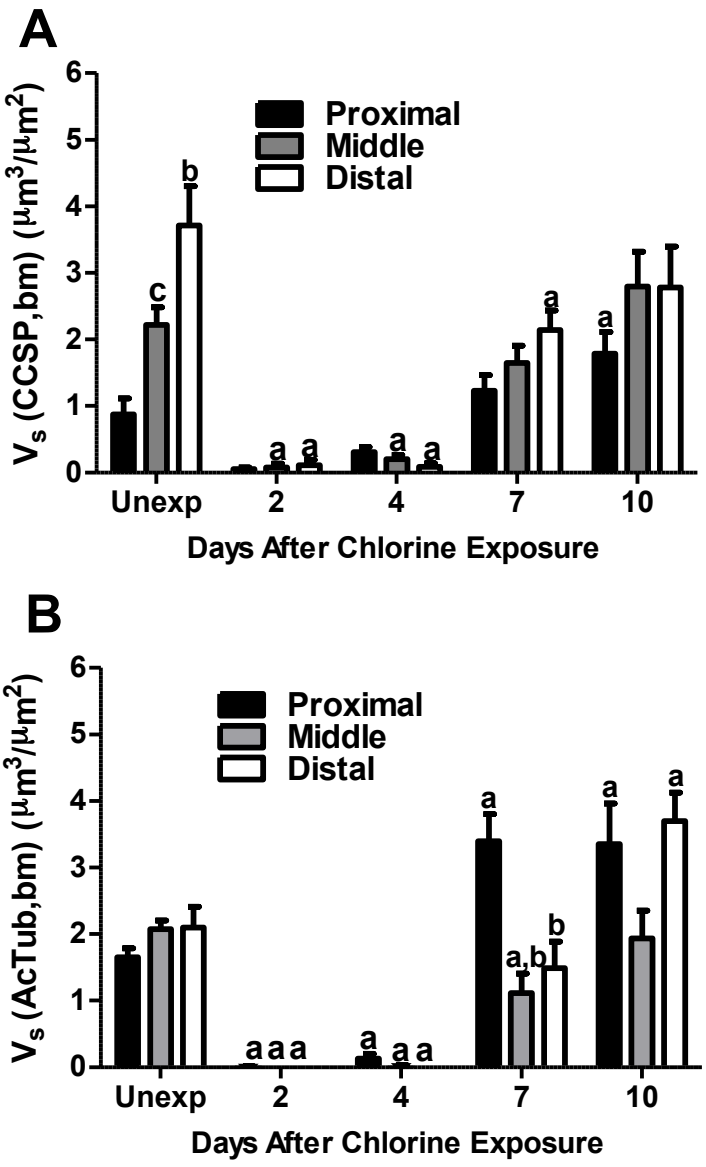

Figure 14. Morphometric analysis of Clara cell and ciliated cell markers in tracheal epithelium after chlorine injury. Tracheal sections stained for EdU in conjunction with either CCSP or AcTub were evaluated as described in Materials and Methods. (A) Volume of CCSP staining relative to basement membrane surface area. a, $p < 0.05$ vs. unexposed; b, $p < 0.05$ vs. proximal; c, $p < 0.05$ vs.

distal. (B) Volume of AcTub staining relative to basement membrane surface area. a, $p < 0.05$ vs. unexposed; b, $p < 0.05$ vs. proximal.

Discussion

The results define the nature and time course of epithelial repair following chlorine injury of the trachea. Exposure of mice to chlorine led to the loss of most of the tracheal epithelium, including virtually all Clara and ciliated cells. During steady state, minimal cell proliferation was detected; however after chlorine injury, an upsurge in cell proliferation was observed. The proximal trachea had an earlier initiation of repair and faster restoration of pseudostratified epithelium than did the distal trachea. During repair, numerous proliferating K5- and K14-expressing basal cells were detected. In contrast, Clara and ciliated cells were absent during the proliferative stage of repair, and markers for these differentiated cell types were only observed at later time points. Fibroproliferative lesions developed in areas where epithelial repair was inefficient.

The results presented here provide evidence that basal cells function as progenitor cells in the initiation of repair in the tracheal epithelium after chlorine injury. With the loss of most epithelial cells after chlorine injury, basal cells were the only surviving cells initially observed in the tracheal lumen as a thin layer of squamous epithelium that served to repopulate the trachea. The abundant and widespread distribution of basal cells across the tracheal epithelium during the repair process is more consistent with basal cells functioning as progenitor cells rather than as a rare population of stem cells. Prior studies have demonstrated that basal cells of the tracheobronchial epithelium constitute a multipotent progenitor cell population capable of self-renewal and of differentiation into Clara and ciliated cells after injury [49-53]. Our results are consistent with basal cells

being the major progenitor cell effecting repair after chlorine injury. Clara cells have also been identified as a cell population capable of self-renewal that can contribute to the restoration of injured airway epithelium [70, 71], including the trachea [77]. In the present study, however, few if any Clara cells were detected during the peak period of cell proliferation, and no EdU-labeled Clara cells were observed after chlorine lung injury. Following sulfur dioxide injury, basal cells are thought to be the major progenitor cells involved in repair, with Clara cells that survived the injury playing a minor role in repopulating the trachea with Clara and ciliated cells [50, 77]. We exposed mice to chlorine doses high enough to kill virtually all the Clara cells of the trachea, so the Clara cells observed starting 7 days after exposure appear to be derived from basal cells that survive chlorine exposure. As we did not detect proliferation in these regenerated Clara cells, they do not appear to play any major role as progenitor cells for tracheal repair following a high dose of chlorine.

Following chlorine injury we identified a dynamic pattern in the expression of cytokeratins that have been used as basal cell markers. During normal steady state, most basal cells express K5 but a smaller subset expresses K14 [49, 51, 53] as we observed in this study. The increase we observed in K14-expressing cells during repair is similar to findings reported after naphthalene injury [51-53]. In other tissues such as skin and cornea, K5 and K14 are typically co-expressed and represent binding partners in heterodimeric keratins [78]. The binding partner for K5 in normal mouse tracheal epithelium appears to be keratin 15 [49, 51]. The upregulation of K14 following injury and its association with the

proliferative stage suggests a specific function for this molecule in the repair of the tracheobronchial epithelium. We observed drastic changes in the size and shape of K5- and K14-expressing cells during the course of repair, progressing from thin cells covering the basement membrane to larger cells with enlarged nuclei in the pluristratified reparative epithelium and then returning to small pyramidal cells coincident with loss of K14 expression. As keratins are involved in controlling cell shape and motility, the transient expression of K14 may play a role in the dynamic changes in epithelial morphology that occur during the repair process.

Repair of the tracheal epithelium varied along the proximal-distal axis, with epithelial restoration occurring faster and more completely in the proximal trachea than in the distal trachea or mainstem bronchus. A possible explanation for these observations is that the proximal trachea possesses better intrinsic repair capacity as opposed to the middle and distal trachea or mainstem bronchus. An alternative possibility, which we consider more likely, is that chlorine inhalation results in less initial damage to the epithelium of the proximal trachea. This concept is supported by the observation that initial injury at day 2 after chlorine exposure appeared to be more severe in distal trachea as revealed by an increased percentage of denuded airway surface area. Submucosal glands, which are restricted to the proximal trachea in mice, have been suggested to serve as a protective niche for basal stem cells [45]. The abundance and widespread distribution of basal cell progenitors involved in the repair process that we observed do not support the migration of basal cells from

localized stem cell niches as a major contributor in the restoration of the tracheal epithelium. In distal trachea, we observed a trend toward decreased K5 staining suggestive of fewer basal cells (which could result in less efficient repair), but the difference was not statistically significant. It is possible that other differences in anatomy/architecture may result in differential protection of the proximal airway epithelium, leading to fewer denuded areas and more efficient repair. The trachea narrows considerably distal to the larynx, and the larger, irregularly shaped area of the upper trachea may provide areas of dead space that reduce contact of chlorine with the epithelium. Additionally, regional differences in the concentration of low molecular weight antioxidants in ELF have been demonstrated [79]. Differences in antioxidant concentrations may have resulted in less damage to the proximal trachea compared to the middle and distal portions.

Injury due to chlorine inhalation has been associated with oxidative damage leading to cell death [37]. Histological examination of airways after chlorine inhalation suggests that mechanisms other than apoptosis might be responsible for cell death [26]. Additionally, treatment of the human lung epithelial A549 cell line with chlorine killed cells by necrosis rather than apoptosis (G. Hoyle, unpublished observations). Also, treatment of human monocyte-derived macrophages with HOCl resulted in necrotic cell death [40]. These studies suggest that injury due to chlorine inhalation might result in cell death through necrosis rather than apoptosis.

In unexposed mice, minimal proliferation was detected, but after chlorine inhalation an upsurge in cell proliferation was observed. The molecular trigger that produces this dramatic increase in proliferation has not been identified. Loss of cell-to-cell and cell-to-extracellular matrix interactions may have served as a stimulus for proliferation [80]. Thus, stimulation of cell proliferation through manipulation of signaling activated by cell adhesion molecules or cytoskeletal constituents may serve as a potential therapeutic pathway for enhancing epithelial repair after injury. The initial regeneration of the pseudostratified epithelium in well-defined areas occurred within 7 days after chlorine exposure, but it was apparent that the epithelium at this point was not yet repaired to its original state. At 10 days after exposure, even within well repaired areas, significant differences between regenerated and unexposed epithelium could be observed, including increased expression of K14 in basal cells and increased ciliated cells. We did not determine whether these parameters returned to normal within well repaired areas at later times because of the death of a significant number of animals that occurred between days 7 and 14. Delayed lethality 7-14 days after exposure has been observed previously following inhalation of chlorine in mice [81]. In our experiments, lethality appeared to be associated with airway fibrosis and tracheal or bronchial stenosis in areas of inefficient epithelial repair. Chlorine exposure in dogs resulted in chronic effects of bronchiolitis obliterans, which appeared to be a similar process to what we observed in mice except that in dogs it occurred in smaller airways [82]. In mice, a pseudostratified epithelium with basal cells is restricted to the tracheobronchial

region, whereas in larger mammals, including humans, basal cells extend farther into the lung to the level of smaller bronchioles [45]. The more extensive distribution of basal cells in larger mammals may provide for better repair of epithelium in the proximal airways, allowing survival of animals following extensive desquamation of the tracheobronchial epithelium, as was observed in dogs [82].

Previous studies have examined the repair of airway epithelium after chlorine exposure in mice [26] and rats [31]. These studies focused on intrapulmonary airways in contrast to the processes occurring in the trachea that were investigated in the present study. The rodent tracheal epithelium has been proposed as a model of human airway epithelium, which contains a pseudostratified epithelium with abundant basal cells that extends to the smaller airways [45]. Exposure of A/J mice to 800 ppm chlorine for 5 min resulted in sloughing of epithelium from intrapulmonary airways, stimulation of cellular proliferation, and airway remodeling characterized by increased smooth muscle and collagen [26]. The time course of repair appeared similar to what was observed in the trachea, with a peak in cellular proliferation 5 days after exposure and restoration of a normal epithelium by 10 days. The cells types carrying out repair in the intrapulmonary airways were not investigated, but may possibly be basal cells in the larger airways and Clara cells in the bronchioles by analogy to other injury models (discussed below). Exposure of rats to 400 ppm chlorine for 30 min resulted in sloughing of epithelium from large intrapulmonary airways [31]. The epithelium was repaired by day 7 after exposure, but was abnormal in that it

was thickened and contained increased mucus-producing cells. The repaired tracheal epithelium also showed abnormalities, including altered distribution of ciliated cells and increased K14 staining. Thus a common result between these studies is that repair occurs rapidly, but, at least initially, does not restore the epithelium to its normal state. Further studies are required to assess whether any of these epithelial abnormalities resolve over longer time periods.

Our observations are consistent with a model in which surviving basal cells function as progenitor cells to repopulate the tracheal epithelium after chlorine injury. Repair of the airway epithelium has been previously studied using naphthalene [52, 55, 65, 77] and sulfur dioxide [45, 50, 77]. In the tracheal epithelium, naphthalene injury to Clara cells results in depletion of both Clara cells and ciliated cells, and repair is initiated by a hyperplasia of K5 and K14-labeled basal cells that serve as progenitors for Clara and ciliated cells [49]. In this case repair is efficient because, although Clara and ciliated cells are lost, the full complement of basal cells remains. In contrast, sulfur dioxide, like chlorine, has the potential to injure all epithelial cell types, and the dose of sulfur dioxide used in previous studies resulted in extensive sloughing of tracheal epithelial cells [50, 56]. Repair of the tracheal epithelium was found to be carried out primarily by basal cells but also by Clara cells that survived sulfur dioxide exposure [50, 77]. The dose of chlorine used in our studies appears to result in more severe injury, as large areas of the trachea were either denuded or lined with squamous epithelium, rather than a cuboidal monolayer as observed following sulfur dioxide inhalation [56, 77]. This suggests that significant

numbers of basal cells are lost following high-dose chlorine exposure and this limits or delays repair. Despite the differences in mechanism and extent of epithelial damage, the airway injury models reveal a general response to tracheal epithelial loss that involves the migration, proliferation, and differentiation of basal cells to restore the integrity of the epithelium. Understanding these concepts in the context of chlorine lung injury provides the potential opportunity to manipulate the repair process to accelerate normal epithelial healing following exposure to this chemical threat agent.

CHAPTER III: NGFR SIGNALING AND EPITHELIAL REPAIR FOLLOWING CHLORINE-INDUCED INJURY

Introduction

The p75 neurotrophin receptor (NGFR) is a member of the death receptor family to which NGF binds to with a nanomolar affinity [83, 84]. Neurotrophin binding to NGFR leads to either cell death through apoptosis by the mitogen activated protein kinase c-jun N-terminal kinase (MAPK JNK) signaling pathway, or cell survival through nuclear factor κB (NF-κB) signaling. The signaling pathway activated when NGF binds to NGFR is determined by the adaptor protein or co-receptors recruited to the receptor [57].

NGF was initially identified as a growth factor produced by non-neuronal cells that enhanced the growth, survival, and differentiation of neurons [85, 86]. It was later discovered that receptors for NGF, including NGFR, are also expressed by non-neuronal cell populations such mesenchymal and embryonic stem cells [60, 87]. NGFR expression in embryonic stem cells has been shown to stimulate proliferation with NGF treatment [60]. NGFR expression has also been identified in basal cell populations in epithelial cells of various tissues such as the esophagus, oral mucosa, and lung [50, 58, 59]. The role of NGFR in epithelial stem cell function, however, has yet to be examined. Additionally, NGF has been shown to contribute to repair of the lung epithelium by promoting the proliferation and self-renewal of Clara cells after naphthalene injury [55]. We

hypothesized that NGFR expression in basal stem cells regulates the survival and proliferation of airway basal stem cells following chlorine injury and that airway epithelial repair would be stimulated by NGF treatment.

Materials and Methods

Animals

Transgenic mice over-expressing NGF from the Clara cell secretory protein promoter (CCSP-NGF Tg) on a C57BL/6 background were developed in the PI's laboratory [88]. NGF overexpression in CCSP-NGF mice was previously measured in lung homogenates. Results indicated that NGF was overexpressed 28- 31-fold over the levels found in non-transgenic mice of similar genetic background [88].

NGFR knockout (NGFR KO) mice [89] on a C57BL/6 background were obtained from The Jackson Laboratory. C57BL/6 mice were used as wild-type controls. All mice were randomly assigned to either chlorine-exposed or unexposed groups. Mice were exposed to a target dose of 240 ppm-hr chlorine in a whole body exposure chamber [25]; deviation between target and actual doses averaged 3% for CCSP-NGF Tg mice, 3% for NGFR KO mice, and 5% for C57BL/6 mice for the NGF treatment experiment.

For CCSP-NGF Tg and NGFR KO mice time-course experiments, mice were injected intraperitoneally with 10 mg/kg of 5-ethynyl-2'-deoxyuridine (EdU) [73] from Life Technologies (Grand Island, NY) 17 hr prior to euthanasia at different times after exposure (days 2, 4, 7, or 10) to label proliferating cells. Mice were euthanized for collection of tracheal tissue by injection with tribromoethanol (375 mg/kg intraperitoneally) followed by exsanguination. Tracheal tissues were collected, fixed in 10% neutral buffered formalin overnight,

and divided into 3 equal pieces along the proximal-distal axis (designated proximal, middle, and distal) before embedding in paraffin.

Treatment of Mice with NGF

C57BL/6 mice were exposed to chlorine and treated with NGF (Alomone Lab, catalog # N-100) (dissolved in Dulbecco's PBS without calcium and magnesium) at a dose of 1 µg/mouse intranasally 1 hr after exposure and every day thereafter for 7 days. Mice in the vehicle group were treated with PBS. Mice were sacrificed either at day 4 or day 7 after chlorine exposure.

Treatment with TRPA1 Antagonist

C57BL/6 mice were treated with the TRPA1 antagonist HC-030031 (Sigma-Aldrich, catalog # H4415) in 0.5% methyl cellulose (at a dose of 100 mg/kg body weight) 4 hr before chlorine exposure. Lungs were lavaged 6 hr after exposure, and the recovered material was centrifuged at 1,000 x g to remove cells. The lavage fluid supernatant was stored at -80 ^{o}C until subsequent analysis of protein content.

Protein Assay

Protein content was determined in lavage fluid samples from NGFR KO and wild-type (WT) mice exposed to chlorine and lavaged after 6 hr, and also from C57BL/6 mice pre-treated with the TRPA1 antagonist HC-030031 before chlorine exposure and lavaged after 6 hr. Lavage fluid samples were thawed and spun for 2 min to pellet precipitated material, and the supernatant was recovered for assay. Lavage fluid was diluted with water, and each sample was

assayed in duplicate using BioRad Protein Assay (Bio-Rad Laboratories, Hercules, CA).

Isolation and Culture of Primary Airway Epithelial Cells

Epithelial cells were isolated from C57BL/6, CCSP-NGF Tg, and NGFR KO mice according to Rock et al. [50] with slight modifications. Mice were euthanized, and the chests were opened to collect tracheas. Tracheal tissue was placed into a petri dish with 6 ml DMEM media (GIBCO, catalog # 10567) and trimmed to remove excess connective tissue. Trachea was cut longitudinally into two pieces and placed in 2 ml of dispase (BD Biosciences, catalog # 354235) for ~15 to 20 min at room temperature with gentle shaking. Trachea was transferred to 2 ml of DMEM media supplemented with 5% fetal bovine serum (FBS) (Invitrogen, catalog # 10082) to inactivate dispase. Tracheal tissue was placed in PBS (GIBCO, catalog # 14190), and the epithelium was scraped off with a scalpel and placed in 2 ml of pre-warmed trypsin-EDTA (Invitrogen, catalog # 25200) containing 20 µl of 10 mg/ml DNase I (Sigma-Aldrich, catalog # DN-25) and incubated at 37 ^{o}C for 20 min. Cells were then strained through a 40 µm strainer and spun at 400 x g for 10 min. Pelleted cells were resuspended in 2 ml DMEM supplemented with 10% FBS and incubated at 37 ^{o}C for 2 hr. The cell suspension was centrifuged at 400 x g for 10 min, and the cell pellet was resuspended in MTEC/PLUS media (DMEM/F-12 + GlutaMAX supplemented with 3.6 mM sodium bicarbonate, 1.5 mM L-glutaMAX, 100 µg/ml penicillin/streptomycin, 0.01% insulin-transferase-selenium, 0.1 µg/ml cholera toxin, 25 ng/ml epidermal growth factor, 30 µg/ml bovine pituitary extract, 5%

FBS, and 0.01 μM vitamin A). Ten thousand cells per well were diluted in a 1:1 ratio with growth factor reduced Matrigel (BD Biosciences, catalog # 356230) for a total volume of 500 μl and seeded into 0.4 μm Transwell inserts. 1.5 ml of MTEC/PLUS media was added to the lower chamber of each Transwell insert, and media was changed every other day. On day 7, media was replaced with MTEC/SF media (DMEM/F-12 + GlutaMAX supplemented with 3.6 mM sodium bicarbonate, 1.5mM L-glutaMAX, 100 μg/ml penicillin/streptomycin, 0.01% insulin-transferase-selenium, 0.025 μg/ml cholera toxin, 5 ng/ml epidermal growth factor, 30 μg/ml bovine pituitary extract, 0.01 μM vitamin A, and 1 mg/ml bovine serum albumin) and changed every other day. For NGF treatment experiments, cells were treated with either 100 ng/ml or 1,000 ng/ml NGF (Alomone labs, catalog # N245) on the day cells were seeded and every other day with media change until day 7. For other experiments, cells were treated with 100 ng/ml brain derived neurotrophin factor (BDNF), 100 ng/ml neurotrophin 3 (NT-3), 1,000 ng/ml anti-NGF antibody, or 1,000 ng/ml IgG control. Tracheospheres were counted in each well on days 10 and 13 using a dissecting microscope. At the end of the culture period, tracheospheres were fixed in 10% neural buffered formalin (NBF), embedded in 3% agarose, processed, paraffin embedded, and sectioned onto slides. Immunofluorescence for K5, CCSP, and AcTub was performed on tracheosphere sections.

Isolation and Culture of Primary Lung Fibroblasts

Primary lung fibroblasts were isolated from NGFR KO and WT mice as described by Tomic and colleagues [90]. Briefly, mice were euthanized and

lungs were excised. Primary lung fibroblasts were obtained by cutting lung into 1-mm pieces. Lung tissue pieces were washed in sterile PBS and incubated in a culture dish in DMEM with 4.5 g/L glucose (GIBCO, catalog # 10566) supplemented with 10% FBS (Invitrogen, catalog # 10082) and 1% antibiotic-antimycotic solution (GIBCO, catalog # 15240-096) in a humidified 5% CO_2 incubator at 37 ^{o}C. Media was changed every 3 days while allowing cells to migrate out of tissue pieces. When the cells reached 80 to 90% confluency, they were treated with 2.5% trypsin (Corning, catalog # 25-051-CI), passaged into T-75 flasks, and designated as passage 1. Cells were passaged when they reached ~90% confluency and either passaged into T-75 flasks or plated into 96-well plates for experiments. Cells between passages 3 to 6 were used for experiments.

Characterization of Isolated Primary Lung Fibroblasts

Isolated primary lung fibroblasts were seeded into wells of chamber slides for 48 hr, after which cells were fixed in 100% ethanol for 10 min and rinsed with PBS three times for 5 min each time. Slides were kept at 4 ^{o}C until immunofluorescence was performed. Immunofluorescence was performed using antibodies against the mesenchymal marker vimentin (Sigma, catalog # V2258) at a dilution of 1: 100, alpha smooth muscle actin (α-SMA) (Sigma, catalog # A5228) at a dilution of 1:5,000, and pan-cytokeratin (Sigma, catalog # P2871) at a dilution of 1:100 as described in Histology, EdU Detection, and Immunofluorescence under Material and Methods in Chapter II. The following secondary antibodies (Life Technologies, Grand Island, NY) were used at a

dilution of 1:500: Alexa Fluor 594 donkey anti-mouse IgG for vimentin and pan-cytokeratin, and Alexa Fluor 488 donkey anti-mouse IgG for α-SMA.

Cell Proliferation Assay

Cell proliferation was determined for primary lung fibroblasts isolated from NGFR KO and WT mice using BrdU Cell Proliferation Assay Kit (Cell Signaling Technology, catalog # 6813) according to the manufacturer's protocol with slight modifications. Briefly, 3,300 cells/well were plated for each genotype in DMEM with 4.5 g/L glucose supplemented with 10% FBS for 24 hr. After this time, cells were serum starved in Opti-MEM media (GIBCO, catalog # 31985) supplemented with 1% penicillin/streptomycin (Invitrogen, catalog # 15140) for 48 hr. To determine the viability of cells between genotypes after serum starvation, MTT assay (Roche Diagnostics, catalog # 11465007001) was performed. Cell proliferation was determined by incubating cells with 10 μM BrdU in DMEM with 4.5 g/L glucose for 24 hrs. For NGF treatment experiments, cells were treated with either 100 ng/ml or 1,000 ng/ml NGF (Alomone Labs, catalog # N-100) for 24 hr followed by BrdU incubation. Incorporated BrdU was detected thereafter according to the manufacturer's protocol.

mRNA Expression of NGF and Collagen in Isolated Lung Fibroblasts

Isolated lung fibroblasts from NGFR KO and WT mice were plated in 96 well plates for approximately 24 hr. cDNA was extracted from cells using the TaqMan Gene Expression Cells-to-CT kit (Ambion, catalog #AM1728) according to the manufacturer's protocol. Quantitative PCR was performed with cDNA samples

using the TaqMan Gene Expression Assay (Foster City, CA) with NGF (Ngfb) and collagen type I, α1 (Col1a1) probe/primer pairs and ß-2 microglobulin (B2m) as control.

Morphometry

See Morphometry in Materials and Methods under Chapter II.

Statistical Analysis

Data are presented as group means ± standard error of the mean (SEM). Statistical analysis was performed using Prism 4.0a (GraphPad; La Jolla, CA). For in vitro tracheosphere experiments with CCSP-NGF Tg and NGFR KO mice, differences between WT and genetically manipulated mice were analyzed by t test. For in vitro tracheosphere experiments with NGF, BDNF, NT-3, and anti-NGF antibody treatment, group means were analyzed using one-way analysis of variance (ANOVA) with Dunnett's multiple comparison test. For MTT assay and cell proliferation experiments for primary lung fibroblasts, data was analyzed by t test. For fibroblast cell proliferation experiments with NGF treatment, results were analyzed by one-way ANOVA followed by Bonferroni's multiple comparison test. Data for mRNA expression for Ngfb and Col1a1 from isolated fibroblasts was analyzed by t test. For in vivo epithelial repair experiments, effects of chlorine exposure among groups (e.g. proximal, middle, and distal trachea), and analysis of protein content from lavage fluid was analyzed by one-way ANOVA with Bonferroni's multiple comparison test. Survival curves in NGFR KO and WT

mice were analyzed by Wilcoxon-Gehan test. Differences were considered statistically significant at $p < 0.05$.

Results

Effect of Neurotrophins and NGFR on Growth and Differentiation of Tracheal Epithelial Stem Cells

To investigate the role of neurotrophins and NGFR in the survival and proliferation of tracheal epithelial stem cells, a three-dimensional cell culture system was used in which isolated tracheal epithelial cells form hollow, spherical structures with a differentiated polarized epithelium referred to as tracheospheres [50]. These structures have been shown to be clonal and derived from a subpopulation of NGFR-expressing basal cells [50], so the assay gives an indication of the number of tracheosphere-forming basal stem cells in the isolated cell population. A representative image of a Transwell insert with tracheospheres is shown in Fig 15A. Characterization of cellular differentiation in tracheospheres revealed the presence of basal cells with the basal cell marker K5, and luminal ciliated cells with the ciliated cell marker AcTub (Fig 15B). Staining for the Clara cell marker CCSP indicated that no Clara cells formed in any of the tracheospheres (not shown). Pharmacological and genetic manipulations were performed to determine whether neurotrophins or NGFR affected the formation of tracheospheres. Treatment of cultures with neurotrophin ligands for NGFR (NGF, BDNF, or NT-3) did not alter the number of tracheospheres that formed (Fig 16). Likewise, treatment with anti-NGFR antibody did not affect tracheosphere formation (Fig 16). NGF treatment did not alter the proportion or distribution of differentiated cell types (basal and ciliated cells) within tracheospheres (not shown). Transgenic mice in which NGF is

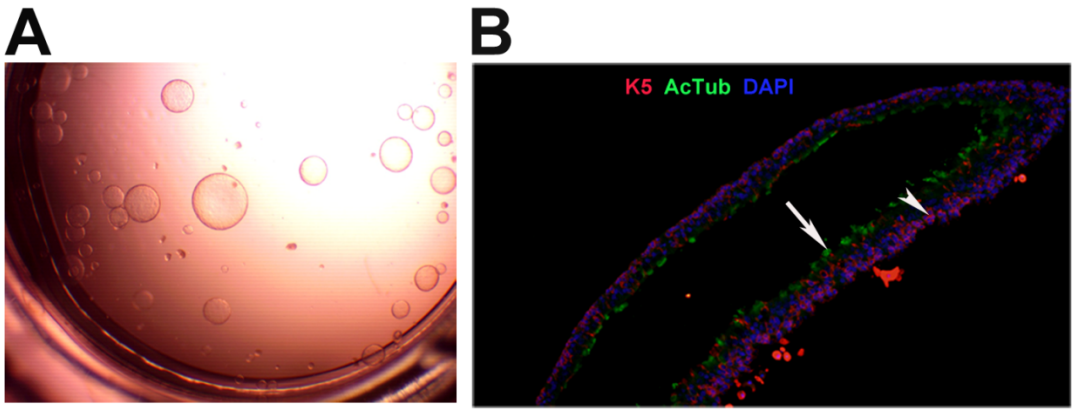

Figure 15. Representative tracheosphere images. Tracheal epithelial cells were isolated and cultured in 3D Matrigel Transwell inserts. (A) Representative image of tracheospheres in a Transwell insert in the 3D culture system. (B) Immunofluorescence image of a tracheosphere section stained for the basal cell marker K5 and ciliated cell marker AcTub. Arrow indicates a ciliated cell (green) and arrowhead indicates a basal cell (red).

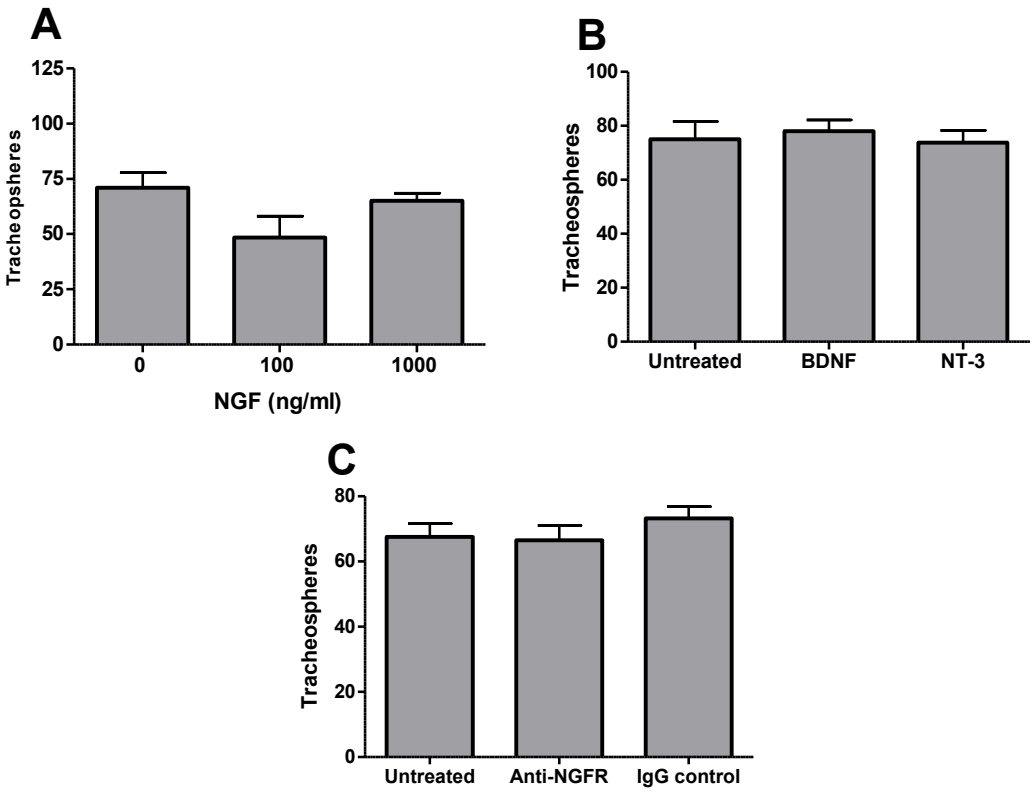

Figure 16. Effect of neurotrophin treatment on tracheosphere formation in isolated tracheal epithelial cells. Tracheal epithelial cells were isolated and cultured in 3D Matrigel Transwell inserts. Cells were treated with (A) NGF, (B) BDNF and NT-3, or (C) anti-NGF antibody (data provided by Jing Chen) on days 1, 3, and 5 during cell culture with media change every other day. Tracheospheres were counted on day 13.

overexpressed in the lung from the CCSP promoter (CCSP-NGF Tg; Hoyle et al., 1998) and knockout mice with mutated NGFR (NGFR KO; Lee et al., 1992) were used to examine the effect of altering NGFR and cognate ligand. Increased tracheosphere counts were observed following culture of cells from CCSP-NGF Tg and NGFR KO mice compared to their WT counterparts (Fig 17A and 17B respectively). There was no difference in the proportion and location of basal and ciliated cells in tracheospheres derived from CCSP-NGF Tg and NGFR KO mice compared to WT (not shown). These results indicated that activation of NGFR signaling with neurotrophin treatment did not alter the survival, proliferation, or differentiation of tracheal basal stem cells in vitro. However, genetic manipulation by over-expression of NGF or deletion of NGFR resulted in increased tracheosphere numbers without influencing differentiation in vitro.

Effect of NGF Treatment on Tracheal Epithelial Repair Following Chlorine Injury

To determine if exogenous NGF could stimulate tracheal epithelial repair, mice were exposed to chlorine and treated intranasally with NGF. Injury and re-epithelialization of the tracheal were assessed by morphometric analysis of histological sections. In this analysis, the presence of squamous epithelium is indicative of early repair, reparative epithelium represents a more advanced stage of repair, and areas with no epithelium indicate inefficient epithelial repair. In unexposed mice, no difference in the pseudostratified epithelium was observed between vehicle and NGF treatment in proximal, middle, or distal trachea (Fig 18A). Four days after chlorine exposure, the tracheal epithelium

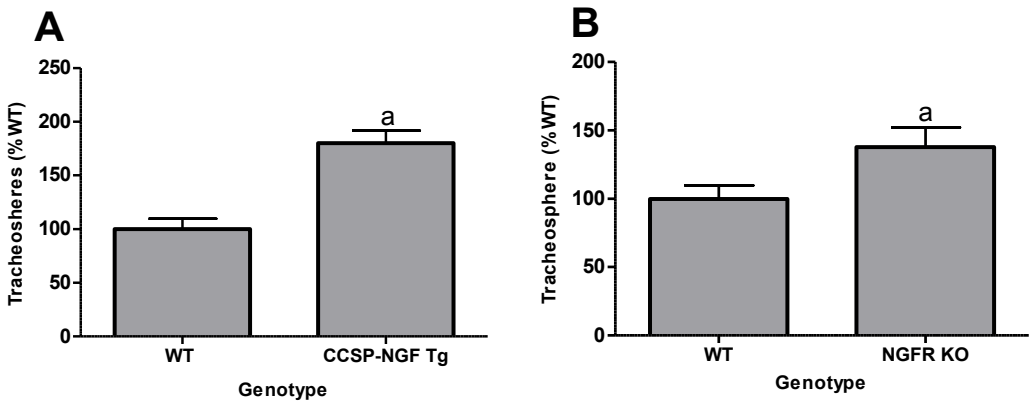

Figure 17. Effect of NGF over-expression or NGFR KO on tracheosphere formation. Tracheal epithelial cells were isolated from (A) CCSP-NGF Tg or (B) NGFR KO mice and cells were cultured in 3D Matrigel Transwell inserts. Media was changed every other day, and tracheospheres were counted on day 13. Graphs depict counts from pooled experiments. a, $p < 0.05$ vs WT.

was mostly composed of pseudostratified and reparative epithelium in vehicle and NGF treated mice (Fig 18A and C). An increase in the percentage of pseudostratified (i.e. repaired) epithelium was observed in NGF-treated mice compared to vehicle-treated mice in middle trachea at this time point (Fig 18A). By day 7, the percentage of pseudostratified epithelium had increased for vehicle- and NGF-treated mice but there was no longer a significant difference among any of these groups (Fig 18A).

Effect of Transgenic Overexpression of NGF on Epithelial Repair

To determine whether NGF overexpression stimulated repair of the tracheal epithelium in vivo, CCSP-NGF Tg and WT mice were exposed to chlorine at a dose of 240 ppm-hr, and tracheas were collected on days 2, 4, 7, 10, and 14 after exposure. In unexposed mice, a normal pseudostratified tracheal epithelium was observed in both WT and CCSP-NGF Tg mice (Fig 19A). Chlorine exposure resulted in extensive sloughing of tracheal epithelial cells in both WT and CCSP-NGF Tg mice (Fig 19D). Two days after chlorine exposure, a higher percentage of squamous epithelium was observed in the middle trachea of CCSP-NGF Tg mice compared to WT mice (Fig 19B). At this same time point, a lower percentage of denuded epithelium was observed in the middle trachea of CCSP-NGF Tg mice compared WT mice (Fig 19D). In CCSP-NGF Tg mice, fewer areas with denuded epithelium were also observed in the middle trachea at day 4, and in the distal trachea at day 14 (Fig 19D). This ultimately translated into a greater percentage of repaired, pseudostratified epithelium by day 7 in the middle trachea of CCSP-NGF Tg mice compared with WT mice (Fig 19A).

Sections were stained for EdU to detect proliferating cells, K5 and K14 for basal cells, CCSP for Clara cells, and AcTub for ciliated cells followed by morphometric analysis. In unexposed mice, minimal cell proliferation was observed. In chlorine-exposed mice, a peak in proliferation was observed on day 4 in both proximal and middle trachea with increased proliferation detected in CCSP-NGF Tg mice compared with their WT counterparts in middle trachea (Fig 20A and B). In the distal trachea, however, cell proliferation peaked on day 4 for CCSP-NGF Tg mice and on day 7 for WT mice (Fig 20C). No significant differences in the expression of the basal cell markers K5 and K14 were observed between CCSP-NGF Tg mice and WT mice in proximal, middle, or distal trachea (Fig 21 and Fig 22). Increased expression of these basal cell markers was, however, observed in both CCSP-NGF Tg and WT mice compared to unexposed mice on days 4 and 7 for proximal trachea (Fig 21A) and days 7 and 10 for middle trachea (Fig 21B). By day 14, expression of K5 was similar to that observed in unexposed mice (Fig 21A, B, and C) but expression of K14 remained elevated (Fig 22A, B, and C). Chlorine exposure resulted in decreased Clara and ciliated cells in CCSP-NGF Tg and WT mice which was concomitant with sloughing of epithelial cells due to chlorine injury (Fig 23A, B, C and Fig 24A, B, C respectively). Re-expression of these differentiated cell markers was observed at later time points (from day 7 onwards) (Fig 23A, B, C, and Fig 24A, B, and C).

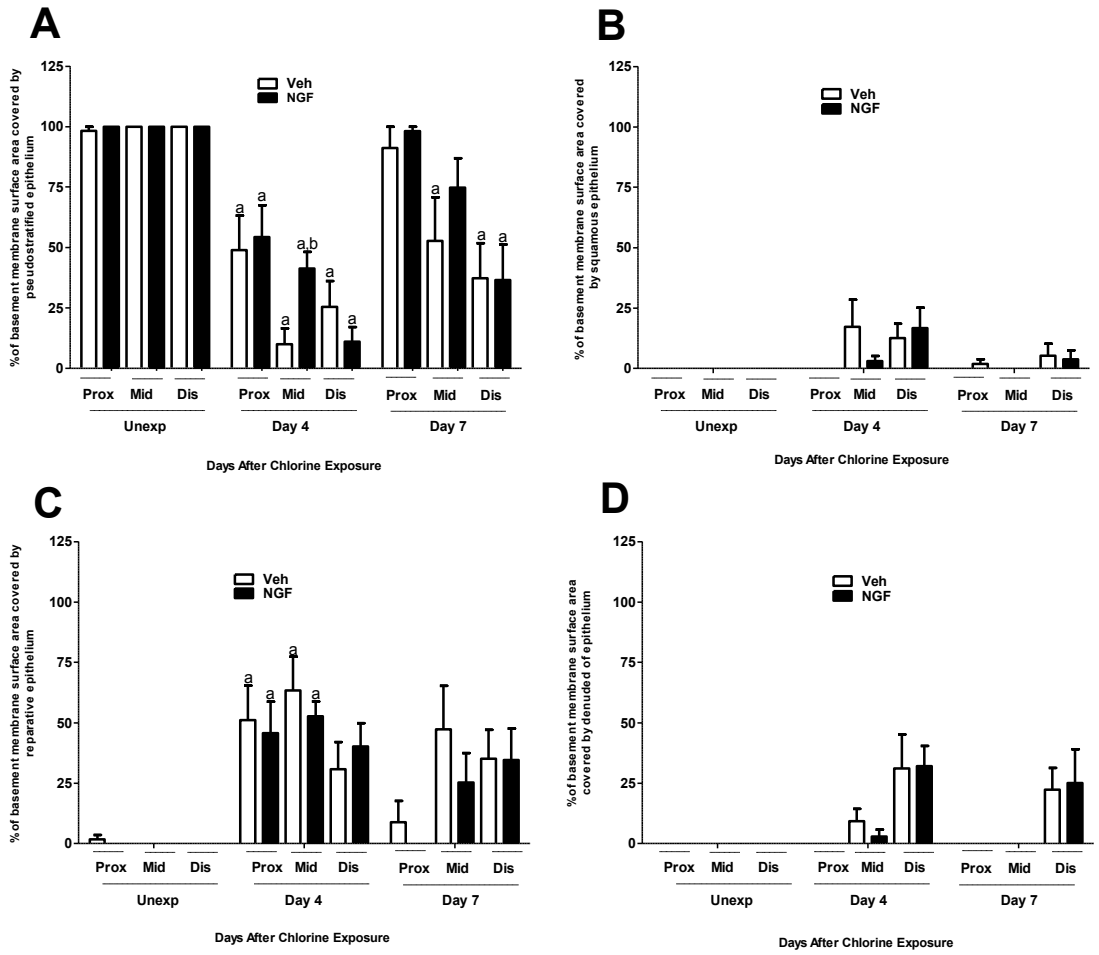

Figure 18. Morphometric analysis of tracheal epithelium in chlorine-exposed mice treated with NGF. Mice were exposed to chlorine and treated with NGF at a dose of 1 µg/mouse or PBS for 4 or 7 days after exposure. Tracheas were collected, processed, paraffin embedded, and sectioned onto slides. Tracheal epithelium was evaluated in H&E-stained sections as described in Materials and Methods. The graphs depict the percentage of basement membrane surface area covered by normal (A), squamous (B), reparative (C), or no epithelium (D) in proximal, middle, and distal trachea. a, $p < 0.05$ vs Unexp; b, $p < 0.05$ vs Veh.

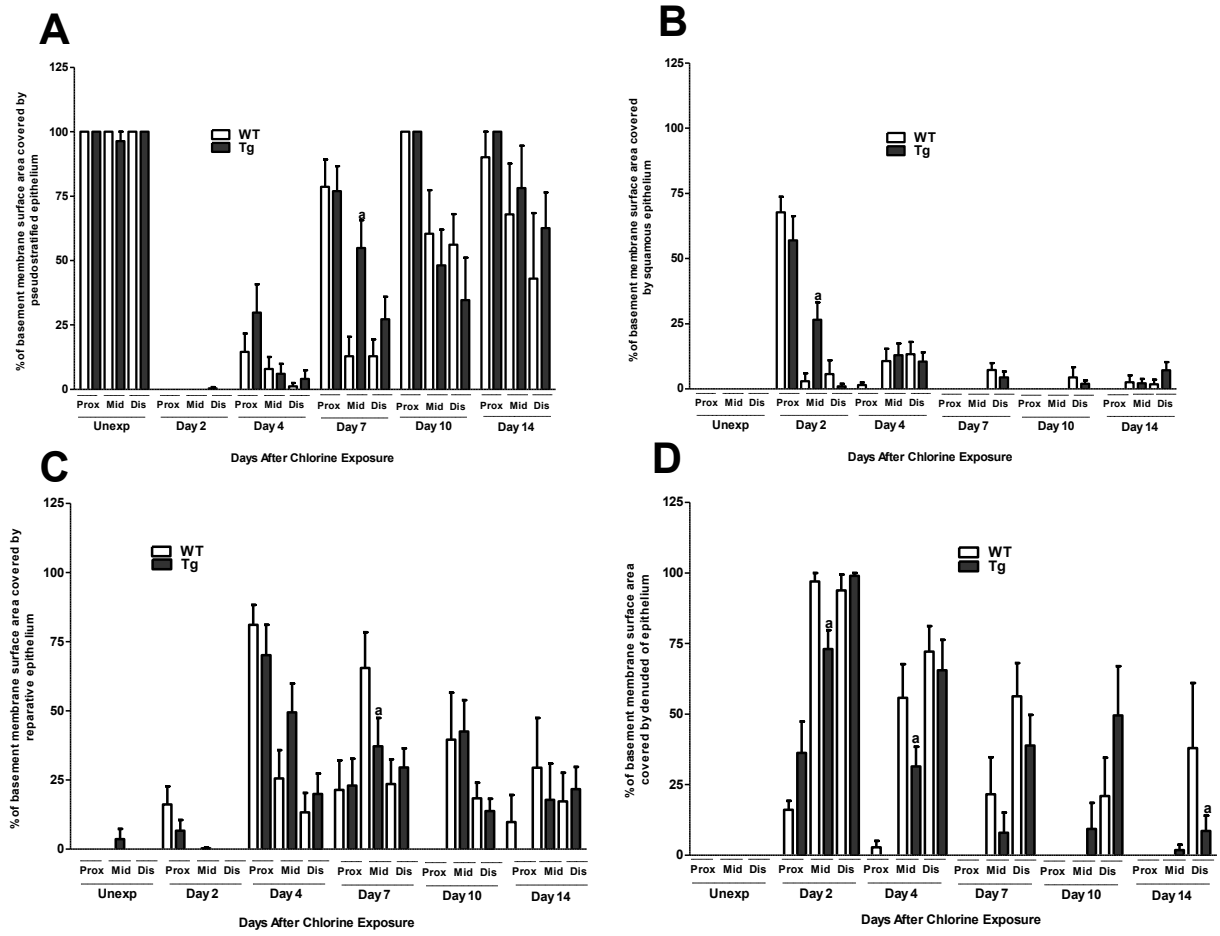

Figure 19. Morphometric analysis of tracheal epithelium in chlorine-exposed CCSP-NGF Tg mice. Mice were exposed to chlorine and tracheas were collected 2, 4, 7, 10, and 14 days after exposure, processed, paraffin embedded, and sectioned onto slides. Tracheal epithelium was evaluated in H&E-stained sections as described in Materials and Methods. The graphs depict the percentage of basement membrane surface area covered by pseudostratified (A), squamous (B), reparative (C), or no (D) epithelium in proximal, middle, and distal trachea. a, $p < 0.05$ vs WT.

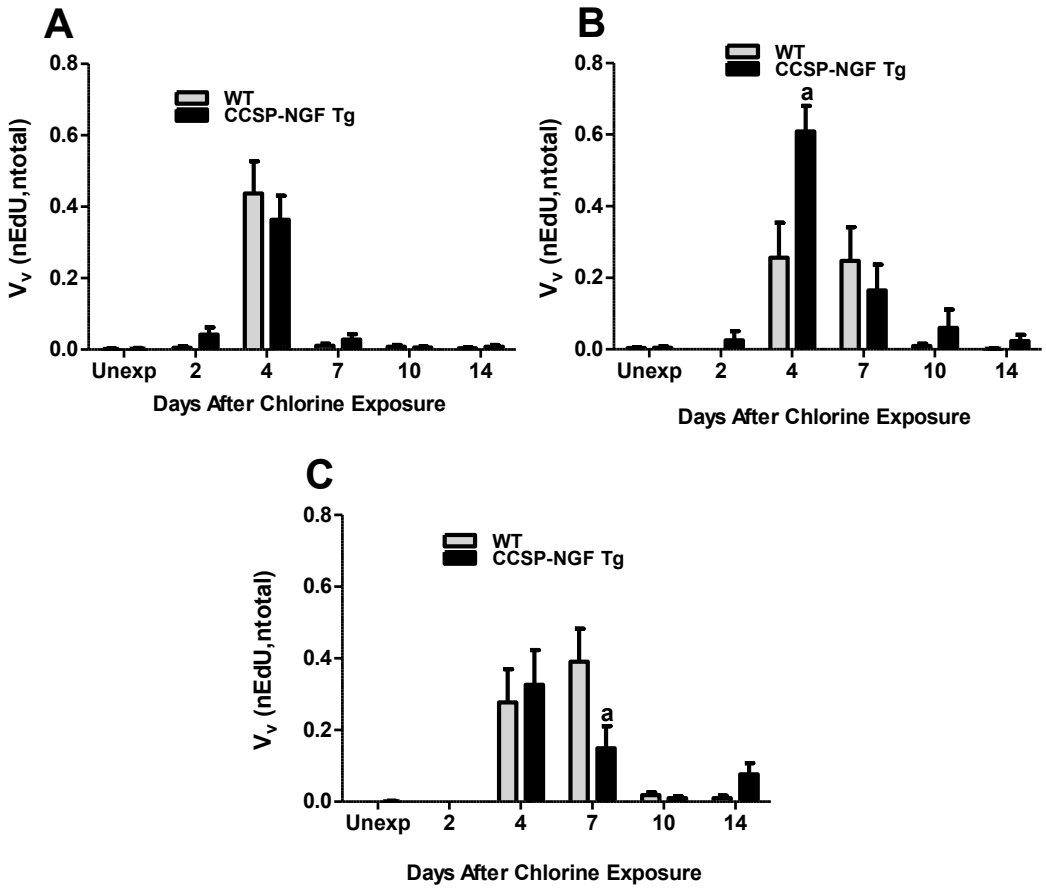

Figure 20. Cell proliferation in tracheal epithelium of CCSP-NGF Tg mice after chlorine injury. CCSP-NGF Tg and WT mice were exposed to chlorine and treated with EdU 17 hr prior to euthanization and collection of tracheas. Tracheas were collected 2, 4, 7, 10, or 14 days after chlorine exposure, processed, paraffin embedded, and sectioned onto slides for immunohistochemistry. Cell proliferation was assessed in EdU-stained tracheal sections as described in Materials and Methods. The graphs depict the volume density (Vv) of EdU-labeled nuclei (nEdU) relative to total nuclei in tracheal epithelium (nTotal) in (A) Proximal, (B) Middle, and (C) Distal trachea. a, $p<0.05$ vs WT.

Overall, staining for Clara cells (Fig 23A, B, and C) or ciliated cells (Fig 24A, B, and C) was not generally different between CCSP-NGF Tg and WT mice. However, on day 7, increased ciliated cells were observed in middle trachea in CCSP-NGF Tg compared to WT mice (Fig 24B), and trends toward increased ciliated cells in distal trachea (Fig 24C) and increased Clara cells in middle and distal trachea (Fig 23B and C) were observed.

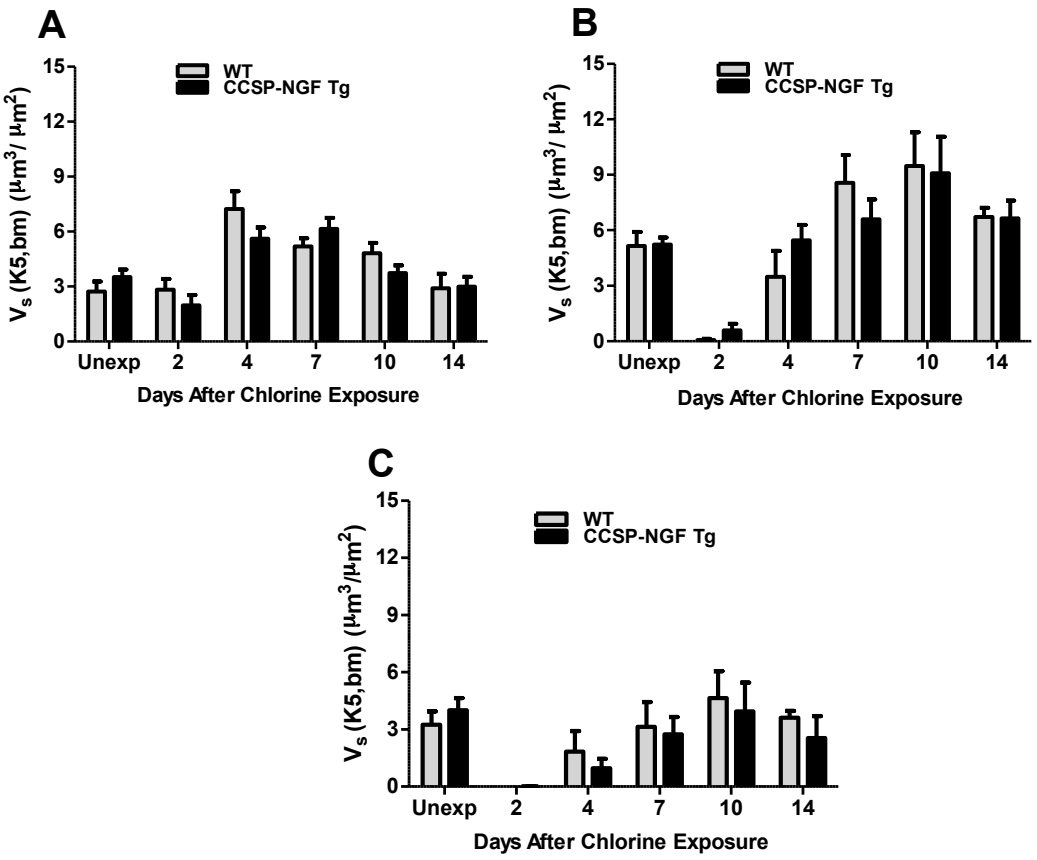

Figure 21. K5 expression in tracheal epithelium of CCSP-NGF Tg mice after chlorine injury. CCSP-NGF Tg and WT mice were exposed to chlorine, and tracheas were collected 2, 4, 7, 10, or 14 days after chlorine exposure. Tracheal tissue was processed, paraffin embedded, and sectioned onto slides for immunohistochemistry. Tissue sections were stained for K5 and were evaluated as described in Materials and Methods. Graphs depict volume of K5-expressing cells relative to basement membrane surface area in (A) Proximal, (B) Middle, and (C) Distal trachea. No significant differences between CCSP-NGF Tg and WT mice were observed.

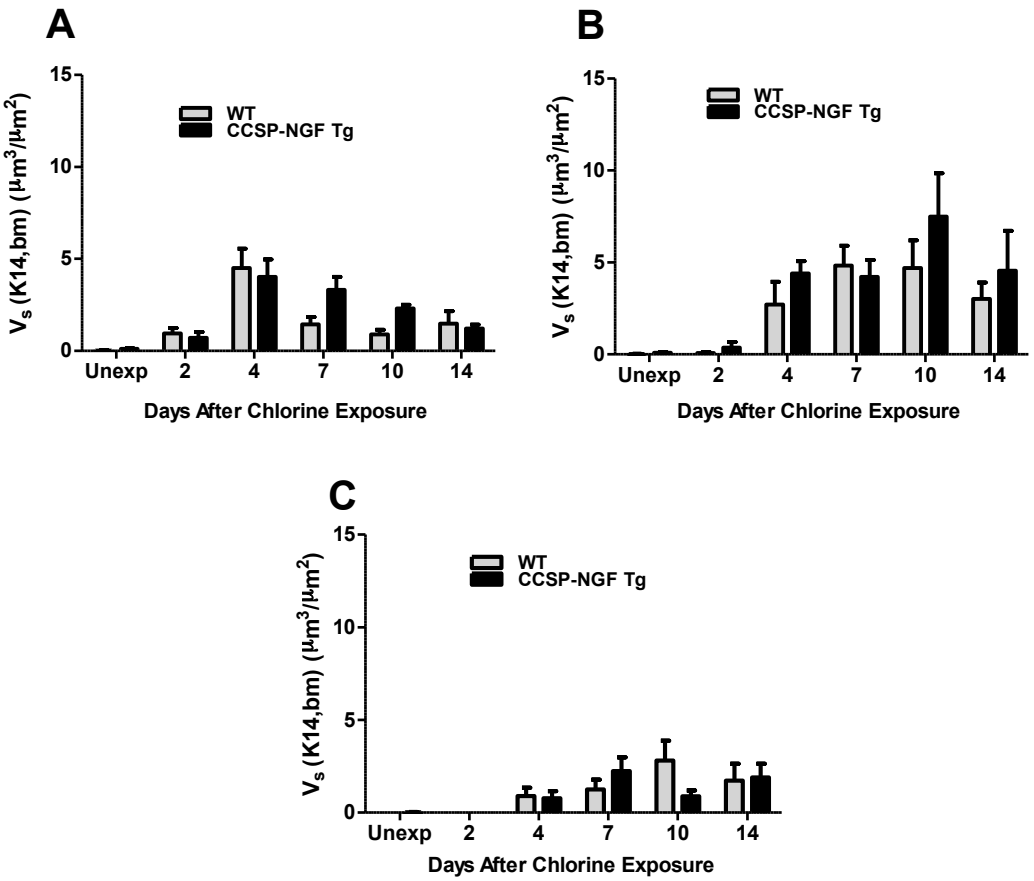

Figure 22. K14 expression in tracheal epithelium of CCSP-NGF Tg mice after chlorine injury. CCSP-NGF Tg and WT mice were exposed to chlorine and sacrificed for collection of trachea 2, 4, 7, 10, or 14 days after chlorine exposure. Tracheal tissue was processed, paraffin embedded, and sectioned onto slides for immunohistochemistry. Tissue sections were stained for K14 and evaluated as described in Materials and Methods. Graphs depict volume of K14-expressing cells relative to basement membrane surface area in (A) Proximal, (B) Middle, and (C) Distal trachea. No significant differences between CCSP-NGF Tg and WT mice were observed.

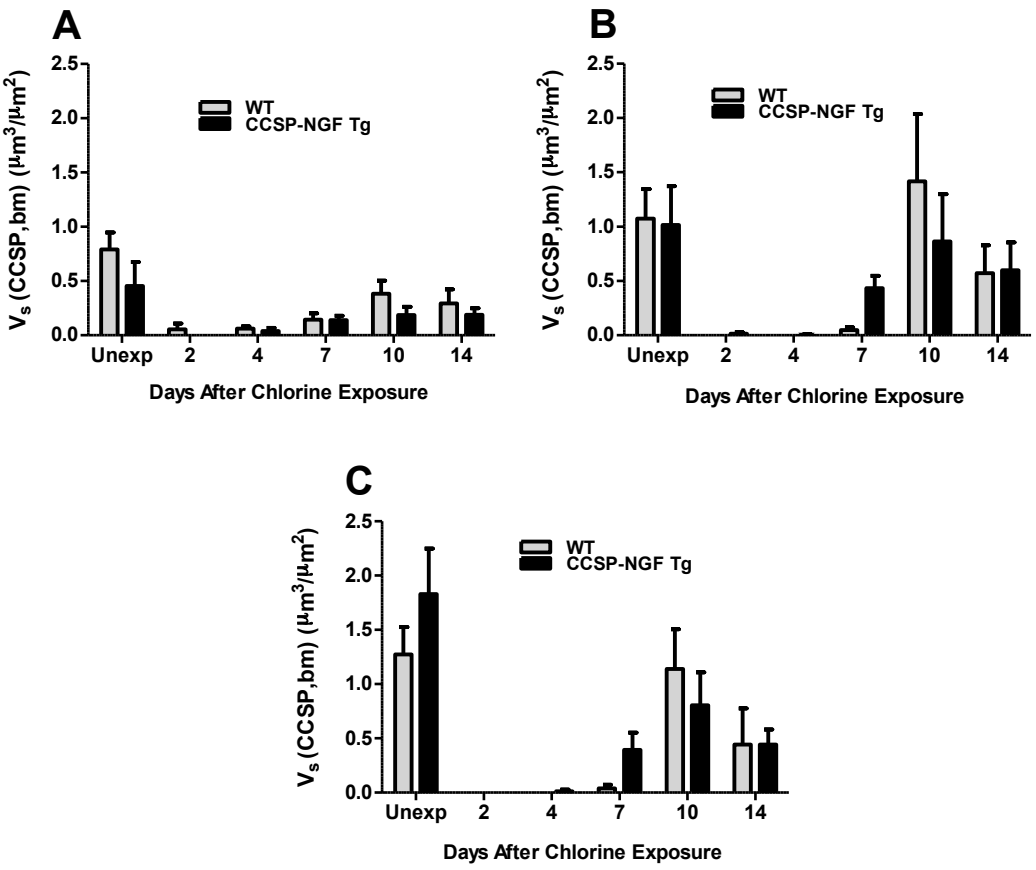

Figure 23. Expression of Clara cell marker CCSP in tracheal epithelium of CCSP-NGF Tg mice after chlorine injury. CCSP-NGF Tg and WT mice were exposed to chlorine and euthanized for collection of tracheas 2, 4, 7, 10, or 14 days after chlorine exposure. Tracheal tissue was processed, paraffin embedded, and sectioned onto slides for immunohistochemistry. Tissue sections were stained for CCSP and evaluated as described in Materials and Methods. Graphs depict volume of CCSP staining relative to basement membrane surface area in (A) Proximal, (B) Middle, and (C) Distal trachea. No significant differences between CCSP-NGF Tg and WT mice were observed.

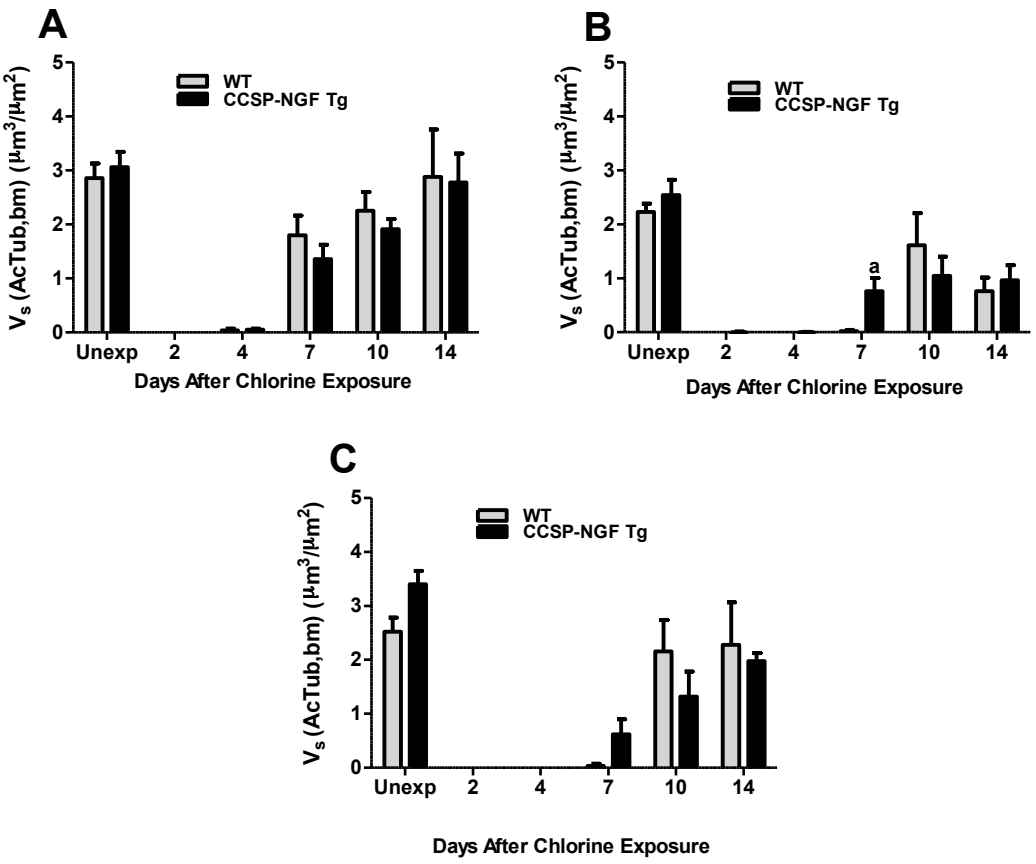

Figure 24. Expression of ciliated cell marker acetylated tubulin in tracheal epithelium of CCSP-NGF Tg mice after chlorine injury. CCSP-NGF Tg and WT mice were exposed to chlorine and euthanized for collection of tracheas 2, 4, 7, 10, or 14 days after chlorine exposure. Tracheal tissue was processed, paraffin embedded, and sectioned onto slides for immunohistochemistry. Tracheal sections were stained for AcTub and evaluated as described in Materials and Methods. Graphs depict volume of AcTub staining relative to basement membrane surface area in (A) Proximal, (B) Middle, and (C) Distal trachea. a, $p<0.05$ vs WT.

Effect of NGFR Knock-out on Epithelial Repair

To determine whether inhibition of NGFR signaling hampered tracheal epithelial repair, NGFR KO mice and their WT counterparts were exposed to chlorine, and tracheas were collected on days 2, 4, and 7 after exposure. In unexposed mice, a normal pseudostratified tracheal epithelium was observed in both WT and NGFR KO mice, indicating that loss of NGFR function did not result in gross abnormalities in the development of the tracheal epithelium (Fig 25A and B, Fig 26A). Chlorine exposure resulted in extensive sloughing of tracheal epithelial cells in both WT and NGFR KO mice (Fig 25C and D, Fig 26D). Two days after chlorine exposure, a higher percentage of squamous epithelium was observed in the proximal trachea of WT mice compared to the proximal trachea of NGFR KO mice (Fig 25C and D, Fig 26B). This observation, coupled with the increase in denuded area in the proximal trachea of NGFR KO mice (Fig 26D) indicates a delayed repair in NGFR KO mice. Initiation of epithelial repair was observed earlier in WT mice compared with NGFR KO mice by day 4 (Fig 25E and F, Fig 26A). At this time, NGFR KO mice had greater areas of denuded trachea compared with WT mice (Fig 26D). Large areas of reparative epithelium were observed at days 4 and 7 in both NGFR KO and WT mice at sites where repair was efficient (Fig 25G and H, Fig 26C). In distal trachea, the development of fibrotic lesions was observed to a greater extent in WT compared with NGFR KO mice 7 days after chlorine exposure in areas where repair was inefficient (Fig 26C and D).

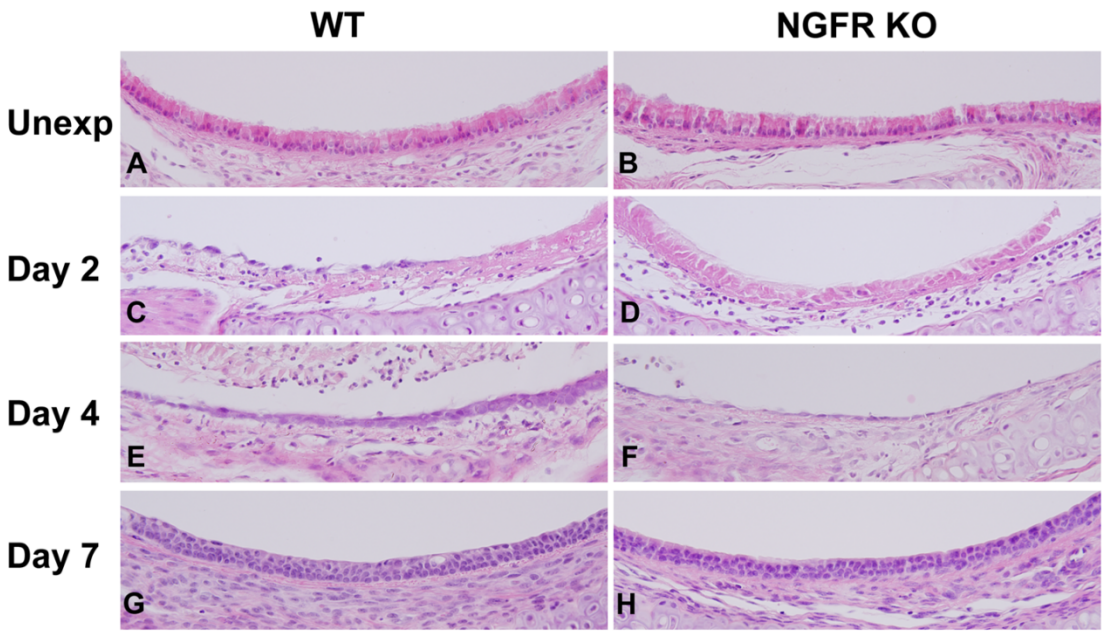

Figure 25. Histology of middle trachea from NGFR KO and WT mice after chlorine exposure. Mice were exposed to chlorine and sacrificed for collection of tracheas 2, 4, and 7 days after exposure. Tracheal sections were examined by H & E.

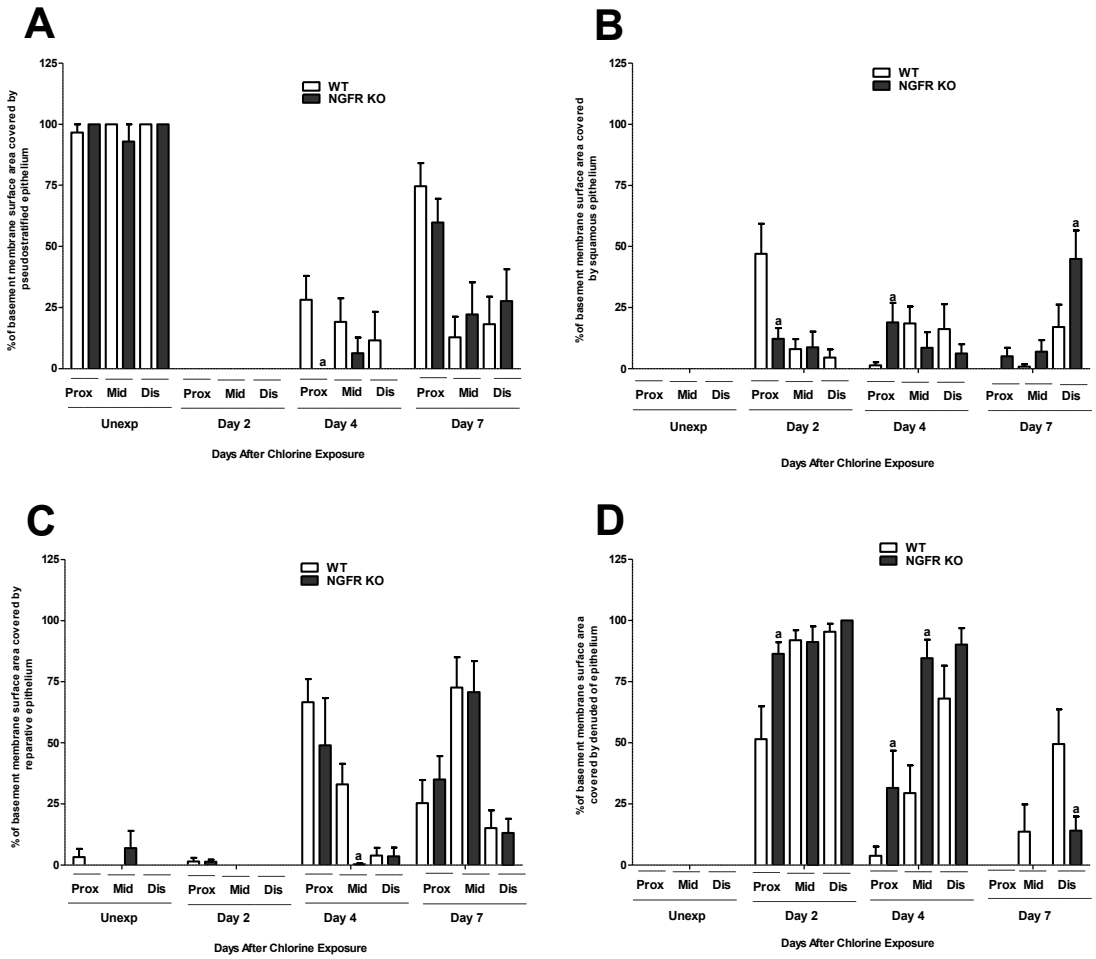

Figure 26. Morphometric analysis of tracheal epithelium in chlorine-exposed NGFR KO mice. Mice were exposed to chlorine and tracheas were collected 2, 4, and 7 days after exposure, processed, paraffin embedded, and sectioned onto slides. Tracheal epithelium was evaluated in H&E-stained sections as described in Materials and Methods. The graphs depict the percentage of basement membrane surface area covered by pseudostratified (A), squamous (B), reparative (C), or no (D) epithelium in proximal, middle, and distal trachea. a, $p < 0.05$ vs WT.

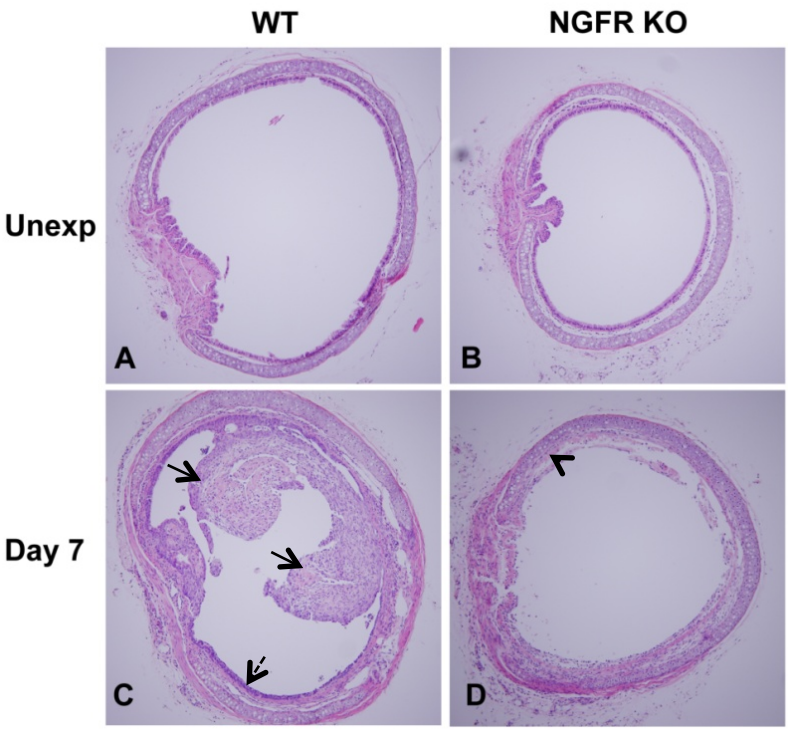

Figure 27. Histology of distal trachea from NGFR KO and WT mice after chlorine exposure. NGFR KO and WT mice were exposed to chlorine, and distal tracheas were examined after 7 days by H & E. Arrows with solid lines indicate fibrotic lesions. Arrow with dashed line indicates area with efficient epithelial repair. Arrowhead indicates denuded epithelium.

To determine the effect of NGFR knockout on cell proliferation during tracheal epithelial repair, proliferative marker EdU was detected in tracheal tissues by histochemistry and the results were analyzed by morphometry (Fig 28 and Fig 29). Minimal cell proliferation was detected in unexposed mice (Fig 28A and B, Fig 29A, B, and C). A peak in cell proliferation was, however, observed 4 days after chlorine exposure with a significantly greater increase in NGFR KO compared with WT mice in proximal trachea (Fig 29A). In middle trachea, decreased proliferation was observed in NGFR KO mice compared with WT mice (Fig 28E and F, 29B). At day 7, cell proliferation was still detected in some areas of the middle and distal trachea (Fig 28G and H, Fig 29B and C), and this increase was significantly greater in NGFR KO mice compared with WT in distal trachea (Fig 29C).

To investigate the contribution of basal cells to epithelial repair in NGFR knockout mice, immunohistochemistry for the basal cell marker K5 was performed. In unexposed mice, no significant difference in K5 expression was observed between NGFR KO and WT mice (Fig 30A and B, Fig 31). By day 4 after chlorine exposure, K5 expression recovered in proximal trachea for both NGFR KO and WT to at least normal levels (Fig 31B). During the peak in cell proliferation in middle trachea at this time point, a statistically significant decrease in K5 expression was observed in NGFR KO mice compared to WT mice (Fig 30E and F, Fig 31B). This observation indicates a reduced volume of basal cells in the epithelium and is consistent with the delayed repair observed in the epithelial scoring analysis.

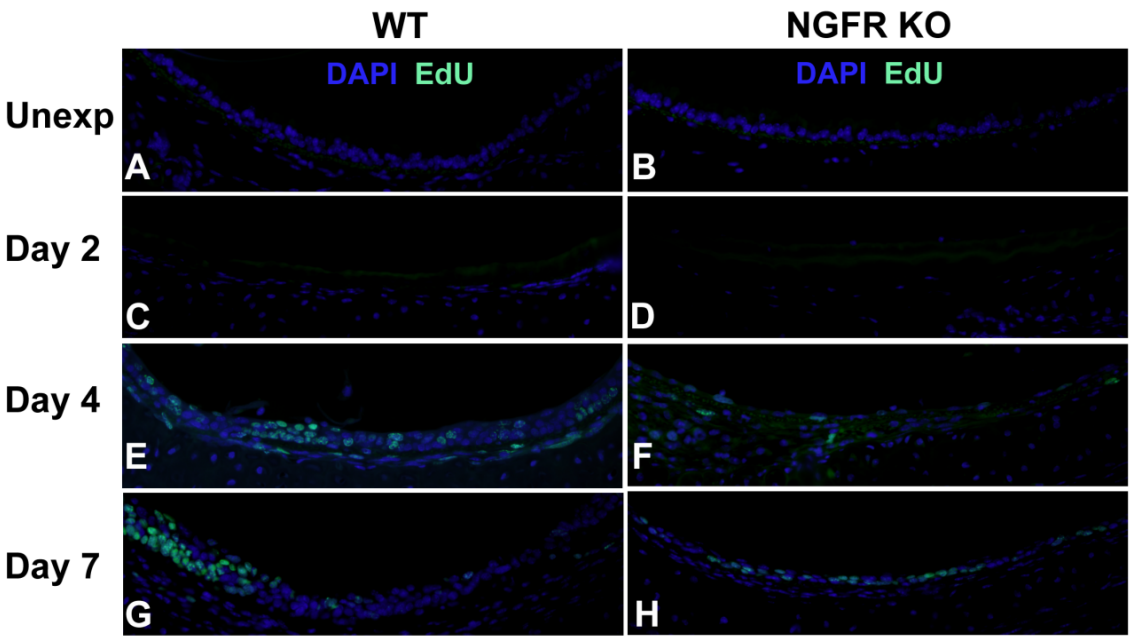

Figure 28. Cell proliferation in NGFR KO mice after chlorine injury. WT and NGFR KO mice were exposed to chlorine and injected with EdU 17 hr prior to sacrifice and collection of tracheas 2, 4, and 7 days after exposure. Images show representative sections of middle trachea after EdU detection to identify proliferating cells during tracheal repair.

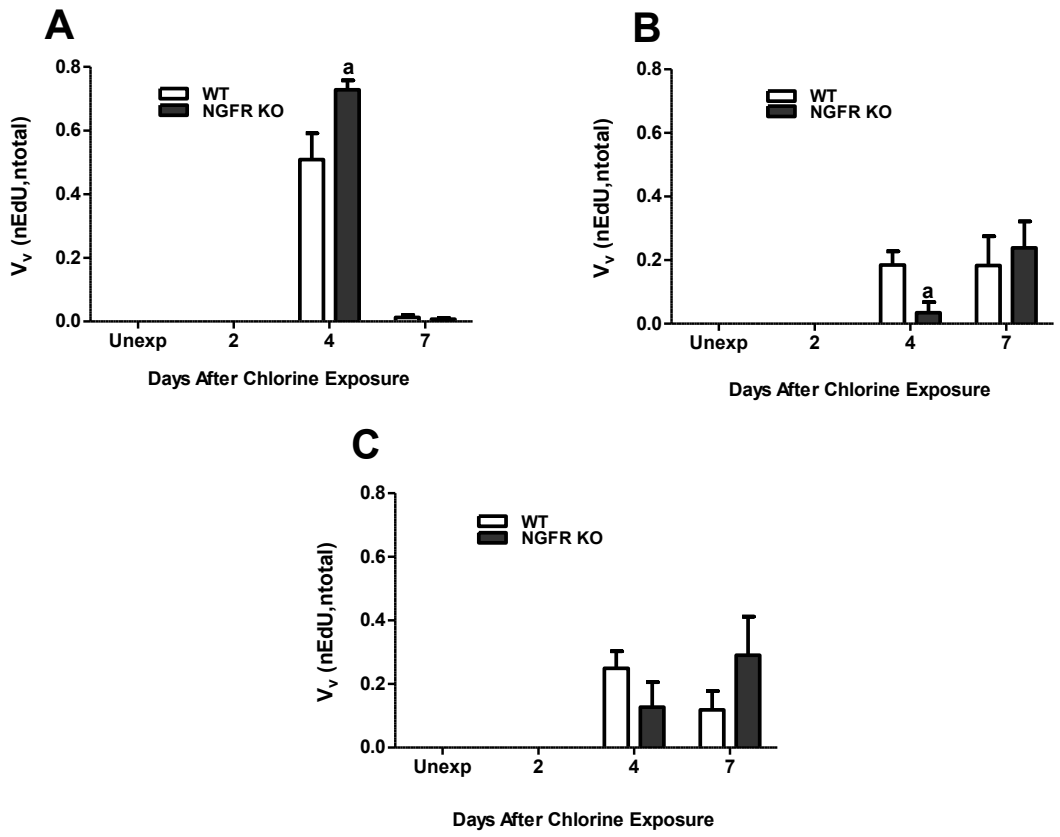

Figure 29. Morphometric analysis of cell proliferation in tracheal epithelium of NGFR KO mice after chlorine injury. WT and NGFR KO mice were exposed to chlorine and injected with EdU 17 hr prior to sacrifice and collection of tracheas 2, 4, and 7 days after exposure. Cell proliferation was assessed in EdU-stained tracheal sections as described in Materials and Methods. The graphs depict the volume density (Vv) of EdU-labeled nuclei (nEdU) relative to total nuclei in tracheal epithelium (nTotal) in (A) Proximal, (B) Middle, and (C) Distal trachea. a, $p<0.05$ vs WT.

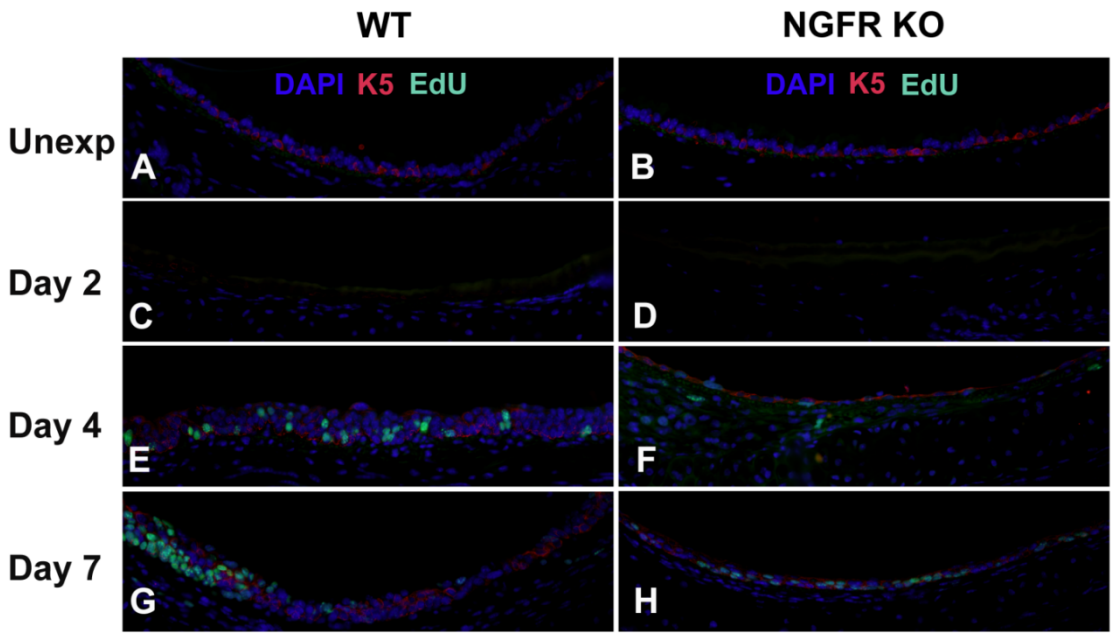

Figure 30. K5 expression in NGFR KO mice during tracheal epithelial repair. WT and NGFR KO mice were exposed to chlorine and injected with EdU 17 hr prior to sacrifice and collection of tracheas 2, 4, and 7 days after exposure. Images show representative sections of middle trachea after EdU detection and immunofluorescence for the basal cell marker K5 during tracheal epithelial repair.

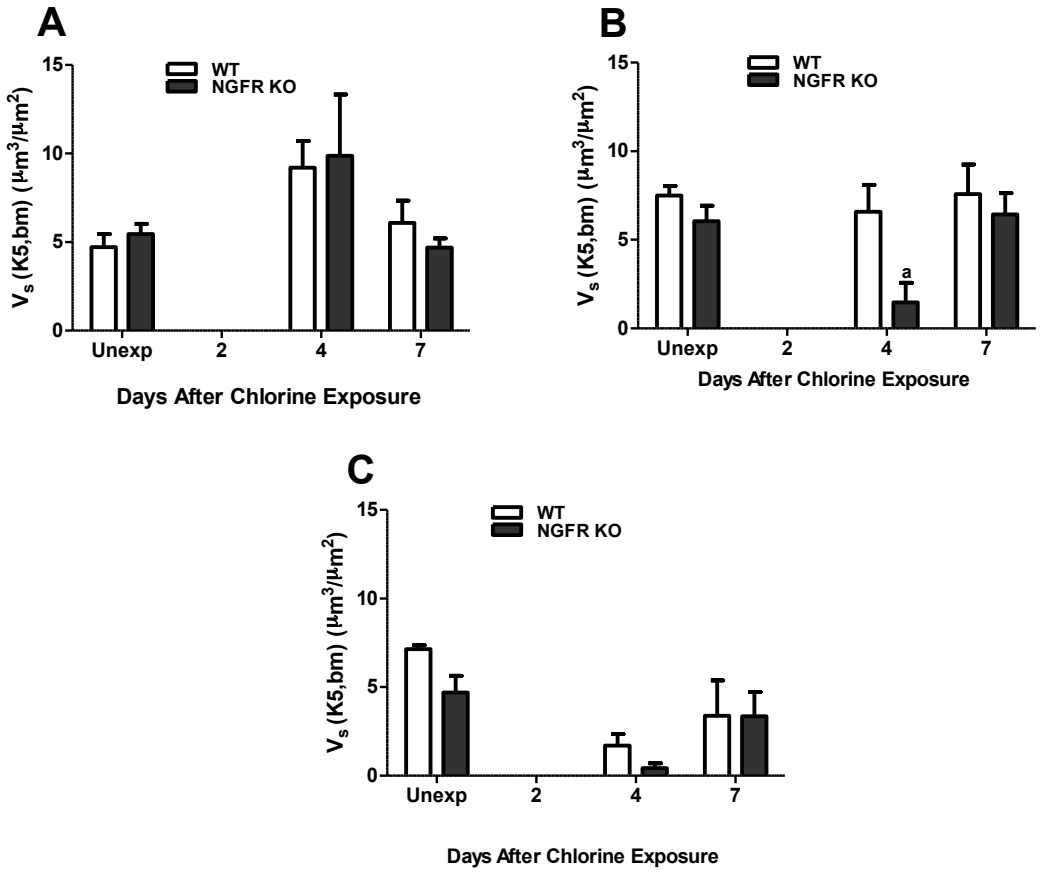

Figure 31. Morphometric analysis for K5 in tracheal epithelium of NGFR KO mice after chlorine injury. WT and NGFR KO mice were exposed to chlorine and sacrificed for collection of tracheas 2, 4, and 7 days after exposure. Tissues were processed, paraffin embedded, and sectioned onto slides for immunohistochemistry. Tracheal sections were stained for K5 and evaluated as described in Materials and Methods. Graphs depict volume of K5-expressing cells relative to basement membrane surface area in (A) Proximal, (B) Middle, and (C) Distal trachea.

Histological analysis and K5 immunostaining indicated that repair of NGFR KO tracheal epithelium was delayed relative to that in WT mice. To distinguish whether this was caused by intrinsic differences in repair capacity or by differences in initial chlorine injury, lung injury was measured 6 hr after exposure before the initiation of repair. Protein content in lung lavage fluid was measured as an indicator of epithelial/endothelial barrier disruption caused by chlorine injury to the respiratory tract. Increased protein content was observed in NGFR KO mice compared with WT mice, indicating a greater extent of chlorine injury (Fig 32A). An additional indicator of increased susceptibility of NGFR KO mice to chlorine-induced injury was provided by an experiment in which mice were inadvertently exposed to a higher chlorine dose than the target of 240 ppm-hr. NGFR KO and WT mice were exposed to 249 ppm-hr, and survival was monitored for 7 days. One day after exposure, survival was 22% in NGFR KO and 75% in WT mice (Fig 32B). By day 2, no NGFR KO mice remained alive while 75% of WT survived until day 7 (Fig 32B).

NGFR KO mice have been shown to have reduced innervation by irritant-responsive sensory nerves. We hypothesized that mice with decreased sensory innervation may exhibit altered breathing patterns that would affect the dose of inhaled chlorine, which may account for the increased susceptibility to injury observed in NGFR KO mice compared with WT mice. In a preliminary experiment to test this hypothesis, we pre-treated C57BL/6 mice with an antagonist for the TRPA1 channel responsible for the detection of pungent and irritant compounds before chlorine exposure. To determine if treatment with the

TRPA1 antagonist had any effect on protective breathing patterns, we measured the respiratory rate in mice immediately after exposure. No statistically significant difference was observed in the respiratory rate between vehicle- and HC-030031 treated mice [113 ± 8.4 and 94 ± 19.1 respectively (mean ± SEM, n=12)]. Additionally, the protein assay results after the 6 hr lavage revealed no statistically significant difference in protein content between vehicle and HC-030031 treatment (Fig 33).

Characterization of Isolated Primary Lung Fibroblasts

To examine NGFR regulation of fibroblast growth as a possible profibrotic mechanism, an in vitro cell culture system using isolated primary lung fibroblasts was employed. Immunofluorescence was performed for vimentin, α-SMA, and pan-cytokeratin to characterize the population of isolated primary fibroblasts used for the cell proliferation experiments. The cells displayed the expected spindle-shaped morphology and stained positive for vimentin (Fig 34A) indicating that the cells are of mesenchymal origin. The cells were negative for α-SMA (Fig 34B) (smooth muscle and myofibroblast marker) and pan-cytokeratin (Fig 34C) (epithelial marker). These are expected results for normal lung fibroblasts, which should have a low prevalence of myofibroblasts.

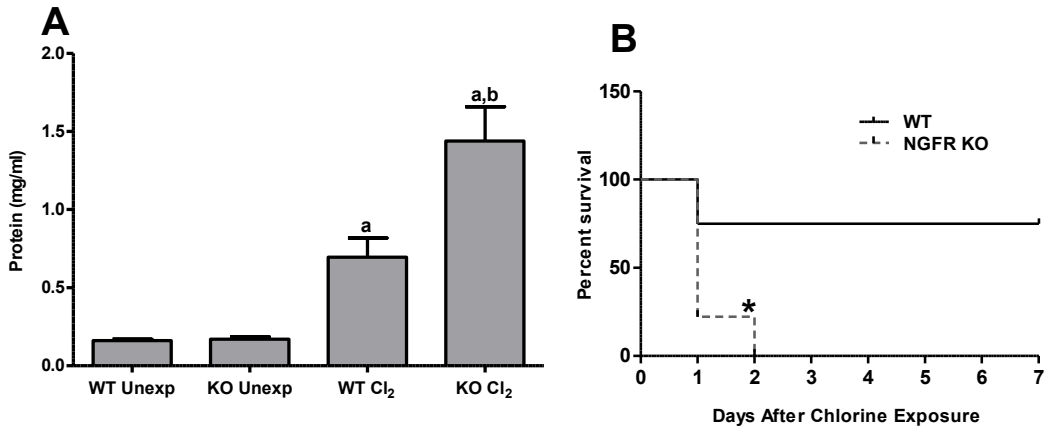

Figure 32. Lavage fluid protein content and survival of NGFR KO mice after chlorine exposure. (A) NGFR KO mice and WT mice were exposed to a target dose of 240 ppm-hr chlorine. Chlorine-exposed mice were lavaged 6 hr after exposure, and lavage fluid was analyzed by Bio-Rad protein assay. a, $p < 0.01$ vs Unexp; b, $p < 0.001$ vs WT Cl_2. n= 4-5 mice per group. (B) Survival curve for NGFR KO and WT mice after exposure to 249 ppm-hr chlorine. n=12 per group. *, $p < 0.01$ vs WT.

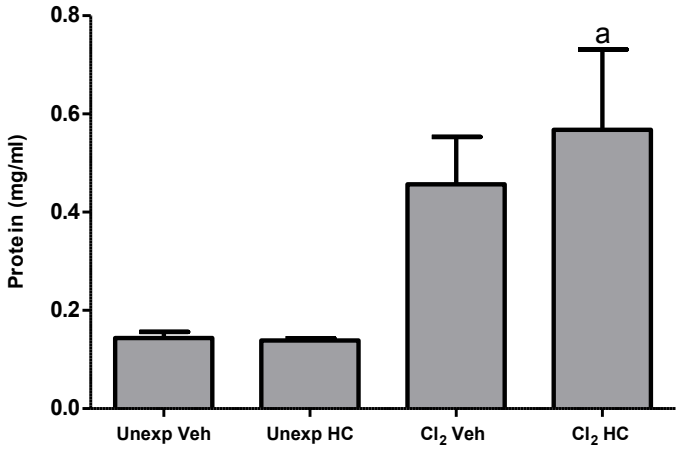

Figure 33. Lavage fluid protein content after pre-treatment with TRPA1 antagonist HC-030031. C57BL/6 mice were exposed to a target dose of 240 ppm-hr chlorine. Mice were lavaged 6 hr after exposure, and lavage fluid was analyzed by Bio-Rad protein assay. n=5 mice per group. a, $p < 0.05$ vs Unexp HC.

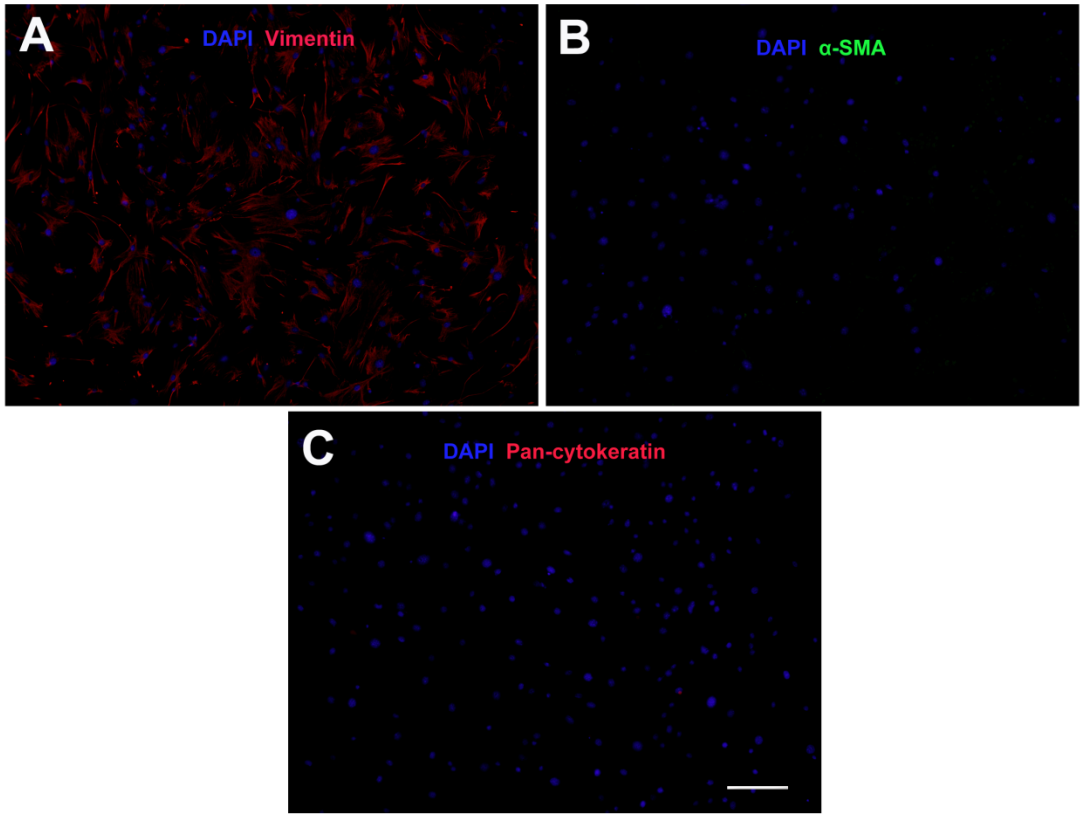

Figure 34. Immunostaining of isolated primary lung fibroblasts. Primary lung fibroblasts were isolated from mice according to Materials and Methods. Immunostaining was performed for (A) Vimentin, (B) α-SMA, and (C) Pan-cytokeratin. Scale bar in Panel C represents 200 μm for all panels.

In Vitro Proliferation of Isolated Primary Lung Fibroblasts

To determine if there was any difference in fibroblast proliferation with or without NGFR function, lung fibroblasts were isolated from NGFR KO and WT mice. MTT assay was performed to demonstrate similar viability of fibroblasts and equal seeding of cells between genotypes (Fig 35A). Interestingly, a statistically significant increased proliferative capacity was observed in NGFR KO compared to WT fibroblasts (Fig 35B). Treatment with NGF ligand resulted in a dose-dependent increase in proliferation in WT fibroblasts but not in NGFR KO cells (Fig 35C and D).

NGFb and Col1a1 Gene Expression in Isolated Primary Lung Fibroblasts

To investigate whether isolated fibroblasts from NGFR KO and WT mice differed in the expression of NGF (NGFb) and collagen type I, α1 (Col1a1), mRNA expression of these genes was assessed. A nonsignificant decrease in expression of NGFb was observed in fibroblasts from NGFR KO compared to WT mice (Fig 36A), and a nonsignificant increase in expression of Col1a1 was detected in NGFR KO fibroblasts compared to WT fibroblasts (Fig 36B).

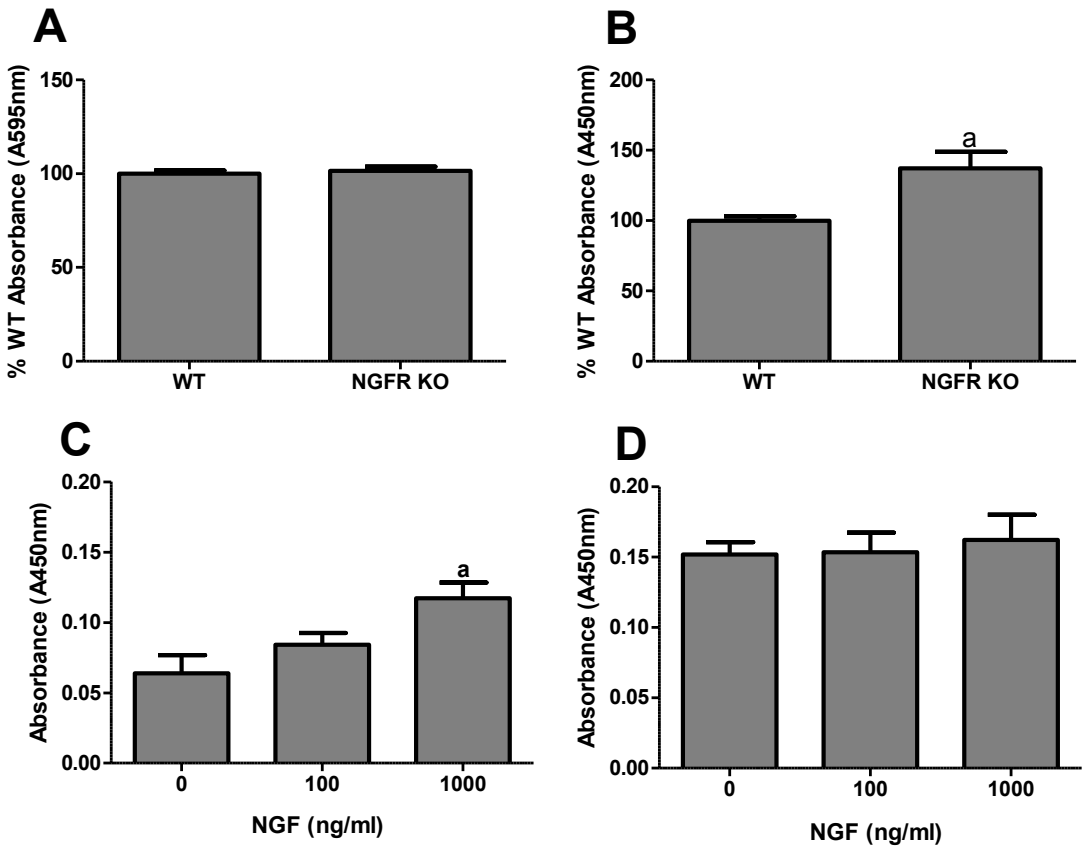

Figure 35. Cell Proliferation assay for isolated lung fibroblasts. Primary lung fibroblasts were isolated from WT and NGFR KO mice as described in Materials and Methods. Cell viability was assessed by MTT Assay (A) and BrdU incorporation into cells was detected by the BrdU cell proliferation assay (B), a, $p < 0.01$ vs WT. Isolated fibroblasts from WT mice (C) and NGFR KO mice (D) were treated with NGF prior to BrdU cell proliferation assay. a, $p < 0.01$ vs no NGF treatment.

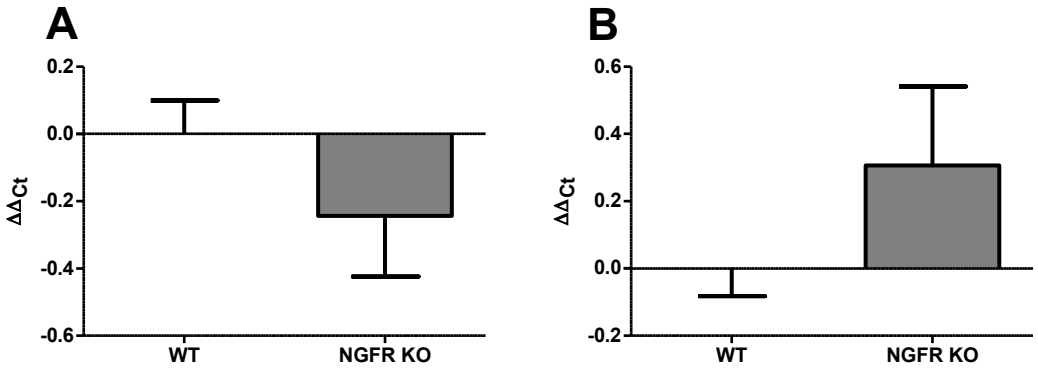

Figure 36. mRNA expression for NGFb and Col1a1 from isolated primary lung fibroblasts. RNA was isolated from primary lung fibroblasts of NGFR KO and WT mice and transcribed into cDNA as described in Materials and Methods. Levels of NGFb (A) and Col1a1 (B) were assessed by qPCR.

Discussion

The goal of the present study was to determine the contribution of neurotrophins and signaling through NGFR to the repair of the tracheal epithelium after chlorine injury. The experimental models employed involved treatment with exogenous neurotrophin ligands, or use of genetically manipulated mice that either overexpressed NGF (CCSP-NGF Tg mice) or had a mutation in NGFR (NGFR KO mice) in cell culture and animal experiments. In the cell culture model, no effect of neurotrophin treatment was observed on tracheosphere formation. In experiments using cells from genetically manipulated mice, increased numbers of tracheospheres grew from cells derived from CCSP-NGF and NGFR KO compared to WT mice. In vivo NGF treatment did not alter epithelial repair. Lung-specific overexpression of NGF in CCSP-NGF transgenic mice did not result in a generalized improvement in epithelial repair, although a suggestion of some localized effects was observed. However, delayed tracheal epithelial repair was observed in NGFR KO mice, as well as decreased development of fibrosis relative to WT mice.

The in vitro cell culture model employed in this study sought to define the ability of a sub-population of basal cells with stem cell properties to survive, self-renew, and differentiate to form lumen-containing structures known as tracheospheres. These structures have been shown to be clonal and serve as an indication of the number of tracheosphere-forming stem cells in the isolated cell population. Pharmacological manipulations did not produce any additional cells with stem cell properties, as there was no change in the number of

tracheospheres formed either with neurotrophin treatment or treatment with NGF blocking antibody. These results indicated that the pharmacological treatments within the culture period did not stimulate stem cell activity. With the hypothesis that NGF would stimulate repair through NGFR signaling in CCSP-NGF Tg mice, initial experiments were designed to manipulate tracheal stem cells in vitro with the tracheosphere culture model. Cells isolated from CCSP-NGF Tg mice formed more tracheospheres than cells from WT mice. A possible explanation for this observation is that continued NGF production in the lung, and/or production during lung development, may increase the pool of stem cells, resulting in an increased number of tracheospheres growing from CCSP-NGF Tg mice. Unexpectedly, more tracheospheres also grew from cells isolated from NGFR KO compared to WT mice. NGF binds to either NGFR or the trkA receptor [57], and both receptor types are widely expressed in the lung [91]. TrkA receptor activation has been implicated in cell survival, proliferation, and differentiation [86, 92]. It has been demonstrated that although NGFR binds all neurotrophins with equal low affinity, the NGF ligand binds to trkA preferentially [93]. A possible explanation for the increased number of tracheospheres observed in NGFR KO mice is activation of trkA to promote the survival and growth of tracheospheres in the absence of NGFR. TrkA receptor activation may therefore compensate for the loss of NGFR function. Complex interactions between NGFR and the trkA receptor have been previously demonstrated [57]. As such, loss of NGFR may distort the balance between these two receptors, and the absence of NGFR may result in complete inhibition of the pro-apoptotic

signaling pathway [94-96]. This may have prevented death of potential stem cells in NGFR KO mice resulting in increased ability to form tracheospheres.

Although the tracheosphere assay is useful for examining the biology of basal epithelial stem cells, it possesses limitations that stimulated us to retain a main focus on the in vivo airway epithelial repair model. For one, this assay gives an indication of the ability of a rare stem cell population to proliferate and differentiate. After chlorine injury in vivo, however, more abundant progenitor cells appeared to be the cells responsible for repair, as basal cells with a widespread distribution across the tracheal epithelium were involved in airway epithelial repair [97]. The in vitro assay therefore, is not indicative of what happens in vivo during repair after chlorine injury. Also, basal cells are directly attached to the basement membrane in vivo and although in the in vitro culture system a Matrigel basement membrane matrix was employed, this may not fully represent the extracellular matrix that underlies basal cells in vivo. This might have influenced cellular interactions with the extracellular matrix. Additionally, since tracheal basal cells in the in vitro culture model are outside of their normal environment and are devoid of interactions with other cell types within their in vivo micro-environment, this model may have failed to mimic the effect of such interactions and their contribution to the survival and growth of tracheal basal cells.

Treatment with exogenous NGF was employed in an animal model of airway epithelial repair, to determine whether epithelial repair could be stimulated through neurotrophin signaling after chlorine injury. NGF treatment did not

produce any significant changes in epithelial repair. NGF levels are upregulated following various types of wounding [98]. Positive effects of exogenous NGF treatment on tissue repair after cutaneous injury have been previously demonstrated [99, 100]. However, these were most pronounced in diabetic mice with reduced endogenous production of NGF, raising the possibility that endogenous levels of NGF after wounding are sufficient to stimulate local NGF receptors. Thus the current findings indicate either that NGF is not involved in airway epithelial repair after chlorine exposure or that endogenous NGF production is sufficient for maximal effect so that exogenous NGF does not accelerate the repair process after chlorine injury.

Lung-specific overexpression of NGF in CCSP-NGF Tg mice produced some localized acceleration of epithelial repair, but no significant generalized effect was observed. A previous study by Sonar and colleagues revealed that NGF overexpression in CCSP-NGF Tg mice did promote the renewal of Clara cells in the bronchiolar epithelium following naphthalene injury [55]. In mice, a pseudostratified epithelium with basal cells is confined to the tracheobronchial region, whereas a simple epithelium is characteristic of the bronchiolar region [45]. Basal cells function as progenitor cells to repair tracheal epithelium, whereas Clara cells function as progenitor cells in the bronchiolar epithelium [45, 48, 49]. The variation in cellular composition and consequent repair processes in the tracheobronchial region versus the bronchiolar region may account for the differences in the observed results. Variations in the cell types responsible for epithelial repair might have similarly influenced the contribution of NGF

overexpression to repair after injury. Also, the fact that naphthalene injury is specific to Clara cells, but chlorine injures all cell types (including Clara cells), may have contributed to the observed differences between the two studies. Furthermore, since the increased tracheosphere formation observed in CCSP-NGF Tg mice in the in vitro assay is an indication of the proliferative capacity of only a small population of tracheal basal cells, the contribution of this subpopulation to epithelial repair in vivo may be minimal, hence, the insignificant contribution of this stem cell population to epithelial repair in CCSP-NGF Tg mice. These findings indicate that NGF overexpression by genetic manipulation does not significantly enhance epithelial repair driven by basal cells in vivo.

To determine whether mutation of NGFR would alter tracheal epithelial repair, this process was examined in NGFR KO mice after chlorine injury. NGFR KO mice exhibited delayed repair in the tracheal epithelium, but also reduced occurrence of fibrotic lesions, suggesting a potential role of NGFR in airway remodeling. NGF and its receptors have been implicated in tissue repair after injury [101, 102]. Following chlorine injury in NGFR KO mice, middle and distal trachea showed a delayed progression from denuded basement membrane through squamous and reparative epithelial stages to restoration of normal pseudostratified epithelium. This observation could be attributed to either a greater initial injury from chlorine exposure in NGFR KO mice, or to an impaired repair process in NGFR KO compared with WT mice. Analysis of injury at an early time after chlorine exposure before initiation of epithelial repair was employed to distinguish between these possibilities. The increased protein

concentration in lavage fluid from NGFR KO compared to WT mice soon after injury supports the premise that NGFR KO mice experienced a greater extent of initial injury after chlorine exposure. The increased early mortality in NGFR KO mice observed in some chlorine exposures is also consistent with this conclusion. NGFR KO mice exhibit decreased sensory innervation by irritant-responsive sensory nerve fibers [89], which control changes in breathing pattern initiated by irritant exposure [103]. Therefore decreased innervation by these sensory fibers in NGFR KO mice may have resulted in decreased sensitivity to the detection of chlorine during exposure which in turn, might have altered their breathing pattern leading to increased chlorine inhalation. An attempt was made to develop an assay to detect chlorine and/or chlorine adducts in blood as an indicator of the amount chlorine that was inhaled, but efforts toward this end were unsuccessful. Treatment with an antagonist to TRPA1, a channel protein that has been implicated in the detection of pungent and irritant compounds, did not result in increased initial injury, a finding that did not support the concept of irritant detection as the difference in injury between NGFR KO and WT mice. An alternative test of this hypothesis involves the use of TRPA1 knockout mice to determine whether they exhibit increased sensitivity to chlorine-induced lung injury.

During tracheal epithelial repair after chlorine-induced injury in NGFR KO mice, areas with denuded epithelium were observed more frequently in NGFR KO mice than in WT mice. In WT mice on the other hand, increased fibrotic lesions were observed more often in distal trachea compared to NGFR KO mice.

Without further studies, it is difficult to ascertain whether the delayed epithelial repair observed in NGFR KO mice would resolve later on in the repair process. In the current study, examining repair at later time points was not possible due to a higher sensitivity of NGFR KO mice to chlorine exposure that led to increased mortality in these mice, apparently from respiratory failure. Perhaps additional exposures with lower concentrations of chlorine to examine the repair process at later time points in NGFR KO mice might prove useful. The reduced fibrotic lesions in NGFR KO mice may suggest that NGFR mutation confers a protection against the development of fibrosis. The development of pulmonary fibrosis has been associated with inflammation [43, 104], and NGF has been shown to exert multiple pro-inflammatory effects. For example, ozone-induced lung inflammation was increased in CCSP-NGF Tg mice and inhibited in NGFR KO mice [105]. A possible role of NGF in promoting airway inflammation has also been demonstrated in CCSP-NGF Tg mice after allergen sensitization [106, 107]. Treatment with NGF blocking antibodies has been shown to decrease the levels of inflammatory cytokines produced after such allergen challenges [106, 108]. The involvement of NGFR in NGF-mediated inflammation has been studied using NGFR blocking antibodies as well as in NGFR KO mice [109, 110]. Furthermore, decreased levels of inflammatory and pro-fibrotic cytokines such as interleukin 4 (IL-4) and interleukin 5 (IL-5) have been observed in NGFR KO mice compared to WT after such allergen sensitization [109, 110]. Although the expression of inflammatory markers was not examined in the current study, it is possible that the decreased occurrence of fibrotic lesions observed in NGFR KO mice may be

associated with decreased inflammation. Future studies examining cytokines and inflammatory cells in NGFR KO mice would shed more light as to the role of NGFR on the development of fibrosis and whether this is associated with decreased inflammation during epithelial repair. Although the mechanisms by which NGFR signaling contributes to fibrosis are unclear, the results of the current study identify this receptor as a potential therapeutic target for preventing airway fibrosis.

To examine the contribution of NGFR signaling to fibroblast proliferation in the development of fibrosis, an in vitro cell culture system with isolated primary lung fibroblasts was employed. Findings revealed increased baseline fibroblast proliferation in NGFR KO fibroblasts, but decreased responsiveness to exogenous NGF. The expression of NGF, NGFR, and trkA receptor has been demonstrated in human dermal fibroblasts and myofibroblasts [111], human lung fibroblasts [112], and primary human fibroblastic-keratocytes [113]. In the present study, fibroblasts from WT mice were stimulated to proliferate more when treated with NGF, but fibroblasts from NGFR KO mice were not responsive. This was not unexpected, as the knockout cells lack one of the receptors for responding to NGF. Although NGFR can bind ligand independently, it has also been demonstrated to act as a co-receptor that enhances the affinity of the trkA receptor for proliferation in dermal fibroblasts [111]. Impaired NGFR function in knockout fibroblasts could therefore potentially impact fibroblast proliferation through both main NGF receptors. Interestingly, results from the present study also revealed that primary fibroblasts from NGFR KO mice showed a higher

basal proliferative rate in the absence of exogenous NGF compared to fibroblasts from WT mice. Lack of NGFR apparently releases these cells from a dependence on NGF for maximal proliferation, but the mechanisms responsible for this were not investigated. Finally, a trend toward increased collagen mRNA expression was observed in NGFR KO fibroblasts compared to WT fibroblasts, which represents an additional profibrotic pathway that may be stimulated in NGFR KO mice.

Findings from this study reveal that the addition of exogenous NGF did not affect the proliferation of tracheal basal cells in vitro, nor did it impact tracheal epithelial repair in vivo after chlorine injury. NGF overexpression in vivo contributed minimally to epithelial repair. Deletion of NGFR however, did appear to confer protection to the development of fibrosis. Future studies examining NGFR signaling as a potential pathway for the inhibition of fibrosis would provide insight into the mechanisms that underlie this finding and also identify this receptor as a potential therapeutic target for preventing the development of airway fibrosis.

CHAPTER IV: WNT/β-CATENIN SIGNALING AND EPITHELIAL REPAIR FOLLOWING CHLORINE-INDUCED INJURY

Introduction

Wnt/β-catenin is a signaling pathway with an essential role in embryonic development and adult tissue homeostasis [63, 114]. During embryonic development, Wnt/β-catenin signaling regulates proliferation, specifies cell fate, and controls cellular differentiation [115]. The canonical Wnt/β-catenin pathway is regulated by stabilization of the transcriptional co-activator β-catenin [114]. Wnt signaling occurs through the Frizzled and the LDL receptor-related proteins 5 and 6 (LRP5 and LRP6) receptors [116]. Wnt ligands (a family of secreted glycoproteins) bind to the Frizzled and LRP6/6 receptors to activate canonical Wnt/β-catenin signaling [63, 114].

The Wnt/β-catenin pathway has been implicated in regeneration and repair of lung epithelium after injury [65, 67]. Activation of Wnt/β-catenin signaling has been demonstrated in mechanical ventilated-associated lung injury with increased expression of Wnt target genes [117]. In addition to its role in epithelial repair, activation of Wnt/β-catenin signaling has been associated with pulmonary fibrosis [118]. In patients with idiopathic pulmonary fibrosis (IPF), increased Wnt signaling has been reported [119, 120]. Inhibition of Wnt/β-catenin signaling with β-catenin siRNA or the Wnt signaling inhibitor ICG-001 resulted in decreased bleomycin-induced pulmonary fibrosis [121, 122].

Although the influence of Wnt/β-catenin signaling has been demonstrated in various models of lung injury, its role in lung repair after chlorine injury has yet to be examined. The objective of this study was to determine if Wnt/β-catenin signaling was activated following chlorine lung injury and if manipulating components of this pathway could alter the course of lung repair.

Materials & Methods

In Vitro LiCl Treatment of Tracheal Epithelial Cells

Epithelial cells were isolated from mouse trachea and grown in a three-dimensional tracheosphere culture described under Materials and Methods in Chapter III. To determine the effect of LiCl treatment on tracheosphere formation, tracheal epithelial cells were treated with LiCl at different times during the culture period. Lithium stimulates ß-catenin function by inhibiting glycogen synthase kinase 3β (GSK-3β) leading to activation of β-catenin target genes [123]. Cells were treated with 20 mM LiCl at the start of culture, halfway through the culture, or late during tracheosphere culture. In early treatment experiments, cells were treated with LiCl or NaCl on days 1, 3, and 5 during cell culture. For LiCl treatments halfway through tracheosphere culture, cells were treated with LiCl on days 11, 13, and 15 after the start of culture. For late LiCl treatments, tracheospheres were treated with LiCl 15 and 17 days from start of culture.

Animals

Experiments involving animals were approved by the University of Louisville Institutional Animal Care and Use Committee and were conducted in accordance with the Institute of Laboratory Animal Resources Guide for the Care and Use of Laboratory Animals [72]. TOPGAL mice (a reporter strain that expresses beta-galactosidase under the control of a promoter containing lymphoid enhancer binding factor 1/transcription factor 3 (LEF/TCF) binding sites) on a CD1 background [124] were purchased from The Jackson Laboratory. Male FVB/N mice were also purchased from The Jackson Laboratory. TOPGAL

and FVB/N mice were randomly assigned to chlorine exposed or unexposed groups. Mice were exposed to chlorine at a target dose of 240 ppm-hr in a whole body exposure chamber [25]. Deviation from target dose for chlorine exposure was 3% for experiment with TOPGAL mice. For chlorine exposure experiments with FVB/N mice, deviation form target dose was 7% for LiCl treatment, 3% for ICG-001 treatment, and 2% for Wnt/β-catenin target gene expression.

X-gal Staining

TOPGAL mice were exposed to chlorine and were euthanized 3, 5, and 7 days after exposure for tracheal tissue collection and X-gal staining. Tracheas were collected in PBS and fixed in 4% paraformaldehyde at 4 ^{o}C for 1 hr. Tracheal tissues were then rinsed in LacZ rinse buffer (0.2 M sodium phosphate, pH 7.3, 2 mM magnesium chloride, 0.02% Igepal, and 0.01% sodium deoxycholate) three times for 30 min each time at room temperature. Tissues were incubated overnight with agitation in LacZ staining solution (LacZ buffer containing 5 mM potassium ferricyanide, 5 mM potassium ferrocyanide, and 1 mg/ml X-gal) at 37 ^{o}C. The following day, tracheas were rinsed in PBS and visualized with a dissecting microscope.

Treatment of Animals

To manipulate components of the Wnt/β-catenin pathway that could alter the course of epithelial repair, mice were treated with either the Wnt/β-catenin pathway stimulator LiCl or regulator ICG-001 (this drug inhibits β-catenin interaction by binding to cyclic AMP response-element binding protein binding protein (CBP) to inhibit β-catenin-dependent transcription through this co-

activator [125]. For LiCl treatment experiment, FVB/N mice were exposed to chlorine and treated with either LiCl (at a dose of 200 mg/kg body weight) or vehicle (water) 1 hr after chlorine exposure and every day thereafter for 7 days by intraperitoneal injection. For treatment with the Wnt pathway regulator ICG-001, FVB/N mice were exposed to chlorine and treated with either ICG-001 (at a dose of 5 mg/kg body weight) or vehicle (0.14% ethanol in saline) 1 hr after chlorine exposure and twice a day thereafter for 7 days by subcutaneous injection. In LiCl and ICG-001 treatment experiments, mice were euthanized after 7 days for collection of lungs for the analysis of airway fibrosis.

Analysis of Fibrosis

Airway fibrosis was assessed in the left lungs by hydroxyproline analysis and in the right lungs by histology using picro-Sirius Red staining. To analyze collagen content in left lung by hydroxyproline assay, left lungs were weighed and the assay was performed as previously described [126, 127]

To assess fibrosis by histology, right lungs were fixed in 10% neutral buffered formalin overnight, processed, embedded in paraffin and sectioned onto slides. Fibrosis around large airways was assessed by staining of tissue sections for collagen with picro-Sirius Red. Sections were deparaffinized in xylene, rehydrated in ethanol, and rinsed in water. Slides were then placed in picric acid (1.3% in water) containing 0.1% Fast Green and 0.1% Sirius Red for 40 min at room temperature. Slides were rinsed briefly in water, dehydrated in ethanol, changed to xylene, and mounted with Permount.

To quantify fibrosis after picric-Sirius Red staining, digital images of sections containing cross sections of lobar bronchi were captured and analyzed by morphometry using ImageJ. Captured images were first converted to grayscale, and the area around the large airway that stained red for collagen was analyzed on the green channel. Areas that stained red for collagen were isolated using Moments automatic threshold. Collagen content was quantified as the area of collagen staining normalized to airway perimeter.

Statistical Analysis

Statistical analysis was performed using Prism 4.0a (GraphPad; La Jolla, CA). Data are presented as group means ± standard error of the mean (SEM). Group means for in vitro LiCl treatment experiments were compared between control and treatment group using t test. Group means for in vitro LiCl and NaCl treatment experiments were compared between control and treatment groups using one-way analysis of variance (ANOVA) with Bonferroni's multiple comparison. Data for LiCl treatment at different times were analyzed by one-way ANOVA with Dunnett's multiple comparison test. For animal experiments, group means were compared between chlorine exposed and unexposed animals using ANOVA with Bonferroni's multiple comparison test. Differences were considered to be statistically significant at $p < 0.05$.

Results

Effect of Wnt/β-catenin Signaling in Airway Epithelial Cells In Vitro

To investigate the effect of Wnt/β-catenin signaling on the growth of epithelial cells in vitro, isolated mouse tracheal epithelial cells were treated with LiCl which stimulates β-catenin activation by inhibiting GSK-3β [123]. Activation of Wnt/β-catenin signaling has been shown to regulate airway stem cells numbers [65]. The purpose of this manipulation was to determine if Wnt/β-catenin signaling stimulation would alter tracheosphere formation. Treatment with LiCl starting on the first day of culture completely inhibited tracheosphere formation (Fig 37A) suggesting a profound effect of β-catenin on this process. To verify that failure of tracheosphere formation with LiCl treatment was not due to a change in osmolarity with addition of LiCl, parallel cultures in a subsequent experiment were supplemented with an equivalent concentration of sodium chloride (NaCl). Again, LiCl inhibited tracheosphere formation, but NaCl treatment had no effect (Fig 37B). Due to the complete inhibition of tracheosphere formation observed with LiCl treatment at the start of tracheosphere culture, subsequent experiments were designed with LiCl treatments at different times (either halfway through culture, or towards the end of the culture period) to determine effect of LiCl treatment at these different times on tracheosphere formation. LiCl treatment starting halfway through the culture period on days 11, 13, and 15 resulted in decreased numbers of tracheospheres formed compared to control (Fig 37C). However, late LiCl treatment on days 15 and 17 after start of cell culture did not have any observed effect on

tracheosphere counts (Fig 37C). These results indicate that early stimulation of Wnt signaling inhibits tracheosphere formation but has no effect on tracheosphere survival after tracheospheres are completely formed.

Activation of β-catenin after Chlorine Injury In Vivo

To determine the timing and spatial distribution of β-catenin activation in the tracheal epithelium after chlorine injury, TOPGAL mice (a reporter strain that expresses beta-galactosidase under the control of a ß-catenin-responsive promoter) [124] were exposed to chlorine, and β-catenin activation was examined in the trachea by whole mount X-gal staining. Activation of β-catenin was not observed in unexposed TOPGAL mice (Fig 38A). After exposure to chlorine, X-gal staining indicative of β-catenin activation was observed in the trachea throughout the study period from day 2 to day 7 (Fig 38B, C, and D). Three days after chlorine exposure, β-catenin activation was restricted mostly to the proximal trachea (Fig 38B). By day 5, β-catenin activation was still observed in the proximal trachea, although widespread activation was also observed in the middle to distal trachea (Fig 38C). Activation of β-catenin was observed on day 7 in the distal trachea even although staining for this was weak (Fig 38D). In the proximal trachea at this same time point however, strong staining for β-catenin activation was observed (Fig 38D).

Expression of Wnt/β-catenin Signaling Target Genes in Distal Trachea/Mainstem Bronchi after Chlorine Exposure

Increased functional Wnt/β-catenin signaling has been observed in association with lung fibrosis [118-120]. To determine whether development of

fibrosis after chlorine exposure was associated with altered expression of Wnt target genes, mRNA levels for Wnt target genes were analyzed in the distal trachea/mainstem bronchi. The expression of Wnt target genes Lef1, Tcf7, and Axin2 was analyzed 4 and 7 days after chlorine exposure. Although not statistically significant, a trend towards increased expression of Lef1, Tcf7, and Axin2 was observed 4 and 7 days after chlorine exposure (Fig 39A, B, and C). The expression of Axin2 in the tracheal epithelium after chlorine exposure was also verified by immunofluorescence. In unexposed mice, Axin2 expression was detected in basal cells and other differentiated cells of the epithelium (Fig 39A). Four days after chlorine, Axin2 expression was observed although expression was weak (Fig 40B). At day 7, increased Axin2 expression was observed in multiple layers of the repairing trachea (Fig 40C) suggesting the association of Axin2 re-expression with differentiation after chlorine injury.

Effect of Wnt/β-catenin Stimulation on the Development of Airway Fibrosis

To examine the effect of stimulation of Wnt/β-catenin signaling on the development of fibrosis in the lung after chlorine exposure, FVB/N mice were exposed to chlorine and treated with the Wnt/β-catenin signaling stimulant LiCl every day for 7 days. Collagen content, a feature in the development of fibrosis, was measured in the left lung by hydroxyproline assay. Results revealed increased collagen content after chlorine exposure in vehicle-treated mice compared to unexposed mice (Fig 41A). However, collagen content in chlorine-exposed LiCl-treated mice was significantly reduced compared to chlorine-exposed vehicle-treated mice, suggesting that stimulation of Wnt/β-catenin

inhibits the development of fibrosis after chlorine injury (Fig 41A). Collagen content in the lobar bronchus of the lower right lung was also assessed by picro-Sirius Red staining. Chlorine exposure resulted in increased collagen content in the large airway of both vehicle-treated and LiCl-treated mice compared to unexposed mice (Fig 41B). Decreased collagen content was observed in LiCl-treated mice compared to vehicle-treated mice after chlorine exposure, although this decrease was not statistically significant (Fig 41B).

Effect of Wnt/β-catenin Signaling Regulator on the Development of Fibrosis In Vivo

To determine the effect of Wnt signaling regulation on the development of fibrosis, mice were treated with the Wnt/β-catenin pathway regulator ICG-001 which blocks β-catenin interaction with CBP to inhibit activation of ß-catenin-responsive genes dependent on CBP [125]. Mice were treated with ICG-001 twice a day for 7 days after chlorine exposure. Hydroxyproline content in the left lung was increased in chlorine-exposed mice treated with vehicle and ICG-001 compared to unexposed mice (Fig 42A). There was no observed difference in left lung hydroxyproline content between vehicle-treated and ICG-001-treated mice after chlorine exposure (Fig 42A). Interestingly, histological assessment of the collagen content in the lower right lung revealed significantly decreased collagen staining in ICG-001-treated compared to vehicle-treated mice (Fig 42B) suggesting that modulation of Wnt signaling with ICG-001 may produce beneficial effects by attenuating the development of fibrosis after chlorine injury.

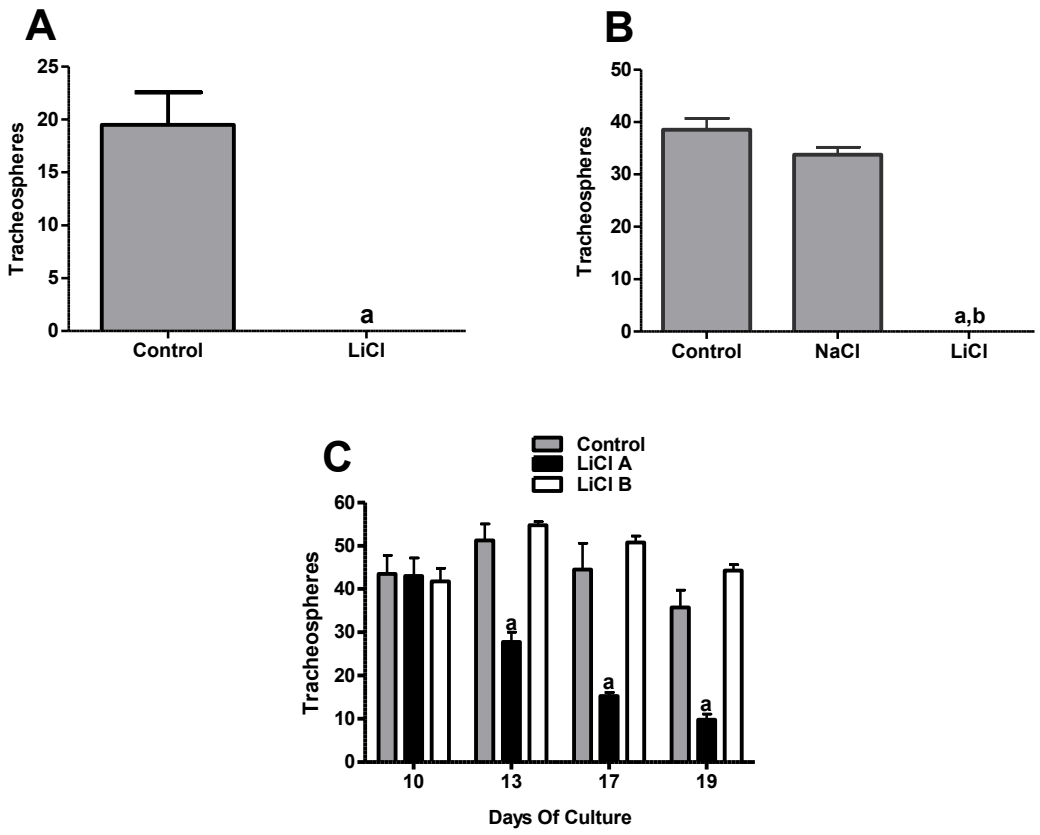

Figure 37. Effect of Wnt/β-catenin stimulation by LiCl on tracheosphere formation. Tracheal epithelial cells were isolated from C57BL/6 mice and cultured in Matrigel in Transwell inserts with media change every other day. Epithelial cells were treated with 20 mM LiCl (A) or 20 mM LiCl and 20 mM NaCl (B) on days 1, 3, and 5 during the culture period. Tracheospheres were counted on day 13 after start of culture. a, $p < 0.0001$ vs Control; b, $p < 0.0001$ vs NaCl. (C) Epithelial cells were treated with 20 mM LiCl on days 11, 13, and 15 after start of cell culture (LiCl A), or days 15 and 17 after start of culture (LiCl B). Tracheospheres were counted on days 10, 13, 17, and 19 after start of culture. a, $p < 0.01$ vs Control.

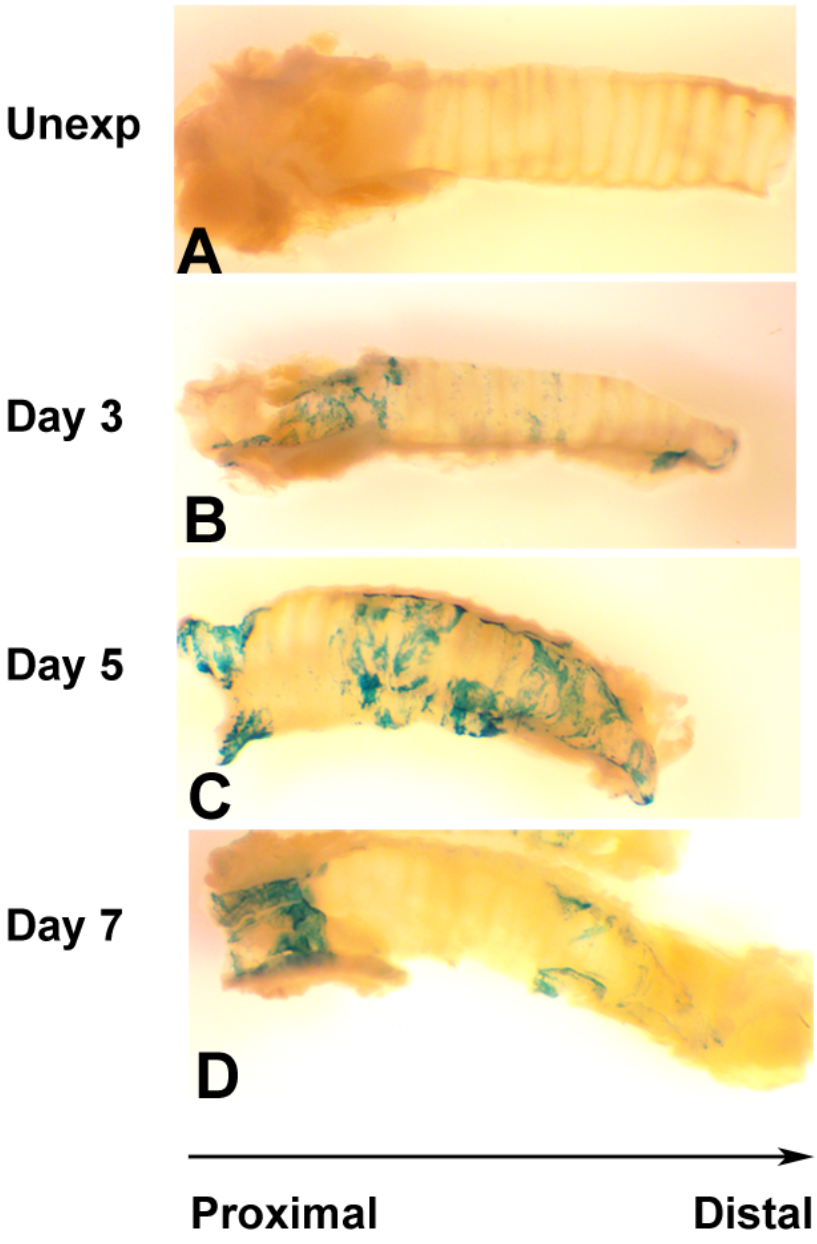

Figure 38. X-gal staining in TOPGAL mice after chlorine exposure.

TOPGAL mice were exposed to chlorine, and tracheas were collected for whole mount X-gal staining 3, 5, and 7 days after exposure as described in Materials and Methods.

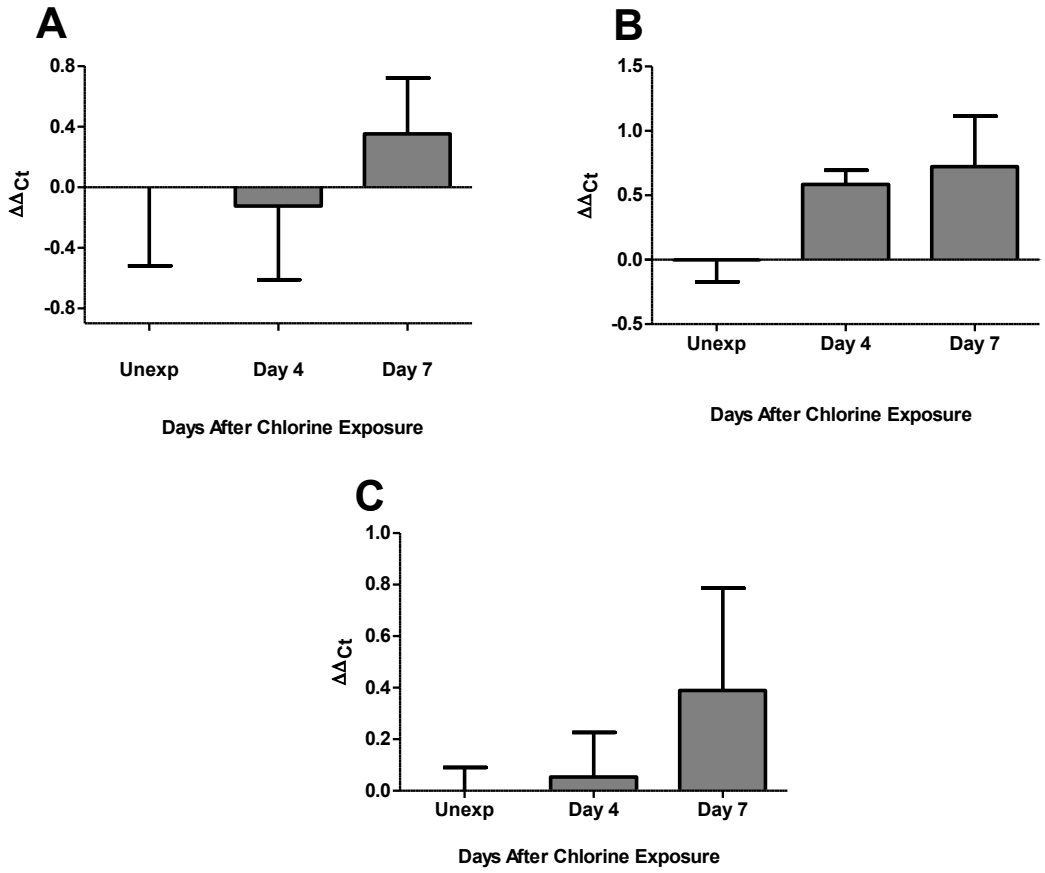

Figure 39. Expression of Wnt signaling target genes in distal trachea/mainstem bronchi after chlorine exposure. FVB/N mice were exposed to chlorine, and distal trachea/ mainstem bronchi were collected on days 4 and 7 for RNA isolation. Gene expression for Lef1 (A), Tcf7 (B), and Axin2 (C) was determined by quantitative RT-PCR.

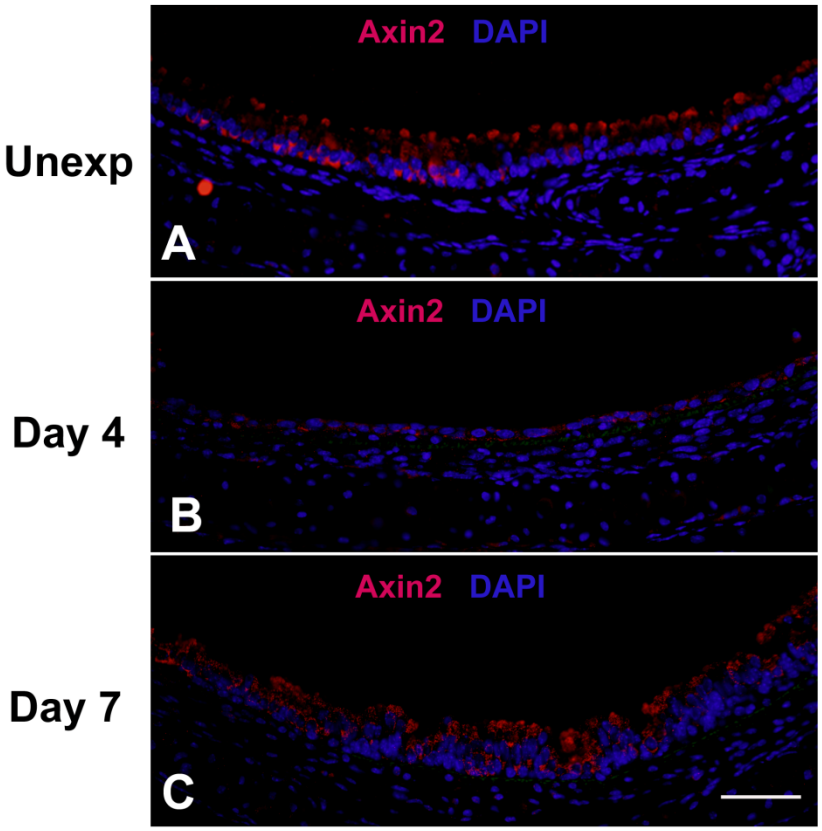

Figure 40. Expression of Axin2 in distal trachea after chlorine exposure. Mice were exposed to chlorine and euthanized for collection of tracheas 4 and 7 days after exposure. Tracheal sections were stained for Axin2 (red), and nuclei were labeled with DAPI (blue). Scale bar in Panel C represents 50 μm for all panels.

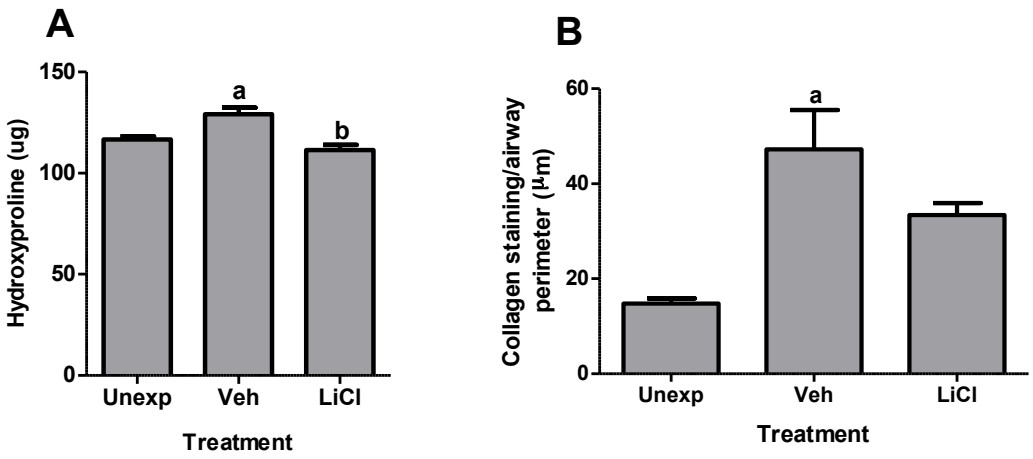

Figure 41. Effect of Wnt/β-catenin stimulation by LiCl on collagen content in the lungs of chlorine-exposed mice. FVB/N mice were exposed to chlorine and treated with either vehicle (water) or LiCl every day for 7 days. Mice were sacrificed for collection of lungs after 7 days to assess collagen content. (A) Determination of collagen content in left lung by hydroxyproline assay. a, $p < 0.05$ vs Unexp; b, $p < 0.0001$ vs Veh. (B) Right lungs were fixed, processed, paraffin embedded, and sectioned onto slides. Tissue sections were stained for collagen by picro-Sirius Red staining. Morphometry was performed as described in Materials and Methods on the largest airway of the lower right lung to quantify collagen content. a, $p < 0.05$ vs Unexp.

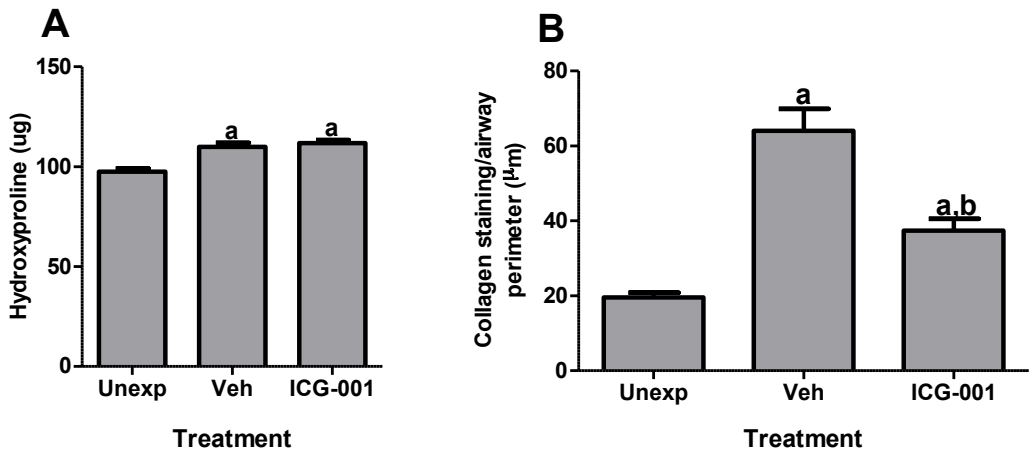

Figure 42. Effect of the Wnt signaling regulator ICG-001 on collagen content in chlorine-exposed mice. FVB/N mice were exposed to chlorine and treated with either vehicle (0.14% ethanol in saline) or ICG-001 twice a day for 7 days. (A) Collagen content was determined in left lung by hydroxyproline assay. a, $p < 0.05$ vs Unexp. (B) Right lungs were fixed, processed, and sectioned onto slides. Tissue sections were stained for collagen using picro-Sirius Red staining. Morphometry was performed on the largest airway of the lower right lung to quantify collagen content. a, $p < 0.01$ vs Unexp; b, $p < 0.0001$ vs Veh.

Discussion

The present study aimed to determine the role of Wnt/β-catenin signaling in the formation of tracheospheres in vitro, and in epithelial repair after chlorine injury in vivo. A complete inhibition of tracheosphere formation was observed with early treatment with LiCl in vitro. LiCl treatment halfway through cell culture resulted in decreased tracheosphere formation, while LiCl treatment towards the end of culture did not have any observed effect on tracheosphere survival. Chlorine exposure resulted in the activation of β-catenin signaling in the tracheal epithelium of TOPGAL mice. Stimulation of Wnt/β-catenin pathway with LiCl treatment decreased collagen content in the lung after chlorine exposure. Additionally, in vivo regulation of Wnt/β-catenin signaling with ICG-001 treatment resulted in decreased collagen 7 days after chlorine exposure. Altered mRNA expression of Wnt target genes in distal trachea/mainstem bronchi was observed after chlorine exposure.

Activation of Wnt/β-catenin signaling has been associated with inhibition of differentiation in stem cells [65, 67]. LiCl stimulates Wnt/β-catenin signaling by inhibiting GSK-3β thus leading to β-catenin activation. The complete inhibition of tracheosphere formation observed with early LiCl suggests that stimulation of Wnt/β-catenin signaling may have inhibited the differentiation of tracheal epithelial cells into tracheospheres. Inhibition of cellular differentiation has been shown to promote apoptosis [128]. Inhibition of differentiation by inappropriate Wnt/β-catenin signaling may have resulted in apoptosis, hence, the complete inhibition of tracheosphere formation. Stimulation of Wnt/β-catenin signaling

halfway through the cell culture period may have prevented the formation of new tracheospheres by inhibiting their differentiation and as such, the observed decreased tracheosphere counts. Also, formed tracheospheres that were not completely differentiated may have been susceptible to LiCl treatment and this may have resulted in cell death. Stimulation of Wnt/β-catenin signaling towards the end of the culture period did not have any observed effect on tracheosphere counts. During this period, all formed tracheospheres may have been fully differentiated and were no longer susceptible to inappropriate Wnt/β-catenin activation by LiCl stimulation. LiCl treatment after differentiation may therefore have contributed to the maintenance of a differentiated epithelium and this may have promoted the survival of tracheospheres. This suggests that activation of Wnt/β-catenin signaling during differentiation may prevent tracheosphere formation. However, activation after differentiation may help maintain a differentiated epithelium and promote survival of tracheospheres. Immunohistochemical analysis of tracheospheres sections for basal cell and differentiated cell markers would provide insight into the effect(s) of the different LiCl timing treatments on the differentiation of formed tracheospheres.

Activation of Wnt/β-catenin signaling has been demonstrated in epithelial injury and repair models in the lung [46, 65, 117, 129, 130]. The chlorine-induced injury model employed in the current study resulted in activation of β-catenin signaling in a proximal-distal spatial distribution in the tracheal epithelium of TOPGAL mice. This observed pattern of β-catenin activation after chlorine exposure is similar to the pattern of tracheal epithelial repair after chlorine

exposure previously reported [97]. The appearance of β-catenin activation in proximal trachea is correlated with repair and re-differentiation in that part of the trachea [97]. This finding indicates that β-catenin activation may be associated with tracheal epithelial differentiation after chlorine exposure as has been previously reported [62, 65, 68]. Activation of Wnt/β-catenin signaling also suggests the expression of β-catenin target genes. The expression of Wnt target genes during homeostasis and their subsequent re-activation after injury has been reported [68, 130]. Elevated expression of Wnt target genes has been shown with activation of Wnt signaling after naphthalene injury [68]. Increased functional Wnt/ β-catenin signaling was also observed in idiopathic pulmonary fibrosis (IPF) [120]. In the present study, expression of Axin2 was decreased after chlorine injury, and was later re-activated in the repair process in the distal trachea, associating Axin2 with maintenance of a differentiated epithelium. A similar finding was reported by Zemke and colleagues [131]. Future studies examining cell proliferation, and the expression of basal cell and differentiated cell markers with β-catenin activation in TOPGAL mice after chlorine exposure would provide information as to the role of β-catenin activation in the repair process after chlorine injury.

The effect of stimulating the Wnt/β-catenin signaling pathway by LiCl treatment has been examined in lung epithelial repair [129]. The mechanism of action by which LiCl lithium stimulates Wnt pathway is by inhibition of GSK-3β, a component of the scaffolding protein complex responsible for targeting β-catenin for degradation [123]. Inhibition of GSK-3β by LiCl thus prevents β-catenin

phosphorylation and in turn, promotes β-catenin translocation into the nucleus for activation of target genes [123]. Stimulation of this process by LiCl treatment in our current study resulted in decreased collagen content in the lung after chlorine exposure. Similarly, the activation of Wnt signaling by LiCl stimulation reduced collagen content in an experimental model of emphysema [129]. The decreased collagen content observed with LiCl treatment in the present study can be attributed to decreased fibrosis more so than the contribution of LiCl to promoting efficient epithelial repair. Also, results from the in vitro LiCl treatments in the current study suggest that early LiCl treatment might have an adverse effect on epithelial repair but later treatment may contribute to maintenance of a differentiated epithelium. Subsequent studies with LiCl treatments starting later during repair would determine if this treatment would result in more efficient epithelial repair in addition to attenuating the development of fibrosis. Our current findings, however, suggest that LiCl stimulation of Wnt/β-catenin signaling inhibits the development of fibrosis in the lung after chlorine injury.

In the present study, modulation of Wnt/β-catenin signaling using the small molecule ICG-001 resulted in decreased collagen content in large airways of the lung. ICG-001 alters β-catenin activation by selectively blocking its interaction with CBP without interfering with its interaction with p300 (another co-activator responsible for T-cell factor/β-catenin transcription) [125]. The decreased collagen content observed with ICG-001 treatment can be explained by the fact that although ICG-001 may have inhibited β-catenin/CBP interaction, it is possible that signaling may have been skewed towards β-catenin/ p300

activation and this may have resulted in the upregulation of ß-catenin target genes dependent on p300 activity. Beneficial effects of ICG-001 supported by Zemans and colleagues who also observed that treatment with ICG-001 promoted epithelial repair after lung injury [132]. An additional study reported that treatment with ICG-001 promoted epithelial repair and decreased fibrosis associated with bleomycin-induced injury [121]. In future studies, analysis of the expression of Wnt signaling components and/or target genes following ICG-001 treatment would further explore mechanisms by which ICG-001 promotes epithelial repair and inhibits fibrosis.

Taken together, our results demonstrate that Wnt/β-catenin signaling is activated after chlorine injury. Modulation of Wnt/ β-catenin signaling resulted in decreased fibrosis in the lung after injury. Although further studies providing insights into the mechanisms underlying decreased fibrosis with Wnt/β-catenin signaling is needed, these results implicate Wnt/β-catenin as a potential pathway to manipulate for enhanced epithelial repair and inhibition of fibrosis associated with chlorine injury.

CHAPTER V: CONCLUSION

This study examined airway epithelial repair after chlorine-induced injury and investigated potential signaling pathways that could be manipulated to stimulate efficient repair. Initial work to characterize tracheal epithelial repair after chlorine injury revealed that chlorine inhalation resulted in the death and sloughing of virtually all Clara and ciliated cells and a variable number of basal cells from the trachea. Surviving basal cells spread to cover the injured airway and proliferated to restore a pseudostratified epithelium containing Clara and ciliated cells. In areas with few surviving basal cells, repair was inefficient, leading to an extended period of denuded basement membrane and the development of airway fibrosis.

To investigate potential signaling pathways that could be stimulated to facilitate epithelial repair, the role of neurotrophins and NGFR signaling was examined in an in vitro cell culture system and in vivo after chlorine-induced injury. Pharmacological treatment and genetically manipulated mice that either overexpressed NGF (CCSP-NGF Tg mice) or had a mutation in NGFR (NGFR KO mice) were employed in in vitro and in vivo experiments. Addition of exogenous NGF did not impact the proliferation of tracheal basal cells in vitro, nor did it influence tracheal epithelial repair in vivo after chlorine injury. NGF overexpression in vivo did not produce major changes in epithelial repair. Mutation of NGFR increased the sensitivity of mice to chlorine-induced airway

injury but also protected mice from the development of fibrosis, implicating NGFR signaling in airway remodeling after injury.

The influence of Wnt/β-catenin signaling on epithelial repair was examined in vitro and in vivo as another potential pathway to facilitate epithelial repair after chlorine injury. Tracheosphere formation was completely inhibited with early treatment with LiCl (a stimulator of the Wnt/β-catenin signaling pathway) in vitro. LiCl treatment halfway through cell culture resulted in decreased tracheosphere formation, whereas LiCl treatment towards the end of culture did not have any observed effect on tracheosphere survival. In animal experiments, chlorine inhalation resulted in the activation of β-catenin signaling in the tracheal epithelium. Stimulation of the Wnt/β-catenin pathway with LiCl reduced collagen content in the lung after chlorine exposure. In vivo regulation of Wnt/β-catenin signaling with ICG-001(a Wnt/β-catenin signaling pathway regulator) resulted in decreased collagen 7 days after chlorine exposure. Additionally, chlorine exposure altered mRNA expression of Wnt target genes in distal trachea/mainstem bronchi. Overall, this study revealed that Wnt/ β-catenin signaling is activated after chlorine injury and that this pathway can be experimentally manipulated to attenuate the development of fibrosis in the lung after chlorine-induced injury.

Taken together, these studies highlight the necessity for efficient epithelial repair after injury. The work characterizing tracheal epithelial repair establishes a model for understanding regenerative processes in the respiratory epithelium that will be valuable for testing therapies for airway injury. Findings from the animal

model of chlorine-induced injury and repair employed can be related to alterations in the pathology of several chronic lung diseases such as chronic obstructive pulmonary disease (COPD), cystic fibrosis, and idiopathic pulmonary fibrosis. Reactivation of developmental pathways such as Wnt/β-catenin signaling after injury as observed in this study has been associated with idiopathic pulmonary fibrosis, a disease state often attributed to aberrant epithelial repair. Findings in this study therefore provide insights into the potential contribution of NGFR signaling and Wnt/β-catenin pathway to the inhibition of fibrosis that will be beneficial to developing interventional therapies for airway injury.

REFERENCES

1. Das R, Blanc PD: **Chlorine gas exposure and the lung: a review.** *Toxicol Ind Health* 1993, **9:**439-455.
2. Evans RB: **Chlorine: state of the art.** *Lung* 2005, **183:**151-167.
3. Van Sickle D, Wenck MA, Belflower A, Drociuk D, Ferdinands J, Holguin F, Svendsen E, Bretous L, Jankelevich S, Gibson JJ, et al: **Acute health effects after exposure to chlorine gas released after a train derailment.** *Am J Emerg Med* 2009, **27:**1-7.
4. Brodsky BH: **Industrial chemicals as weapons: chlorine** [http://www.nti.org/analysis/articles/industrial-chemicals-weapons-chlorine/]
5. Ploysongsang Y, Beach BC, DiLisio RE: **Pulmonary function changes after acute inhalation of chlorine gas.** *South Med J* 1982, **75:**23-26.
6. Schwartz DA, Smith DD, Lakshminarayan S: **The pulmonary sequelae associated with accidental inhalation of chlorine gas.** *Chest* 1990, **97:**820-825.
7. Weill H, George R, Schwarz M, Ziskind M: **Late evaluation of pulmonary function after acute exposure to chlorine gas.** *Am Rev Respir Dis* 1969, **99:**374-379.
8. Jones RN, Hughes JM, Glindmeyer H, Weill H: **Lung function after acute chlorine exposure.** *Am Rev Respir Dis* 1986, **134:**1190-1195.

9. Mohan A, Kumar SN, Rao MH, Bollineni S, Manohar IC: **Acute accidental exposure to chlorine gas: clinical presentation, pulmonary functions and outcomes.** *Indian J Chest Dis Allied Sci* 2010, **52:**149-152.

10. Charan NB, Lakshminarayan S, Myers GC, Smith DD: **Effects of accidental chlorine inhalation on pulmonary function.** *West J Med* 1985, **143:**333-336.

11. Leroyer C, Malo JL, Infante-Rivard C, Dufour JG, Gautrin D: **Changes in airway function and bronchial responsiveness after acute occupational exposure to chlorine leading to treatment in a first aid unit.** *Occup Environ Med* 1998, **55:**356-359.

12. Chierakul N, Rittayamai N, Passaranon P, Chamchod C, Suntiwuth B: **Respiratory health effect of persons accidentally expose to high concentration of chlorine gas.** *J Med Assoc Thai* 2013, **96 Suppl 2:**S17-21.

13. Donnelly SC, FitzGerald MX: **Reactive airways dysfunction syndrome (RADS) due to chlorine gas exposure.** *Ir J Med Sci* 1990, **159:**275-276; discussion 276-277.

14. Malo JL, L'Archeveque J, Castellanos L, Lavoie K, Ghezzo H, Maghni K: **Long-term outcomes of acute irritant-induced asthma.** *Am J Respir Crit Care Med* 2009, **179:**923-928.

15. Schonhofer B, Voshaar T, Kohler D: **Long-term lung sequelae following accidental chlorine gas exposure.** *Respiration* 1996, **63:**155-159.

16. Bherer L, Cushman R, Courteau JP, Quevillon M, Cote G, Bourbeau J, L'Archeveque J, Cartier A, Malo JL: **Survey of construction workers repeatedly exposed to chlorine over a three to six month period in a pulpmill: II. Follow up of affected workers by questionnaire, spirometry, and assessment of bronchial responsiveness 18 to 24 months after exposure ended.** *Occup Environ Med* 1994, **51:**225-228.

17. Gautrin D, Boulet LP, Boutet M, Dugas M, Bherer L, L'Archeveque J, Laviolette M, Cote J, Malo JL: **Is reactive airways dysfunction syndrome a variant of occupational asthma?** *J Allergy Clin Immunol* 1994, **93:**12-22.

18. Boulet LP, Laviolette M, Turcotte H, Cartier A, Dugas M, Malo JL, Boutet M: **Bronchial subepithelial fibrosis correlates with airway responsiveness to methacholine.** *Chest* 1997, **112:**45-52.

19. Lemiere C, Malo JL, Boutet M: **Reactive airways dysfunction syndrome due to chlorine: sequential bronchial biopsies and functional assessment.** *The European respiratory journal* 1997, **10:**241-244.

20. Takeda N, Maghni K, Daigle S, L'Archeveque J, Castellanos L, Al-Ramli W, Malo JL, Hamid Q: **Long-term pathologic consequences of acute irritant-induced asthma.** *J Allergy Clin Immunol* 2009, **124:**975-981 e971.

21. Kennedy SM, Enarson DA, Janssen RG, Chan-Yeung M: **Lung health consequences of reported accidental chlorine gas exposures among pulpmill workers.** *Am Rev Respir Dis* 1991, **143:**74-79.

22. Salisbury DA, Enarson DA, Chan-Yeung M, Kennedy SM: **First-aid reports of acute chlorine gassing among pulpmill workers as predictors of lung health consequences.** *Am J Ind Med* 1991, **20:**71-81.

23. Courteau JP, Cushman R, Bouchard F, Quevillon M, Chartrand A, Bherer L: **Survey of construction workers repeatedly exposed to chlorine over a three to six month period in a pulpmill: I. Exposure and symptomatology.** *Occup Environ Med* 1994, **51:**219-224.

24. Martin JG, Campbell HR, Iijima H, Gautrin D, Malo JL, Eidelman DH, Hamid Q, Maghni K: **Chlorine-induced injury to the airways in mice.** *Am J Respir Crit Care Med* 2003, **168:**568-574.

25. Tian X, Tao H, Brisolara J, Chen J, Rando RJ, Hoyle GW: **Acute lung injury induced by chlorine inhalation in C57BL/6 and FVB/N mice.** *Inhal Toxicol* 2008, **20:**783-793.

26. Tuck SA, Ramos-Barbon D, Campbell H, McGovern T, Karmouty-Quintana H, Martin JG: **Time course of airway remodelling after an acute chlorine gas exposure in mice.** *Respir Res* 2008, **9:**61.

27. Song W, Wei S, Zhou Y, Lazrak A, Liu G, Londino JD, Squadrito GL, Matalon S: **Inhibition of lung fluid clearance and epithelial Na+ channels by chlorine, hypochlorous acid, and chloramines.** *J Biol Chem* 2010, **285:**9716-9728.

28. Li C, Weng Z, Doran SF, Srivastava RK, Afaq F, Matalon S, Athar M: **Chlorine induces the unfolded protein response in murine lungs and skin.** *Am J Respir Cell Mol Biol* 2013, **49:**197-203.

29. Leustik M, Doran S, Bracher A, Williams S, Squadrito GL, Schoeb TR, Postlethwait E, Matalon S: **Mitigation of chlorine-induced lung injury by low-molecular-weight antioxidants.** *Am J Physiol Lung Cell Mol Physiol* 2008, **295:**L733-743.

30. Honavar J, Samal AA, Bradley KM, Brandon A, Balanay J, Squadrito GL, MohanKumar K, Maheshwari A, Postlethwait EM, Matalon S, Patel RP: **Chlorine gas exposure causes systemic endothelial dysfunction by inhibiting endothelial nitric oxide synthase-dependent signaling.** *Am J Respir Cell Mol Biol* 2011, **45:**419-425.

31. Fanucchi MV, Bracher A, Doran SF, Squadrito GL, Fernandez S, Postlethwait EM, Bowen L, Matalon S: **Post-exposure antioxidant treatment in rats decreases airway hyperplasia and hyperreactivity due to chlorine inhalation.** *Am J Respir Cell Mol Biol* 2012, **46:**599-606.

32. Yildirim C, Kocoglu H, Goksu S, Cengiz B, Sari I, Bagci C: **Long-term pulmonary histopathologic changes in rats following acute experimental exposure to chlorine gas.** *Inhal Toxicol* 2004, **16:**911-915.

33. Demnati R, Fraser R, Ghezzo H, Martin JG, Plaa G, Malo JL: **Time-course of functional and pathological changes after a single high acute inhalation of chlorine in rats.** *Eur Respir J* 1998, **11:**922-928.

34. Batchinsky AI, Martini DK, Jordan BS, Dick EJ, Fudge J, Baird CA, Hardin DE, Cancio LC: **Acute respiratory distress syndrome secondary to inhalation of chlorine gas in sheep.** *J Trauma* 2006, **60:**944-956; discussion 956-947.

35. Gunnarsson M, Walther SM, Seidal T, Bloom GD, Lennquist S: **Exposure to chlorine gas: effects on pulmonary function and morphology in anaesthetised and mechanically ventilated pigs.** *J Appl Toxicol* 1998, **18:**249-255.

36. Squadrito GL, Postlethwait EM, Matalon S: **Elucidating mechanisms of chlorine toxicity: reaction kinetics, thermodynamics, and physiological implications.** *Am J Physiol Lung Cell Mol Physiol* 2010, **299:**L289-300.

37. Yadav AK, Bracher A, Doran SF, Leustik M, Squadrito GL, Postlethwait EM, Matalon S: **Mechanisms and modification of chlorine-induced lung injury in animals.** *Proc Am Thorac Soc* 2010, **7:**278-283.

38. Park SY, Shin SW, Lee SM, Park JW: **Hypochlorous acid-induced modulation of cellular redox status in HeLa cells.** *Arch Pharm Res* 2008, **31:**905-910.

39. Whiteman M, Rose P, Siau JL, Cheung NS, Tan GS, Halliwell B, Armstrong JS: **Hypochlorous acid-mediated mitochondrial dysfunction and apoptosis in human hepatoma HepG2 and human fetal liver cells: role of mitochondrial permeability transition.** *Free Radic Biol Med* 2005, **38:**1571-1584.

40. Yang YT, Whiteman M, Gieseg SP: **HOCl causes necrotic cell death in human monocyte derived macrophages through calcium dependent calpain activation.** *Biochim Biophys Acta* 2012, **1823:**420-429.

41. Van Rensburg CE, Van Staden AM, Anderson R: **Inactivation of poly (ADP-ribose) polymerase by hypochlorous acid.** *Free Radic Biol Med* 1991, **11:**285-291.

42. White CW, Martin JG: **Chlorine gas inhalation: human clinical evidence of toxicity and experience in animal models.** *Proc Am Thorac Soc* 2010, **7:**257-263.

43. O'Koren EG, Hogan BL, Gunn MD: **Loss of Basal Cells Precedes Bronchiolitis Obliterans-Like Pathological Changes in a Murine Model of Chlorine Gas Inhalation.** *Am J Respir Cell Mol Biol* 2013.

44. Mo Y, Chen J, Schlueter CF, Hoyle GW: **Differential susceptibility of inbred mouse strains to chlorine-induced airway fibrosis.** *Am J Physiol Lung Cell Mol Physiol* 2013, **304:**L92-102.

45. Rock JR, Randell SH, Hogan BL: **Airway basal stem cells: a perspective on their roles in epithelial homeostasis and remodeling.** *Dis Model Mech* 2010, **3:**545-556.

46. Crosby LM, Waters CM: **Epithelial repair mechanisms in the lung.** *Am J Physiol Lung Cell Mol Physiol* 2010, **298:**L715-731.

47. Hajj R, Baranek T, Le Naour R, Lesimple P, Puchelle E, Coraux C: **Basal cells of the human adult airway surface epithelium retain transit-amplifying cell properties.** *Stem Cells* 2007, **25:**139-148.

48. Stripp BR, Reynolds SD: **Maintenance and repair of the bronchiolar epithelium.** *Proc Am Thorac Soc* 2008, **5:**328-333.

49. Cole BB, Smith RW, Jenkins KM, Graham BB, Reynolds PR, Reynolds SD: **Tracheal Basal cells: a facultative progenitor cell pool.** *Am J Pathol* 2010, **177:**362-376.

50. Rock JR, Onaitis MW, Rawlins EL, Lu Y, Clark CP, Xue Y, Randell SH, Hogan BL: **Basal cells as stem cells of the mouse trachea and human airway epithelium.** *Proc Natl Acad Sci U S A* 2009, **106:**12771-12775.

51. Hong KU, Reynolds SD, Watkins S, Fuchs E, Stripp BR: **In vivo differentiation potential of tracheal basal cells: evidence for multipotent and unipotent subpopulations.** *Am J Physiol Lung Cell Mol Physiol* 2004, **286:**L643-649.

52. Ghosh M, Brechbuhl HM, Smith RW, Li B, Hicks DA, Titchner T, Runkle CM, Reynolds SD: **Context-dependent differentiation of multipotential keratin 14-expressing tracheal basal cells.** *Am J Respir Cell Mol Biol* 2011, **45:**403-410.

53. Hong KU, Reynolds SD, Watkins S, Fuchs E, Stripp BR: **Basal cells are a multipotent progenitor capable of renewing the bronchial epithelium.** *Am J Pathol* 2004, **164:**577-588.

54. Schoch KG, Lori A, Burns KA, Eldred T, Olsen JC, Randell SH: **A subset of mouse tracheal epithelial basal cells generates large colonies in vitro.** *Am J Physiol Lung Cell Mol Physiol* 2004, **286:**L631-642.

55. Sonar SS, Schwinge D, Kilic A, Yildirim AO, Conrad ML, Seidler K, Muller B, Renz H, Nockher WA: **Nerve growth factor enhances Clara cell proliferation after lung injury.** *Eur Respir J* 2010, **36:**105-115.

56. Rawlins EL, Ostrowski LE, Randell SH, Hogan BL: **Lung development and repair: contribution of the ciliated lineage.** *Proc Natl Acad Sci U S A* 2007, **104:**410-417.

57. Freund-Michel V, Frossard N: **The nerve growth factor and its receptors in airway inflammatory diseases.** *Pharmacol Ther* 2008, **117:**52-76.

58. Nakamura T, Endo K, Kinoshita S: **Identification of human oral keratinocyte stem/progenitor cells by neurotrophin receptor p75 and the role of neurotrophin/p75 signaling.** *Stem Cells* 2007, **25:**628-638.

59. Okumura T, Shimada Y, Imamura M, Yasumoto S: **Neurotrophin receptor p75(NTR) characterizes human esophageal keratinocyte stem cells in vitro.** *Oncogene* 2003, **22:**4017-4026.

60. Moscatelli I, Pierantozzi E, Camaioni A, Siracusa G, Campagnolo L: **p75 neurotrophin receptor is involved in proliferation of undifferentiated mouse embryonic stem cells.** *Exp Cell Res* 2009, **315:**3220-3232.

61. Wang Y, Sun Z, Qiu X, Li Y, Qin J, Han X: **Roles of Wnt/beta-catenin signaling in epithelial differentiation of mesenchymal stem cells.** *Biochem Biophys Res Commun* 2009, **390:**1309-1314.

62. Love D, Li FQ, Burke MC, Cyge B, Ohmitsu M, Cabello J, Larson JE, Brody SL, Cohen JC, Takemaru K: **Altered lung morphogenesis,**

epithelial cell differentiation and mechanics in mice deficient in the Wnt/beta-catenin antagonist Chibby. *PLoS One* 2010, **5:**e13600.

63. Akiyama T: **Wnt/beta-catenin signaling.** *Cytokine Growth Factor Rev* 2000, **11:**273-282.

64. Sugimura R, Li L: **Noncanonical Wnt signaling in vertebrate development, stem cells, and diseases.** *Birth Defects Res C Embryo Today* 2010, **90:**243-256.

65. Reynolds SD, Zemke AC, Giangreco A, Brockway BL, Teisanu RM, Drake JA, Mariani T, Di PY, Taketo MM, Stripp BR: **Conditional stabilization of beta-catenin expands the pool of lung stem cells.** *Stem Cells* 2008, **26:**1337-1346.

66. Nakatsu MN, Ding Z, Ng MY, Truong TT, Yu F, Deng SX: **Wnt/beta-catenin signaling regulates proliferation of human cornea epithelial stem/progenitor cells.** *Invest Ophthalmol Vis Sci* 2011, **52:**4734-4741.

67. Zhang Y, Goss AM, Cohen ED, Kadzik R, Lepore JJ, Muthukumaraswamy K, Yang J, DeMayo FJ, Whitsett JA, Parmacek MS, Morrisey EE: **A Gata6-Wnt pathway required for epithelial stem cell development and airway regeneration.** *Nat Genet* 2008, **40:**862-870.

68. Brechbuhl HM, Ghosh M, Smith MK, Smith RW, Li B, Hicks DA, Cole BB, Reynolds PR, Reynolds SD: **Beta-catenin dosage is a critical determinant of tracheal basal cell fate determination.** *Am J Pathol* 2011, **179:**367-379.

69. Reynolds SD, Brechbuhl HM, Smith MK, Smith RW, Ghosh M: **Lung epithelial healing: a modified seed and soil concept.** *Proc Am Thorac Soc* 2012, **9:**27-37.

70. Reynolds SD, Giangreco A, Power JH, Stripp BR: **Neuroepithelial bodies of pulmonary airways serve as a reservoir of progenitor cells capable of epithelial regeneration.** *Am J Pathol* 2000, **156:**269-278.

71. Reynolds SD, Malkinson AM: **Clara cell: progenitor for the bronchiolar epithelium.** *Int J Biochem Cell Biol* 2010, **42:**1-4.

72. Institute of Laboratory Animal Resources (U.S.). *Guide for the care and use of laboratory animals.* Washington, D.C.: National Academy Press; 1996.

73. Salic A, Mitchison TJ: **A chemical method for fast and sensitive detection of DNA synthesis in vivo.** *Proc Natl Acad Sci U S A* 2008, **105:**2415-2420.

74. Hsia CC, Hyde DM, Ochs M, Weibel ER: **An official research policy statement of the American Thoracic Society/European Respiratory Society: standards for quantitative assessment of lung structure.** *Am J Respir Crit Care Med* 2010, **181:**394-418.

75. Miller LA, Gerriets JE, Tyler NK, Abel K, Schelegle ES, Plopper CG, Hyde DM: **Ozone and allergen exposure during postnatal development alters the frequency and airway distribution of CD25+ cells in infant rhesus monkeys.** *Toxicol Appl Pharmacol* 2009, **236:**39-48.

76. **ImageJ: Image processing and analysis in java** [http://rsbweb.nih.gov/ij/]

77. Rawlins EL, Okubo T, Xue Y, Brass DM, Auten RL, Hasegawa H, Wang F, Hogan BL: **The role of Scgb1a1+ Clara cells in the long-term maintenance and repair of lung airway, but not alveolar, epithelium.** *Cell Stem Cell* 2009, **4:**525-534.

78. Hutton E, Paladini RD, Yu QC, Yen M, Coulombe PA, Fuchs E: **Functional differences between keratins of stratified and simple epithelia.** *J Cell Biol* 1998, **143:**487-499.

79. van der Vliet A, O'Neill CA, Cross CE, Koostra JM, Volz WG, Halliwell B, Louie S: **Determination of low-molecular-mass antioxidant concentrations in human respiratory tract lining fluids.** *Am J Physiol* 1999, **276:**L289-296.

80. Schwartz MA, Assoian RK: **Integrins and cell proliferation: regulation of cyclin-dependent kinases via cytoplasmic signaling pathways.** *J Cell Sci* 2001, **114:**2553-2560.

81. Bitron MD, Aharonson EF: **Delayed mortality of mice following inhalation of acute doses of CH2O, SO2Cl2, and Br2.** *Am Ind Hyg Assoc J* 1978, **39:**129-138.

82. Winternitz MC, Lambert RA, Jackson L, Smith GH: **The pathology of chlorine poisoning.** In *Collected studies on the pathology of war gas poisoning.* Edited by Winternitz MC: New Haven: Yale University School of Medicine; 1920: 1-32.

83. Chao MV: **Neurotrophins and their receptors: a convergence point for many signalling pathways.** *Nat Rev Neurosci* 2003, **4:**299-309.

84. Chapman BS, Kuntz ID: **Modeled structure of the 75-kDa neurotrophin receptor.** *Protein Sci* 1995, **4:**1696-1707.

85. Levi-Montalcini R: **The nerve growth factor 35 years later.** *Science* 1987, **237:**1154-1162.

86. Levi-Montalcini R, Dal Toso R, della Valle F, Skaper SD, Leon A: **Update of the NGF saga.** *J Neurol Sci* 1995, **130:**119-127.

87. Quirici N, Soligo D, Bossolasco P, Servida F, Lumini C, Deliliers GL: **Isolation of bone marrow mesenchymal stem cells by anti-nerve growth factor receptor antibodies.** *Exp Hematol* 2002, **30:**783-791.

88. Hoyle GW, Graham RM, Finkelstein JB, Nguyen KP, Gozal D, Friedman M: **Hyperinnervation of the airways in transgenic mice overexpressing nerve growth factor.** *Am J Respir Cell Mol Biol* 1998, **18:**149-157.

89. Lee KF, Li E, Huber LJ, Landis SC, Sharpe AH, Chao MV, Jaenisch R: **Targeted mutation of the gene encoding the low affinity NGF receptor p75 leads to deficits in the peripheral sensory nervous system.** *Cell* 1992, **69:**737-749.

90. Tomic R, Lassiter CC, Ritzenthaler JD, Rivera HN, Roman J: **Anti-tissue remodeling effects of corticosteroids: fluticasone propionate inhibits fibronectin expression in fibroblasts.** *Chest* 2005, **127:**257-265.

91. Ricci A, Felici L, Mariotta S, Mannino F, Schmid G, Terzano C, Cardillo G, Amenta F, Bronzetti E: **Neurotrophin and neurotrophin receptor protein expression in the human lung.** *Am J Respir Cell Mol Biol* 2004, **30:**12-19.

92. Freund V, Frossard N: **[Nerve growth factor (NGF) in inflammation and asthma].** *Rev Mal Respir* 2004, **21:**328-342.

93. Chao MV, Bothwell M: **Neurotrophins: to cleave or not to cleave.** *Neuron* 2002, **33:**9-12.

94. Do H, Park HJ, Sohn EH, Kim BO, Um SH, Kwak JH, Moon EY, Rhee DK, Pyo S: **Ethanol induces cell cycle arrest and triggers apoptosis via Sp1-dependent p75NTR expression in human neuroblastoma cells.** *Cell Biol Toxicol* 2013, **29:**365-380.

95. Gascon E, Vutskits L, Jenny B, Durbec P, Kiss JZ: **PSA-NCAM in postnatally generated immature neurons of the olfactory bulb: a crucial role in regulating p75 expression and cell survival.** *Development* 2007, **134:**1181-1190.

96. Savitz SI, Kessler JA: **Leukemia inhibitory factor requires concurrent p75LNTR signaling to induce apoptosis of cultured sympathetic neurons.** *J Neurosci* 2000, **20:**4198-4205.

97. Musah S, Chen J, Hoyle GW: **Repair of tracheal epithelium by basal cells after chlorine-induced injury.** *Respir Res* 2012, **13:**107.

98. Matsuda H, Koyama H, Sato H, Sawada J, Itakura A, Tanaka A, Matsumoto M, Konno K, Ushio H, Matsuda K: **Role of nerve growth**

factor in cutaneous wound healing: accelerating effects in normal and healing-impaired diabetic mice. *J Exp Med* 1998, **187:**297-306.

99. Graiani G, Emanueli C, Desortes E, Van Linthout S, Pinna A, Figueroa CD, Manni L, Madeddu P: **Nerve growth factor promotes reparative angiogenesis and inhibits endothelial apoptosis in cutaneous wounds of Type 1 diabetic mice.** *Diabetologia* 2004, **47:**1047-1054.
100. Muangman P, Muffley LA, Anthony JP, Spenny ML, Underwood RA, Olerud JE, Gibran NS: **Nerve growth factor accelerates wound healing in diabetic mice.** *Wound Repair Regen* 2004, **12:**44-52.
101. Ebadi M, Bashir RM, Heidrick ML, Hamada FM, Refaey HE, Hamed A, Helal G, Baxi MD, Cerutis DR, Lassi NK: **Neurotrophins and their receptors in nerve injury and repair.** *Neurochem Int* 1997, **30:**347-374.
102. Nithya M, Suguna L, Rose C: **The effect of nerve growth factor on the early responses during the process of wound healing.** *Biochim Biophys Acta* 2003, **1620:**25-31.
103. Bautista DM, Pellegrino M, Tsunozaki M: **TRPA1: A gatekeeper for inflammation.** *Annu Rev Physiol* 2013, **75:**181-200.
104. Ward PA, Hunninghake GW: **Lung inflammation and fibrosis.** *Am J Respir Crit Care Med* 1998, **157:**S123-129.
105. Graham RM, Friedman M, Hoyle GW: **Sensory nerves promote ozone-induced lung inflammation in mice.** *Am J Respir Crit Care Med* 2001, **164:**307-313.

106. Path G, Braun A, Meents N, Kerzel S, Quarcoo D, Raap U, Hoyle GW, Nockher WA, Renz H: **Augmentation of allergic early-phase reaction by nerve growth factor.** *Am J Respir Crit Care Med* 2002, **166:**818-826.

107. Quarcoo D, Schulte-Herbruggen O, Lommatzsch M, Schierhorn K, Hoyle GW, Renz H, Braun A: **Nerve growth factor induces increased airway inflammation via a neuropeptide-dependent mechanism in a transgenic animal model of allergic airway inflammation.** *Clin Exp Allergy* 2004, **34:**1146-1151.

108. Braun A, Appel E, Baruch R, Herz U, Botchkarev V, Paus R, Brodie C, Renz H: **Role of nerve growth factor in a mouse model of allergic airway inflammation and asthma.** *Eur J Immunol* 1998, **28:**3240-3251.

109. Kerzel S, Path G, Nockher WA, Quarcoo D, Raap U, Groneberg DA, Dinh QT, Fischer A, Braun A, Renz H: **Pan-neurotrophin receptor p75 contributes to neuronal hyperreactivity and airway inflammation in a murine model of experimental asthma.** *Am J Respir Cell Mol Biol* 2003, **28:**170-178.

110. Tokuoka S, Takahashi Y, Masuda T, Tanaka H, Furukawa S, Nagai H: **Disruption of antigen-induced airway inflammation and airway hyper-responsiveness in low affinity neurotrophin receptor p75 gene deficient mice.** *Br J Pharmacol* 2001, **134:**1580-1586.

111. Palazzo E, Marconi A, Truzzi F, Dallaglio K, Petrachi T, Humbert P, Schnebert S, Perrier E, Dumas M, Pincelli C: **Role of neurotrophins on**

dermal fibroblast survival and differentiation. *Journal of cellular physiology* 2012, **227:**1017-1025.

112. Micera A, Vigneti E, Pickholtz D, Reich R, Pappo O, Bonini S, Maquart FX, Aloe L, Levi-Schaffer F: **Nerve growth factor displays stimulatory effects on human skin and lung fibroblasts, demonstrating a direct role for this factor in tissue repair.** *Proc Natl Acad Sci U S A* 2001, **98:**6162-6167.

113. Micera A, Lambiase A, Puxeddu I, Aloe L, Stampachiacchiere B, Levi-Schaffer F, Bonini S: **Nerve growth factor effect on human primary fibroblastic-keratocytes: possible mechanism during corneal healing.** *Exp Eye Res* 2006, **83:**747-757.

114. MacDonald BT, Tamai K, He X: **Wnt/beta-catenin signaling: components, mechanisms, and diseases.** *Dev Cell* 2009, **17:**9-26.

115. Vlad A, Rohrs S, Klein-Hitpass L, Muller O: **The first five years of the Wnt targetome.** *Cell Signal* 2008, **20:**795-802.

116. He X, Semenov M, Tamai K, Zeng X: **LDL receptor-related proteins 5 and 6 in Wnt/beta-catenin signaling: arrows point the way.** *Development* 2004, **131:**1663-1677.

117. Villar J, Cabrera NE, Casula M, Valladares F, Flores C, Lopez-Aguilar J, Blanch L, Zhang H, Kacmarek RM, Slutsky AS: **WNT/beta-catenin signaling is modulated by mechanical ventilation in an experimental model of acute lung injury.** *Intensive Care Med* 2011, **37:**1201-1209.

118. Liu L, Carron B, Yee HT, Yie TA, Hajjou M, Rom W: **Wnt pathway in pulmonary fibrosis in the bleomycin mouse model.** *J Environ Pathol Toxicol Oncol* 2009, **28:**99-108.

119. Chilosi M, Poletti V, Zamo A, Lestani M, Montagna L, Piccoli P, Pedron S, Bertaso M, Scarpa A, Murer B, et al: **Aberrant Wnt/beta-catenin pathway activation in idiopathic pulmonary fibrosis.** *Am J Pathol* 2003, **162:**1495-1502.

120. Konigshoff M, Balsara N, Pfaff EM, Kramer M, Chrobak I, Seeger W, Eickelberg O: **Functional Wnt signaling is increased in idiopathic pulmonary fibrosis.** *PLoS One* 2008, **3:**e2142.

121. Henderson WR, Jr., Chi EY, Ye X, Nguyen C, Tien YT, Zhou B, Borok Z, Knight DA, Kahn M: **Inhibition of Wnt/beta-catenin/CREB binding protein (CBP) signaling reverses pulmonary fibrosis.** *Proc Natl Acad Sci U S A* 2010, **107:**14309-14314.

122. Kim TH, Kim SH, Seo JY, Chung H, Kwak HJ, Lee SK, Yoon HJ, Shin DH, Park SS, Sohn JW: **Blockade of the Wnt/beta-catenin pathway attenuates bleomycin-induced pulmonary fibrosis.** *Tohoku J Exp Med* 2011, **223:**45-54.

123. Klein PS, Melton DA: **A molecular mechanism for the effect of lithium on development.** *Proc Natl Acad Sci U S A* 1996, **93:**8455-8459.

124. DasGupta R, Fuchs E: **Multiple roles for activated LEF/TCF transcription complexes during hair follicle development and differentiation.** *Development* 1999, **126:**4557-4568.

125. Emami KH, Nguyen C, Ma H, Kim DH, Jeong KW, Eguchi M, Moon RT, Teo JL, Kim HY, Moon SH, et al: **A small molecule inhibitor of beta-catenin/CREB-binding protein transcription [corrected].** *Proc Natl Acad Sci U S A* 2004, **101:**12682-12687.

126. Li J, Poovey HG, Rodriguez JF, Brody A, Hoyle GW: **Effect of platelet-derived growth factor on the development and persistence of asbestos-induced fibroproliferative lung disease.** *J Environ Pathol Toxicol Oncol* 2004, **23:**253-266.

127. Woessner JF, Jr.: **The determination of hydroxyproline in tissue and protein samples containing small proportions of this imino acid.** *Arch Biochem Biophys* 1961, **93:**440-447.

128. Liu HY, L. Xu,S. Wang, K. Zhang,T.: **Cholestane-3b,5a,6b-Triol Inhibits Osteoblastic Differentiation and Promotes Apoptosis of Rat Bone Marrow Stromal Cells.** *Journal of Cellular Biochemistry* 2005, **96:**198-208.

129. Kneidinger N, Yildirim AO, Callegari J, Takenaka S, Stein MM, Dumitrascu R, Bohla A, Bracke KR, Morty RE, Brusselle GG, et al: **Activation of the WNT/beta-catenin pathway attenuates experimental emphysema.** *Am J Respir Crit Care Med* 2011, **183:**723-733.

130. Konigshoff M, Eickelberg O: **WNT signaling in lung disease: a failure or a regeneration signal?** *Am J Respir Cell Mol Biol* 2010, **42:**21-31.

131. Zemke AC, Teisanu RM, Giangreco A, Drake JA, Brockway BL, Reynolds SD, Stripp BR: **beta-Catenin is not necessary for maintenance or**

repair of the bronchiolar epithelium. *Am J Respir Cell Mol Biol* 2009, **41:**535-543.

132. Zemans RL, McClendon J, Aschner Y, Briones N, Young SK, Lau LF, Kahn M, Downey GP: **Role of beta-catenin-regulated CCN matricellular proteins in epithelial repair after inflammatory lung injury.** *Am J Physiol Lung Cell Mol Physiol* 2013, **304:**L415-427.

CURRICULUM VITAE

Sadiatu Musah
351 Abraham Flexner Way
A702
Louisville, KY 40202

Education

Doctor of Philosophy in Public Health Sciences – Environmental Health, December 2013
University of Louisville

Master of Science – Environmental Sciences, May 2008
University of Northern Iowa

Bachelor of Science – Zoology, August 2004
University of Ghana

Fellowships

Graduate Teaching Assistantship
University of Louisville (2008 – 2013)

Graduate Teaching Assistantship
University of Northern Iowa (2006 – 2008)

Professional Experience

Graduate Research Assistant, University of Louisville, August 2008 – December 2013

- Examined repair of the respiratory epithelium after chlorine-induced injury
- Investigated mechanisms of particulate matter (PM) toxicity in vitro and in vivo
- Examined proteome profile alterations after cigarette smoke exposure

Graduate Research Assistant, University of Northern Iowa, August 2006 – July 2008

- Investigated effects of metolachlor on HepG2 cells

Areas of Expertise

Skilled in laboratory techniques such as

- Culture of cell lines, isolation and culture of primary cells
- Cell proliferation and viability assays
- Western blot analysis
- 2D gel electrophoresis
- PCR
- ELISA
- Inhalation exposure
- Drug administration
- Histology, immunohistochemistry, and morphometry

Affiliations

American Thoracic Society Member In Training

Honors

Winner, Basic Science Research Award Poster at Research Louisville, University of Louisville (2012)

Outstanding Student for the School of Public Health and Information Sciences, Fall 2013

Commencement Speaker, Fall 2013.

Publications

Sean Hartnett, **Sadiatu Musah**, Kavita R. Dhanwada. Cellular effects of metolachlor exposure on human liver (HepG2) cells. Chemosphere, Volume 90, Issue 3, January 2013, Pages 1258–1266.

Sadiatu Musah, Jing Chen, Gary W Hoyle. Repair of tracheal epithelium by basal cells after chlorine-induced injury. Respiratory Research 2012, 13:107.

Lorena Canales, Jing Chen, Elizabeth Kelty, **Sadiatu Musah**, Cindy Webb, M. Michele Pisano, Rachel E. Neal. Developmental cigarette smoke exposure: Liver proteome profile alterations in low birth weight pups. Toxicology, Volume 300, Issues 1–2, 9 October 2012, Pages 1–11.

Sadiatu Musah, Natasha DeJarnett, Gary W. Hoyle. Tumor necrosis factor-α mediates interactions between macrophages and epithelial cells underlying proinflammatory gene expression induced by particulate matter. Toxicology, Volume 299, Issues 2–3, 28 September 2012, Pages 125–132.

Presentations

"Impaired Repair Of Chlorine-Induced Airway Injury In Mice Lacking The Low-Affinity Nerve Growth Factor Receptor"
Sadiatu Musah, Jing Chen, Connie F. Schlueter, and Gary Hoyle. Am. J. Respir. Crit. Care Med. (2013). Vol 187: A1850.

- American Thoracic Society International Conference
- Philadelphia, PA, May 2013

"Repair Of The Tracheal Epithelium After Chlorine-Induced Injury"

- Research Louisville
- Louisville, KY, October 2012

"Repair Of Tracheal Epithelium After Chlorine-Induced Injury"
Sadiatu Musah, Connie Schlueter, Jing Chen, and Gary Hoyle. Am. J. Respir. Crit. Care Med. (2012). Vol 185: A6237.

- American Thoracic Society International Conference
- San Francisco, CA, May 2012

"Repair Of Tracheal Epithelium After Chlorine-Induced Injury"

- Research Louisville
- Louisville, KY, October 2011

"Tumor Necrosis Factor-Alpha (TNF) Mediates Pro-inflammatory Gene Expression Induced By Particulate Matter In Co-Cultures Of Macrophage And Lung Epithelial Cell Lines"
Sadiatu Musah, Natasha DeJarnett, and Gary W. Hoyle. Am. J. Respir. Crit. Care Med. (2011). Vol 183: A3239.

- American Thoracic Society International Conference
- Denver, CO, May 2011

"TNF Mediates Pro-inflammatory Gene Expression Induced by Particulate Matter in Co-cultures of Macrophage and Lung Epithelial Cell Lines"

- Research Louisville
- Louisville, KY, October 2010

“Serum Metabolome and Frontal Cortex Proteome Alterations in C57Bl/6 Mice Persist Past Withdrawal of Chronic Tobacco Smoke Exposure”

- American Society of Mass Spectrometry
- Philadelphia, PA, June 2009

IAS 2008

- Iowa Academy of Science
- Ames, IA, May 2008

SETAC 2007

- Society of Environmental Toxicology and Chemistry
- Milwaukee, WI, 2007